Symmetry breaking signaling mechanisms during cell polarization

Lucas Bruurs

Artwork by:
Василий Васильевич Кандинский
Front: *Untitled*, 1923
Back: *Untitled (drawing for "Diagram 17")*, 1925
Insert: *Free Curve to the Point - Accompanying Sound of Geometric Curves*, 1925

Printed by:
ProefschriftMaken // www.proefschriftmaken.nl // Vianen, The Netherlands

Symmetry breaking signaling mechanisms during cell polarization

Symmetrie-doorbrekende signaleringsmechanismes tijdens cel polarisatie
(met een samenvatting in het Nederlands)

Proefschrift
ter verkrijging van de graad van doctor aan de Universiteit Utrecht op gezag van de rector magnificus, prof. dr. G.J. van der Zwaan, ingevolge het besluit van het college voor promoties in het openbaar te verdedigen op
dinsdag 14 februari 2017 des middags te 12.45 uur
door

Lucas Johan Maria Bruurs

geboren op 21 april 1988 te Veere

Promotor: Prof. dr. J.L. Bos

Dedicated to Willem

Table of Contents

I

General introduction

Mechanisms of symmetry breaking during cell polarization

1

Abstract

Tissue morphogenesis requires orchestrated execution of the epithelial cell polarity program. Small GTPases of the Rho family are central players in the various processes that contribute to cell polarization. Cdc42 in particular has an evolutionary conserved function in apico-basal polarity establishment by pioneering the formation of an apical plasma membrane. In order to function as pioneer factor, Cdc42 must break initial cellular symmetry and establish a polarity axis. Importantly, polarization at multiple sites can be detrimental to cellular function and therefore cells must ensure that only one polarity axis is established.

Here, epithelial cell polarity and signaling by the small GTPase Cdc42 during cellular polarization will be introduced. An overview is provided on symmetry breaking by small GTPases and the mechanisms that safeguard singularity in polarization will be discussed.

Epithelial cell polarity

Cell morphology and function are intimately linked. A paramount example of this are polarized enterocytes that constitute the major cell type of the intestinal epithelium. The primary function of these cells is to transport nutrients from the intestinal lumen to the underlying blood vessels, while providing a barrier to bacteria and xenobiotics. For this enterocytes develop a highly specialized ("apical") front and ("basal") rear. The apical domain (which faces the intestinal lumen) is hallmarked by densely packed microvilli, which increase apical membrane surface and thereby allow efficient nutrient uptake. In addition, apical tight junctions provide a physical barrier between neighboring cells and thus ensure epithelial monolayer integrity. On the other side of the cell, the basal domain regulates nutrient passage to the circulation and contacts the basement membrane, thereby tethering the epithelial monolayer to the underlying tissue. The importance of this specific cellular morphology is highlighted by the notion that disruption of apico-basal polarity is causative to human diseases (e.g. microvillous inclusion disease) and that polarity is almost universally lost during cancer progression[1-3].

Because of this importance, the establishment and maintenance of apico-basal polarization in enterocytes is strictly regulated. Cell polarization is essentially the result of a combination of various cellular processes which need to be executed in a concerted manner[4]. These processes include among others: establishment of an apico-basal axis, rearrangement of the cytoskeleton and organelles, organization of apical and basal vesicular transport, remodeling of the apical plasma membrane and assembly of apical junctional complexes. Signaling by small GTPases is involved in many of these processes and these proteins therefore have a critical function in cell polarization[5,6].

Signaling by small GTPases

The human Ras superfamily of small GTPases comprise a group of approximately 170 membrane-bound proteins, which resemble the Ras oncogene and function as molecular switches[7]. These 170 proteins are further subdivided into Ras, Rho, Rab and Arf families based on structural and functional resemblance. Nonetheless, all have a common biochemical mechanism which allows their binary signaling: when bound to guanosine diphosphate (GDP) the protein is considered inactive, whereas activation results from binding to guanosine triphosphate (GTP). This induces a conformational rearrangement in the switch regions resulting in binding of effector proteins that activate downstream signaling[8,9]. GTP-loading is catalyzed by guanine nucleotide exchange factors (GEFs) which liberate GDP and allow substitution with more abundant GTP[10]. On the other hand, signal termination occurs when GTP is hydrolyzed to GDP. Although intrinsic GTPase activity can reset the system, it is generally too slow to enable dynamic regulation. Instead, GTPase-activating proteins (GAPs) function to boost intrinsic GTPase

activity and thereby induce signal termination. Many GEFs and GAPs are multidomain proteins whose activity is subjected to additional regulation. This therefore allows for precise spatial and temporal control over GTP-loading and consequently over the signaling output of small GTPases[10].

Whereas the GDP/GTP cycle enables switch-like activation of small GTPases, an additional dimension of regulation originates from the localization of small GTPases. All small GTPases are subjected to isoprenyl lipid modification involving the covalent attachment of either a farnesyl or geranylgeranyl moiety to a C-terminal cysteine[11]. This provides membrane affinity to a low degree and therefore secondary membrane targeting motifs are often present in the form of either a polybasic region or cysteines that can be dynamically palmitoylated[12,13]. The composition of these secondary membrane targeting motifs and the presence of additional localization signals differs between small GTPases and thus add to the spatial regulation of GTPase signaling[14].

Furthermore, small GTPases of the Rho family are substrate for guanosine nucleotide dissociation inhibitor (GDI)-mediated membrane dissociation, where GDP-bound Rho proteins are extracted from membranes and sequestered in the cytosol in an inactive complex with the GDI[15]. Importantly, the interaction with RhoGDI can be modulated by phosphorylation of either RhoGDI or client Rho protein[16,17]. Similar GDI-like interactions of PDEδ have been reported to control the localization of polybasic region containing GTPases, like KRas, thereby expanding the mechanisms of spatial regulation[18]. The mechanisms that control GTPase localization act in concert with GEF/GAP mediated control over GTP-loading to achieve high spatiotemporal control over GTPase signaling.

The Rho family of GTPases is composed of 22 proteins in mammals, of which three members are most extensively studied: RhoA, Rac1 and Cdc42[19]. Signaling by Rho proteins regulates the actin cytoskeleton and thereby controls cellular morphology, cell migration, junction formation and cell polarization. For this Rho proteins are activated by RhoGEFs that are hallmarked by the presence of a Dbl-homology (DH) domain, which is typically flanked by a PH domain, and inactivated by RhoGAPs[10]. Humans harbor 70 DH domain and 66 RhoGAP containing proteins that can have different specificities towards different Rho proteins, thereby allowing precise control of Rho activity and enabling selective signaling by related Rho GTPases.

Signaling by Rho GTPases is involved in a variety of processes during epithelial cell polarization. For instance, ß1-Integrin binding to the extracellular matrix of the basement membrane results in activation of Rac1, which instructs orientation of the polarity axis[20-22]. Alternatively, apical RhoA activation is primarily implicated in generating actomyosin contractility to enable apical constriction. This is crucial during epithelial lumen formation *in vivo*, which

involves epithelial sheet invagination at the apical membrane and subsequent folding of the monolayer into an epithelial tube[23,24].

Delineating the specific roles of Rho, Rac and Cdc42 during cell polarization has proven to be challenging and care must be taken to interpret data based on overexpression of constitutively active or dominant negative mutants. Because of the high degree of molecular crosstalk between Rho GTPases these mutants often interfere with signaling by other Rho GTPases. Indeed, phenotypes of dominant negative mutants often do no overlap with knockout phenotypes[25-27].

Cdc42 signaling mechanisms during cell polarization

Whereas Rac and RhoA are primarily implicated in cell polarization by regulating axis establishment and actomyosin contractility respectively, signaling by Cdc42 orchestrates a variety of processes that contribute to cell polarization (Fig. 1). Since Cdc42 is one of the first determinants of apico-basal polarity and because it controls many polarity-defining processes, Cdc42 has been considered to be the center of polarity signaling[28]. Indeed, the pioneering role of Cdc42 in polarity was demonstrated by showing that Cdc42 signaling precedes signaling by other Rho GTPases and that ectopic activation of Cdc42 is sufficient to induce polarization[29,30]. Here, the functions of Cdc42 signaling during epithelial cell polarization will be discussed. A summary of the molecular mechanisms involved in these processes is provided in figure 2.

Apical domain specification

Cdc42 is a pioneering factor in the establishment of an apical domain as it is among the first molecular determinants of an apical membrane. Although it is still unclear which Cdc42GEF(s) activate Cdc42 for apical domain specification, two GEFs have been strongly implicated, namely Tuba and Dbl3[31,32]. Upon activation, Cdc42-GTP recruits and activates atypical protein kinase C (aPKC) via the Cdc42 effector partitioning defective (Par) 6. Together with recruitment by Par3, this mechanism results in apical localization and activation of aPKC[33]. The apical Par3/Par6/aPKC complex, also named Par complex, can be considered the major effector of Cdc42 signaling during epithelial cell polarization as its formation initiates many other processes required for polarity establishment.

Apical membrane specification by the Par complex results from phosphorylation of various basolateral proteins by aPKC, thereby invoking their apical exclusion[34]. Most notably, phosphorylation of Par1, which specifies the basolateral membrane, results in membrane dissociation by the 14-3-3 protein Par5 and apical exclusion of Par1[35,36]. Conversely, Par1 functions as a kinase to prevent apical proteins from trespassing the basolateral membrane. Par3 is among the Par1 phosphorylation targets thus creating a mutual exclusive system for apical and basolateral membrane specification[37].

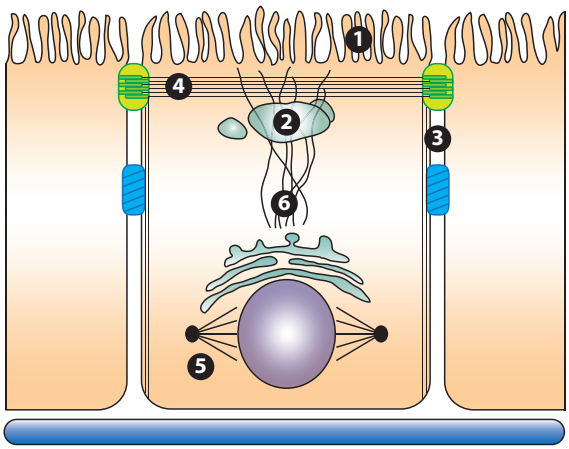

Cdc42-directed processes during cell polarization:

1. ***Apical domain specification***
2. ***Polarized membrane traffic***
3. ***Junction formation***
4. ***Regulation of actin cytoskeleton***
5. ***Spindle orientation***
6. ***Regulation of microtubule network and organelle positioning***

Figure 1: Cdc42-directed processes during epithelial cell polarization
Overview of the cellular processes controlled by Cdc42 that contribute to cell polarization. Note that although listed here as separate processes, most processes are intimately connected.

As Cdc42 is among the first determinants of the apical membrane, the question arises how Cdc42 itself becomes localized. It has been suggested that phosphatase and tensin homolog (PTEN), by generating phosphatidylinositol (4,5)-bisphosphate (PI(4,5)P_2) at the apical membrane, provides a docking site for the scaffold protein Annexin2, which selectively binds GTP-loaded Cdc42 and ensures its apical confinement[38]. Additionally, local Cdc42 activation and consequent apical domain specification has been suggested to involve apical recruitment of the Cdc42GEF Dbl3 by phosphorylated Ezrin[32].
However, because PTEN localization and Ezrin phosphorylation are both dependent on Cdc42 these mechanisms likely reflect positive feedback mechanisms to control Cdc42 localization and activation in cells that are already polarized[39-41]. Alternatively, Cdc42 may become localized in a symmetry breaking process, which does not require pre-existing landmarks but involves positive feedback mechanisms to concentrate Cdc42 at the nascent apical domain[42]. Such a mechanism has been shown to control Cdc42 localization during yeast cell polarization and will be considered later in more detail[43].

Apical protein transport
Directional delivery by vesicular transport functions as a sorting mechanism to segregate apical and basolateral proteins during cell polarization[44,45]. Apical recycling endosomes, as marked by the Rab11 small GTPase, have a seminal function in the sorting and delivery of apical proteins[31,46,47]. Cdc42 is required to target recycling endosomes to the nascent apical plasma membrane and therefore contributes to the delivery of apical membrane components[31].
In the absence of Cdc42 recycling endosomes are formed, indicating that Cdc42 is not required for recycling endosome formation, but they are not transported to the apical membrane[31,48]. Instead, recycling endosomes remain in the cytosol and may ultimately form ectopic lumina[31]. A failure to target recycling endosomes to

the apical membrane underlies the enteropathy Microvillous Inclusion Disease (MVID), a disease caused by mutations in the motor protein for recycling endosomes, MyosinVb[49]. Interestingly, inducible Cdc42 knockout mice develop an MVID phenotype, further indicating that Cdc42 is required for apical targeting of recycling endosomes[50].
Although it is apparent that Cdc42 is required for apical targeting of recycling endosomes, the molecular machinery that Cdc42 employs for this is still largely unclear. Upstream of Cdc42, knockdown of the GEF Tuba fully phenocopies the apical trafficking defects of Cdc42 knockdown in CaCo2 and MDCK cyst cultures, suggesting that Tuba activates Cdc42 to regulate apical transport[31,51]. Downstream of Cdc42, two mechanisms have been proposed to mediate the effects on recycling endosomes directionality, which are not mutually exclusive. On the one hand, Cdc42 interacts with the exocyst complex, which tethers endosomes to the plasma membrane and is required for cargo release[52]. Illustrating this, Cdc42/Par-dependent regulation of the exocyst complex is required for ciliogenesis and therefore explains the polycystic kidney disease (PKD) phenotype of kidney-specific Cdc42 knockout mice[53-55]. On the other hand, Cdc42 may regulate recycling endosomal directionality by modulating the actin cytoskeleton, over which recycling endosomes are transported by the actin-guided motor protein MyosinV[56-58].

Junction formation
The formation of apical tight junctions obstructs lateral diffusion of membrane proteins and thus contributes to the maintenance of cell polarity. In addition, tight junctions ensure the formation of a sealed lumen thereby ensuring epithelial barrier function. Cdc42 signaling is required for the formation and maintenance of tight junctions through diverse mechanisms[59,60].
Tuba is the only GEF implicated in regulating Cdc42 at cell-cell junctions[61,62]. However, Tuba is not required for junction formation or stability and Tuba loss only affects junctional morphology, a phenotype that could originate from the role of Tuba in apical domain specification or modulation of the actin cytoskeleton[61,62]. Therefore, it remains unknown whether there is a specific GEF that regulates Cdc42 activity to control junction formation. Nevertheless, two RhoGAPs are implicated in controlling Cdc42-dependent formation of apical cell-cell junctions: SH3BP1 and Rich1[63,64].

Various effectors where found to be critical for Cdc42-dependent tight junction formation: the Par complex has a critical role in the positioning of the apical junction complex, which in part is controlled by phosphorylation of Crumbs3[65,66]. Other reports have linked the Par complex to the direct regulation of E-Cadherin, thereby contributing to cell-cell junction formation[67,68]. However, the effects of Cdc42/Par on E-Cadherin localization are most likely indirect via regulation of E-Cadherin recycling[69,70].

Next to Par-dependent positioning of apical junctions, Cdc42 signaling controls junction formation via the kinases MRCK and PAK4[71,72]. These effectors have been primarily implicated in junction formation of migrating cells and their effects are believed to be dependent on regulation of the actin cytoskeleton. Given the intimate connectivity between the actin cytoskeleton and cell-cell junctions it is technically challenging to dissect these processes.

Organization of the actin cytoskeleton

The actin and microtubule cytoskeleton contribute to cell polarization by providing the infrastructure required for directional transport[44,73]. This function is best illustrated during yeast cell polarization: upon bud formation, actin cables project towards the apical cap and serve as the track for Myosin-based cargo transport towards the nascent bud[74,75]. As a consequence, disruption of the actin cytoskeleton by Latrunculin B treatment prevents polarized growth and bud establishment[74]. However, apical clustering of Cdc42 is only marginally compromised in Latrunculin B-treated yeast cells, indicating that Cdc42 polarization is actin-independent and suggesting that Cdc42 clustering precedes actin remodeling[75,76].

Whereas the role of actin modulation by Cdc42 in polarizing yeast cells is relatively straightforward, it is far less clear to what extent actin organization by Cdc42 contributes to mammalian cell polarization. In polarized epithelial cells, the adaptor neural Wiskott-Aldrich syndrome protein (NWASP) has been primarily implicated in regulating the actin cytoskeleton in a Cdc42-dependent manner[51,61]. NWASP forms a trimeric complex with Tuba and Cdc42 and depletion of NWASP in MDCK cysts results in the formation of multiple lumen, thus phenocopying Cdc42 and Tuba loss[51,61]. Furthermore, Cdc42 deletion in kidney epithelial cells results in a strong decrease in NWASP activation[55]. Functionally, NWASP stabilizes junctional actin and thereby contributes to the formation of the actin belt that constitutes the zonula adherens[77].

Spindle orientation

The orientation of cell division is a critical regulatory mechanism in stem cell homeostasis and lumen formation[78-80]. In an epithelial tissue cell division is generally oriented in parallel to the monolayer and this configuration requires Cdc42 signaling[79,81]. A failure to ensure this planar orientation can result in defective barrier function but can also cause cell eviction into the lumen, a process that is implicated in breast cancer progression[82,83]. Indeed, mammary-specific Cdc42 deletion results in lumen filling and affects mammary tissue architecture[84].

Deletion of Cdc42 in polarized MDCK cysts causes loss of planar spindle orientation and subsequently leads to the formation of multiple lumen[25].

Also *in vivo*, during *Xenopus laevis* development, Cdc42 is required for planar spindle orientation during neural tube closure[85]. In addition, inducible deletion of Cdc42 in the auditory epithelium results in the formation of ectopic lumen, which may originate from erroneous spindle orientation[86].

Cdc42 controls spindle orientation via multiple signaling routes. A module composed of Tuba/Cdc42/Par complex contributes to spindle orientation and positioning by phosphorylating proteins of the mitotic machinery[87-91]. Whereas this module operates at the apical plasma membrane, a second signaling module controlling spindle orientation composed of Intersectin2/Cdc42/PAK2 is localized to centrosomes[92,93]. Both modules are non-redundant in the control of spindle positioning in polarizing MDCK cysts. Finally, a third Cdc42 module has been implicated in microtubule attachment to the kinetochores, via which it could be involved in spindle orientation[81,94,95]. Whether this function of Cdc42 contributes to spindle orientation in polarized epithelia has not yet been studied.

Regulation of the microtubule network and organelle positioning
The microtubule network is required for polarized organization of organelles and vesicular traffic[44,96]. Polarized epithelial cells typically align the nucleus, golgi and centrosomes/MTOC along the apico-basal polarity axis, with the nucleus located at the basal aspect and the golgi and MTOC located between the nucleus and the apical plasma membrane. A similar distribution is observed in migrating cells, where the MTOC is located between the nucleus and the protrusive front[96].

The microtubule network is critically required to establish this configuration because it serves as the tracks over which dynein-mediated organelle (re)positioning occurs[96]. Cdc42 is required to establish the typical polarized organelle distribution by both regulating the microtubule network and the actin cytoskeleton[28,97]. Although the mechanisms of Cdc42-mediated MTOC orientation have been primarily studied in the context of cell migration, it is likely that similar mechanisms operate during epithelial cell polarization given the strikingly similar organelle distribution.

Cdc42 is activated to induce MTOC reorientation during cell migration upon monolayer scratching[98]. Activated Cdc42 regulates the microtubule network and organelle positioning through various mechanisms which involve a distinct molecular machinery[99]. Firstly, Cdc42 controls MTOC positioning by organizing the microtubule network and by controlling dynein activity[99-102]. Secondly, Cdc42 controls nuclear movement via an actin-based signaling module where Cdc42 activates MRCK and Myosin II[97,103]. Both microtubule-based regulation of MTOC positioning and actin-based control of nuclear movement is ultimately required to establish the typical organelle distribution in polarizing cells[97].

Organization of Cdc42 polarity signaling

Although presented here as distinct functions, many of the Cdc42-governed signaling routes are highly interconnected. For instance, the actin cytoskeleton contributes to junction formation and conversely, cell-cell junctions are instructive cues in the organization of the actin cytoskeleton[104]. Similarly, Cdc42 controls the organization of the actin and microtubule cytoskeleton allowing polarized membrane traffic, but MyosinV-dependent trafficking also controls spindle orientation during yeast cell polarization[105]. Furthermore, although mitotic spindle orientation in an epithelial monolayer is instructed by the apico-basal polarity axis, spindle orientation in turn dictates positioning of the apical membrane[58,106]. Finally, Cdc42 organizes the actin cytoskeleton to control E-cadherin recycling, thereby affecting junction formation[69,70]. These examples therefore illustrate that although Cdc42 employs distinct signaling modules to coordinate different polarization processes, most of the Cdc42-directed processes are ultimately connected. Because of this connectivity, molecular dissection of Cdc42 signaling during cell polarization has proven to be challenging.

A common theme in Cdc42 polarity signaling routes is their organization by feedback mechanisms. For instance: Cdc42-dependent apical membrane specification in enterocytes is followed by brush border formation. During

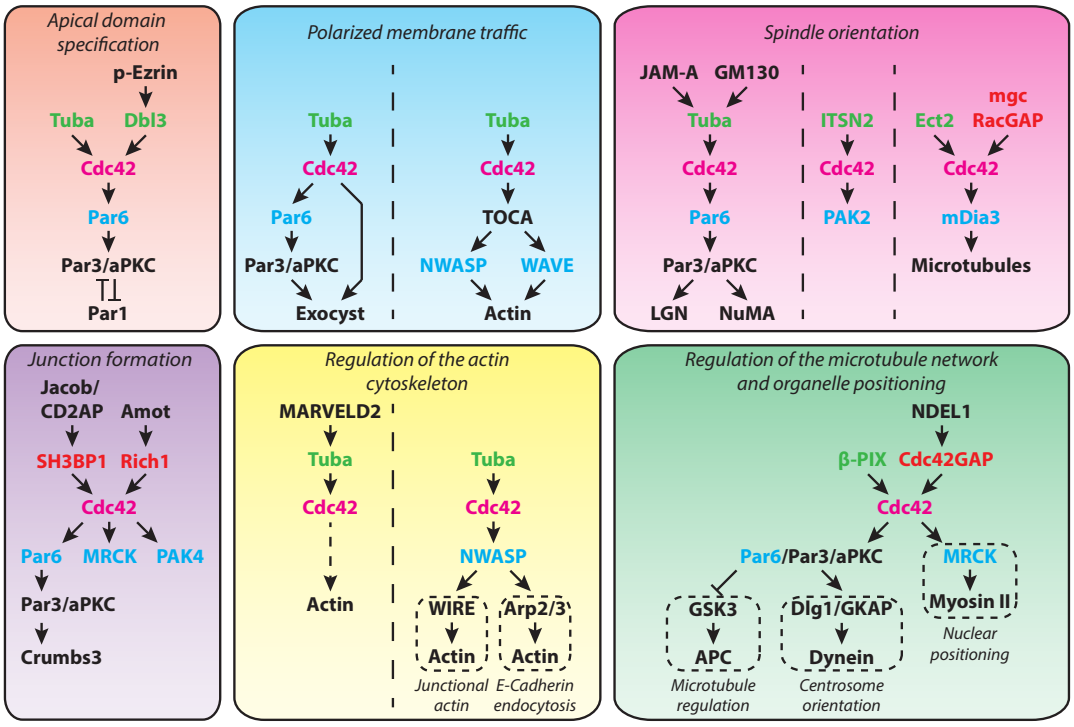

Figure 2: Summary of the molecular mechanisms of Cdc42 signaling during cell polarization
Overview of the signaling pathways involved in various Cdc42-controlled polarity processes. Proteins in green are GEFs, in red are GAPs and in blue are direct Cdc42 effectors.

microvilli formation, ERM phosphorylation is induced and this results in the recruitment of the Cdc42GEF Dbl3[32,107-109]. Apical recruitment of Dbl3 in turn ensures spatially restricted Cdc42 activity to control apical domain specification[32]. Experimentally, this feedback mechanism is partly revealed by the finding that overexpression of Dbl3 or a constitutively active Ezrin mutant results in Cdc42 activation and consequent enlargement of the apical domain[32]. A second example of feedback control over Cdc42 signaling is control of Cdc42 localization by membrane traffic during cell migration. Here, Cdc42/Par complex-mediated organization of polarized membrane trafficking contributes to Cdc42 accumulation at the leading edge because Cdc42 itself is delivered to the leading edge by vesicles[110].

What is the relevance of these feedback regulations in Cdc42 signaling for cell polarization? In general positive feedback mechanisms function to amplify a weak signal, which may be relevant during Cdc42-directed symmetry breaking[111,112]. Additionally, positive feedback mechanisms prevent termination of Cdc42 signaling and thereby create bi-stability in signaling[111-113]. For polarization, this means that once initiated cells are committed to polarizing and that an apical domain is not readily dismantled once formed. Finally, feedback mechanisms in Cdc42 signaling may ensure that a single apical domain is specified by establishing competition[42,114-116]. This aspect will be discussed later in more detail.

From an experimental point of view, the connectivity between the different polarization processes and the existence of feedback mechanisms provide a serious challenge for delineating Cdc42 signaling pathways. Since interference with downstream processes will cause effects upstream in the pathway it is challenging to establish hierarchy in signaling. Furthermore, pathway interference can indirectly affect multiple polarization processes at the same time making it difficult to establish causality. These two factors therefore greatly complicate interpretation of experimental data on polarity signaling pathways.

Small GTPases of the Rho family, and Cdc42 in particular, are crucial signaling molecules in the establishment of cell polarity. Two features of small GTPase signaling are particularly relevant for cell polarization. Firstly, the exquisite spatial and temporal control over GTPase signaling by GEFs and GAPs allows for highly localized activation of downstream signaling pathways in a well-timed manner. For example, the ability to restrict Cdc42 activity to limited part of the cell is crucial to spatially confine Par6/aPKC-dependent apical domain specification[32]. Similarly, Rac1 is locally activated to position the apico-basal polarity axis and an inability to ensure spatially restricted Rac activation prevents axis establishment[117]. Furthermore, temporally distinct waves of Cdc42 activation during yeast cell polarization are required to establish proper bud sites[118]. Secondly, the modular organization of GTPase signaling enables stringent

control over multiple processes by a single GTPase. By engaging different GEFs, GAPs and effectors, Cdc42 can control junction formation, spindle orientation and polarized membrane traffic at the same time without signal interference.

Symmetry breaking during cell polarization

De novo establishment of cell polarity requires breaking of cellular symmetry in order to establish a polarity axis[119,120]. The polarity axis then serves to instruct the next steps in polarization, ultimately leading to the establishment of functionally distinct apical and basal domains. In the context of cell polarity, symmetry breaking often involves the clustering of polarity signaling molecules from an initially homogenous distribution[115,121-123]. In various systems, Cdc42 functions as the pioneering factor in apical membrane specification and its clustering is often a symmetry breaking event[76,124-126].

From a signaling perspective, symmetry breaking provides a very fundamental problem because by definition no pre-existing landmarks are available to instruct segregation of signaling components. Instead, symmetry breaking involves a combination of cell-intrinsic mechanisms via which an initial random fluctuation or an external stimulus triggers complete cell polarization. These mechanisms generally include[115,120,127]:

(1) amplification of a (stochastic) signal by means of positive feedback systems
(2) repression of ectopic clustering by long range inhibition
(3) prevention of cluster dissipation

The combined outcome of these mechanisms is a system where a fluctuation in signaling is amplified to generate a single cluster without the need for pre-existing landmarks, thereby breaking the initial cellular symmetry[115,120].

Spatial control over symmetry breaking

Although no pre-existing landmarks are required for symmetry breaking, spatial cues can be used to bias the location where symmetry breaking takes place. This is best exemplified in polarizing yeast cells where clustering of Cdc42 is a symmetry breaking event in the establishment of an apical domain[76].

Although Cdc42 clustering is sufficient to induce bud formation, yeast cells prevent re-usage of previous bud sites by means of a bud site selection machinery, which ensures that Cdc42-mediated symmetry breaking always takes place adjacent to the previous bud site[136-138]. Nevertheless, when bud site selection is disabled, Cdc42 clustering and concomitant bud formation still occurs, though in a spatially randomized manner[139]. This therefore demonstrates that bud site selection is not required for Cdc42-dependent symmetry breaking and only functions to provide spatial bias to where Cdc42 clustering will initiate[137].

Box 1: Turing-type pattern formation and symmetry breaking

Based on the three aforementioned mechanisms, Alan Turing in his 1952 paper "the Chemical Basis of Morphogenesis" established a mathematical framework that provided a paradigm for symmetry breaking and pattern formation in biology[128].

In a prototypical Turing reaction-diffusion system, symmetry is broken by two interacting molecules ("morphogens"): a rapidly-diffusing inactive molecule, that is capable of long range inhibition, and a slowly-diffusing active signaling molecule, that is able to promote its own synthesis. In such a system, a relatively immobile cluster of active molecules will grow locally, while the rapidly diffusing inhibitor curbs clusters expansion. Importantly, the function of a diffusible inhibitor is dispensable as other means of long range inhibition (e.g. sequestering of a critical factor for activation) will result in a similar network behavior[115,120,127-129].

The resulting Turing system is able to break symmetry and can mathematically account for the formation of a variety of biological patterns, including those of fish skin pigmentation, insect corneal surfaces and digit patterns[130-133]. In the context of cell polarization, Turing-like reaction-diffusion dynamics have been used to model symmetry breaking clustering of Cdc42 during yeast cell polarization, of Rop during root hair cell polarization in plants and of HRas in axon specification[43,134,135]. Because of its straightforward biochemical requirements and its ability to account for complex biological phenomena such as symmetry breaking and singularity in polarization, Turing-type reaction-diffusion dynamics provide an attractive framework to study cell polarization.

Often though, the trigger for symmetry breaking also provides spatial information, thereby ultimately dictating the position of the polarity axis. This is exemplified during *C. elegans* embryo development, where symmetry breaking upon fertilization is initiated when the sperm microtubule organizing center (MTOC) moves towards the cell cortex[121,140]. This causes a local inactivation of RHO-1 and cessation in actomyosin contractility. Local loss of actomyosin contractility establishes an actomyosin flow that drives anterior deposition of the 'apical' Par proteins (PAR-3, PAR-6 and PKC-3) ultimately generating cortical asymmetry[141]. Importantly, the sperm MTOC reaching the cell cortex is both the initiating trigger for symmetry breaking as well as the spatial cue that dictates positioning of the polarity axis.

Singularity in cell polarization

In order to successfully polarize, cells must ensure that one – and only one – polarity axis is established during symmetry breaking. For some cells, limiting polarization to a single domain is pivotal. For instance, if yeast cells form more than one bud, DNA missegregation occurs, resulting in aneuploidy[142].

Alternatively, migrating cells could split apart when opposing migratory fronts are formed[143-145]. In order to ensure singularity in polarization, cells must either suppress formation of secondary polarization sites or be capable of resolving multiple polarization sites. The first mechanism is dependent on long range inhibition and frequently involves mechanochemical signaling[144]. The second mechanism requires the establishment of a 'winner-takes-all' competition between co-existing clusters to establish a single dominant polarization site[146]. Examples of both mechanisms will be discussed here with a focus on the role of small GTPases.

Competition between scarce polarity factors

In polarizing yeast cells, singularity in bud formation is ensured by Cdc42[147]. The mechanisms of Cdc42-dependent singularity regulation have been thoroughly investigated and it provides the prime example of how singularity in polarization is enforced by competition for limited polarity factors.

During yeast cell polarization, nascent polarity clusters engage in a greedy competition for scarce polarity factors such as Cdc42, Bem1 and Cdc24[146]. Positive feedback recruitment of these factors to growing clusters ultimately creates a competition in which larger clusters are more effective in sequestering polarity factors, thereby eliminating smaller clusters[146,148]. This ensures that one winning Cdc42 cluster is formed and thereby prevents formation of multiple buds.

As a consequence of this, slowing the competition between clusters, by reducing the mobility of polarity factors, impairs the ability to resolve multiple clusters and thereby results in yeast cells with multiple buds. In yeast, this has been demonstrated using various approaches: Howell et al. engineered an artificial feedback mechanism involving actin-dependent endocytic recycling of Bem1, which is a critical polarity factor for yeast[148]. As a consequence, this feedback occurs at a slower rate compared to the endogenous diffusion-based feedback circuit and thus slows down competition between growing clusters. This slow feedback mechanism was able to support polarization, but resulted in the formation of multiple buds[148]. Alternatively, Bendezu et al. showed that a Cdc42 mutant that is insensitive to RhoGDI- and endocytosis-dependent plasma membrane removal has reduced mobility but can support cell polarization[149]. Nonetheless, yeast cells expressing this mutant frequently formed multiple buds in a randomized pattern.

Whereas these experiments used artificial mechanisms to demonstrate that competition for polarity factors ensures singularity in bud formation, various mechanisms regulate this competition under endogenous conditions. Cdc42 mobility is a crucial factor in this as already indicated by the finding of Bendezu et al. that a mutant of Cdc42 with decreased mobility violates singularity in

budding[149]. Decreasing Cdc42 mobility by deletion of RhoGDI slows competition between co-existing polarity clusters and results in the formation of multiple buds in a fraction of cells[142,146]. In addition, Cdc42 mobility is regulated by interaction with membrane lipids and by endocytosis[150-152]. Although important for Cdc42 cluster establishment, it remains unclear whether these mechanisms governing Cdc42 mobility contribute to singularity enforcement[153].
Taken together, these findings support the idea that singularity in yeast cell budding is ensured by a fast competition for a limited pool of polarity factors between nascent clusters.

A similar competition may ensure singularity in root hair formation of *Arabidopsis* trichoblast cells[154]. Evidence for this is the finding that mutations in SUPERCENTIPEDE1 (SCN1), which encodes a RhoGDI that controls the mobility of Rop GTPases, result in trichoblast cells with multiple root hairs[155]. Furthermore, competition between two clusters for available Cdc42 and its activator GEF1 facilitate bipolar growth in fission yeast and controls cell morphology[156,157].

A mammalian example where competition between polarity factors ensures singularity is the specification of a single axon out of multiple dendrites during neuronal polarization[158]. In this process, the small GTPase HRas has a crucial function as illustrated by the finding that expression of constitutively activated HRas(Q61L) results in neurons with multiple axons[122]. A positive feedback mechanism which involves PI3K and vesicular transport drives confinement of HRas activity to a single neurite and thereby specifies the nascent axonal growth cone[122]. Therefore, singularity in axon formation is considered to originate from a winner-takes-all competition for HRas between neurites.

Mechanical control of singularity
Next to establishing a competition for scarce polarity factors, singularity in polarization can be achieved via long range inhibition by means of mechanical regulation[129,159,160]. This means of singularity enforcement has been primarily studied in the context of unidirectional cell migration, where a dominant migratory front suppresses the formation of additional protrusions. For instance in migrating neutrophils, where membrane tension functions as a long range inhibitory signal to prevent secondary pseudopod formation[144]. Similarly, membrane tension prevents the formation of multiple fronts during unidirectional migration of fish keratocytes[161].

A seminal question that arises from this is how membrane tension is able to safeguard singularity in polarization during cell migration. Two general mechanisms have been proposed: firstly, increases in membrane tension provide a direct physical barrier to the actin polymerization required for the formation

of secondary protrusions[161,162]. Indeed loss of membrane tension, induced by vesicles fusion, results in the formation of multiple protrusive fronts in migrating keratocytes and causes cell splitting[145]. Secondly, increased membrane tension can trigger negative feedback signaling that inhibits actin polymerization[163]. During neutrophil migration for instance, this mechanochemical signaling route involves tension dependent activation of PLD2 and mTORC2 which subsequently inhibits actin polymerization by inhibiting the WAVE2 complex[163]. At least for polarizing neutrophils, both mechanisms are required to ensure the formation of a single leading edge and consequently for efficient chemotaxis.

Another example of how singularity can be enforced by mechanical cues is the establishment of a polar tube outgrowth during *Schizosaccharomyces pombe* spore germination. Here, the physical constraint imposed by the rigid outer spore wall inhibits Cdc42 clustering, thereby preventing cell polarization[125]. At the first crack of the outer spore wall during hatching, this constraint is relieved and a polar cap can stabilize. The release from this physical constraint therefore ensures that polar growth initiates at the site of outgrowth where mechanical inhibition of cell polarization is lost.

Singularity in apical domain specification during epithelial cell polarization

Apico-basal polarization in epithelial cells almost universally results in the formation of a single apical domain. A notable exception are hepatocytes that typically polarize with multiple, smaller apical domains that form the bile canaliculi. It is generally considered that cell-cell contacts are instructive in apical domain specification and thereby safeguard singularity in polarization[1,2,164,165]. However, this is challenged by the finding that various epithelial cell lines can fully polarize *in vitro* in the absence of cell-cell contacts, either by forced activation of polarity signaling or by applying physiological stimuli[166,167]. Strikingly, these single cell model systems for epithelial cell polarization rarely form multiple apical domains, raising the question how epithelial cells ensure singularity in apical domain specification.

Box 2: Model systems for studying cell polarization ***in vitro*****.**

A variety of cell-based *in vitro* model systems have been developed to understand the molecular mechanisms of cell polarization. Some cell lines are able to polarize in 2D cultures when cultured to confluency. Among these cell lines, the CaCo2 colon carcinoma cell line and its derivatives and the canine MDCK cell line have been widely used to study epithelial cell polarization. More exotic cell lines exist that are used to study epithelial cell polarization of specific organs, for example WIF/B9 cells, a rat hepatoma/human fibroblast hybrid cell line used to study hepatocyte polarization[168].

These model systems have provided many insights in the molecular mechanisms of amongst others, epithelial barrier function, microvilli formation and junction assembly. However, because these cells require prolonged culture at confluency to establish full cell polarization, loss of any protein that is required for monolayer establishment will ultimately result in an apparent loss of cell polarization. As a consequence, various proteins were claimed to be required for cell polarization based on studies in CaCo2 cells, but have less severe polarity phenotypes in other model systems[169,170].

Alternatively, when CaCo2 or MDCK cells are cultured in matrigel, a preparation of tumor-derived extracellular matrix components, they self-organize into cyst cultures that are able to form and maintain a central lumen[25,79]. These cyst cultures are considered more biologically relevant for studying cell polarization in particular with respect to spindle orientation. The formation of a central lumen in MDCK and CaCo2 cyst cultures occurs via a hollowing mechanism, during which neighboring cells establish a small lumen at their junctions which is subsequently expanded by pumping in fluid via vacuolar exocytosis[79,171]. Although this mechanism of lumen formation has been studied in great detail *in vitro*, its biological relevance is debated because there is no evidence that hollowing contributes to lumen formation *in vivo*[79].

Similar to CaCo2 or MDCK cysts, epithelial breast (cancer) cell lines assemble into organized cyst cultures when grown in matrigel[172]. These 3D breast acini have been used to study breast cancer progression and have contributed greatly to an understanding of how the extracellular matrix affects cell behavior[173,174]. One seminal difference with other cyst cultures is that lumen formation in breast acini is driven by apoptosis of cells in the cyst center. This process, known as cavitation, reflects breast lumen formation *in vivo* and is likely driven by cell detachment from the basement membrane and consequent anoikis[175].

A relatively new model system for cell polarization is the Ls174T:W4 cell line[166]. This engineered cell line is based the Ls174T colon carcinoma cell line which is poorly polarized under normal culture conditions. However, forced

activation of Liver Kinase B1 (LKB1) in these cells is sufficient for complete polarization. To this end, Ls174T cells were transduced to stably overexpress LKB1 and to inducibly express its co-activator STRADα. Upon doxycycline stimulation, STRADα forms a complex with LKB1 and the adaptor protein Mo25 which results in cytosolic translocation of this active signaling complex. Although subsequent signaling by LKB1 remains enigmatic, the end result of this forced LKB1 activation is a complete and rapid (±12h) cell polarization that includes the formation of the iconic apical microvilli that constitute the enterocytic brush border[166].

A striking feature of Ls174T:W4 cells is that their induced polarization is independent of cell-cell junctions. This is in sharp contrast with other 2D model systems like MDCK and CaCo2 cells that require junction formation to initiate cell polarization. This makes Ls174T:W4 cell polarization more robust because unlike MDCK and CaCo2 polarization it is not affected by loss of proteins that compromise monolayer integrity.

Polarized Ls174T:W4 cells have the additional curious features that they almost always form a single apical membrane with relatively uniform size (covering roughly 20% of the plasma membrane). Apical cell-cell junctions are generally considered to safeguard singularity in apical membrane formation and control apical membrane size by functioning as a physical barrier between apical and basolateral membranes. The notion that singularity is not violated and that apical membrane size is uniform in polarized Ls174T:W4 cells suggests that mechanisms exist that control these features in a junction-independent manner.

Therefore, studying polarization of Ls174T:W4 cells may allow deconvolution of cell-intrinsic and junction-derived cell-extrinsic polarity signaling routes. However, one needs to be aware that signaling pathways in Ls174T:W4 cells ignore junctional input which may affect signaling in the context of an epithelial monolayer.

Outlook

In this thesis novel signaling pathways are revealed that contribute to symmetry breaking during enterocyte polarization. The prime model system for studying these pathways are Ls174T:W4 cells, which break cellular symmetry upon forced polarization. The central research question underlying this work is: how are intracellular signaling pathways organized to enable symmetry breaking?

In chapter two it is demonstrated that singularity in apical domain specification during epithelial cell polarization is actively enforced and that this requires Cdc42 signaling. For this Cdc42 mobility at the apical domain is regulated by the disease-associated flippase ATP8B1. Loss of this regulation results in the formation of multiple apical domains and affects apical membrane size in Ls174T:W4 cells. In a 3D context, loss of ATP8B1 affects lumen architecture indicative of an important function for singularity enforcement in tissue morphogenesis.

In chapter three the regulation of Cdc42 mobility during cell polarization is further revealed. Upon activation by the Cdc42GEF Tuba, Cdc42 mobility is drastically reduced to ensure localized signaling. The molecular origin of this immobilization is identified and the importance of this regulation is demonstrated.

In chapter four the role of the tumor suppressor PTEN in apical domain specification is assessed. It is revealed that PTEN is required to restrict apical domain formation and that for this PTEN requires binding to PTPL1.

In chapter five signaling by the Rap2 small GTPases is introduced. An overview is provided on the biochemical mechanisms of Rap2 signaling and the biological functions in which Rap2 signaling is implicated are discussed.

In chapter six the mechanisms of isoform specific Rap2 signaling during brush border formation are elucidated. Rap2A is the sole isoform contributing to enterocytic brush border formation despite expression of the highly similar Rap2B and Rap2C isoforms. A combination of specific localization and selective activation explains how highly similar GTPases can signal independently.

In the summarizing discussion the prime findings are recapitulated and their implications are further discussed. Also, the connectivity of the newly identified signaling pathways is discussed.

References

1 Martin-Belmonte, F. & Perez-Moreno, M. Epithelial cell polarity, stem cells and cancer. Nature reviews. Cancer 12, 23-38, doi:10.1038/nrc3169 (2012).
2 Nelson, W. J. Remodeling epithelial cell organization: transitions between front-rear and apical-basal polarity. Cold Spring Harbor perspectives in biology 1, a000513, doi:10.1101/cshperspect.a000513 (2009).
3 Halaoui, R. & McCaffrey, L. Rewiring cell polarity signaling in cancer. Oncogene 34, 939-950, doi:10.1038/onc.2014.59 (2015).
4 Rodriguez-Boulan, E. & Macara, I. G. Organization and execution of the epithelial polarity programme. Nature reviews. Molecular cell biology 15, 225-242, doi:10.1038/nrm3775 (2014).
5 Iden, S. & Collard, J. G. Crosstalk between small GTPases and polarity proteins in cell polarization. Nature reviews. Molecular cell biology 9, 846-859, doi:10.1038/nrm2521 (2008).
6 Citalán-Madrid, A., García-Ponce, A., Vargas-Robles, H., Betanzos, A. & Schnoor, M. Small GTPases of the Ras superfamily regulate intestinal epithelial homeostasis and barrier function via common and unique mechanisms. Tissue Barriers 2, e26938, doi:10.4161/tisb.26938 (2013).
7 Colicelli, J. Human RAS superfamily proteins and related GTPases. Science's STKE : signal transduction knowledge environment 2004, Re13, doi:10.1126/stke.2502004re13 (2004).
8 Goody, R. S. et al. Studies on the structure and mechanism of H-ras p21. Philos Trans R Soc Lond B Biol Sci 336, 3-10; discussion 10-11, doi:10.1098/rstb.1992.0037 (1992).
9 Stouten, P. F., Sander, C., Wittinghofer, A. & Valencia, A. How does the switch II region of G-domains work? FEBS letters 320, 1-6 (1993).
10 Bos, J. L., Rehmann, H. & Wittinghofer, A. GEFs and GAPs: critical elements in the control of small G proteins. Cell 129, 865-877, doi:10.1016/j.cell.2007.05.018 (2007).
11 Ahearn, I. M., Haigis, K., Bar-Sagi, D. & Philips, M. R. Regulating the regulator: post-translational modification of RAS. Nature reviews. Molecular cell biology 13, 39-51, doi:10.1038/nrm3255 (2012).
12 Ghomashchi, F., Zhang, X., Liu, L. & Gelb, M. H. Binding of prenylated and polybasic peptides to membranes: affinities and intervesicle exchange. Biochemistry 34, 11910-11918 (1995).
13 Hancock, J. F., Paterson, H. & Marshall, C. J. A polybasic domain or palmitoylation is required in addition to the CAAX motif to localize p21ras to the plasma membrane. Cell 63, 133-139 (1990)
14 Laude, A. J. & Prior, I. A. Palmitoylation and localisation of RAS isoforms are modulated by the hypervariable linker domain. Journal of cell science 121, 421-427, doi:10.1242/jcs.020107 (2008).
15 Leonard, D. et al. The identification and characterization of a GDP-dissociation inhibitor (GDI) for the CDC42Hs protein. The Journal of biological chemistry 267, 22860-22868 (1992).
16 Forget, M. A., Desrosiers, R. R., Gingras, D. & Beliveau, R. Phosphorylation states of Cdc42 and RhoA regulate their interactions with Rho GDP dissociation inhibitor and their extraction from biological membranes. The Biochemical journal 361, 243-254 (2002).
17 Garcia-Mata, R., Boulter, E. & Burridge, K. The 'invisible hand': regulation of RHO GTPases by RHOGDIs. Nature reviews. Molecular cell biology 12, 493-504, doi:10.1038/nrm3153 (2011).
18 Chandra, A. et al. The GDI-like solubilizing factor PDEdelta sustains the spatial organization and signalling of Ras family proteins. Nature cell biology, doi:10.1038/ncb2394 (2011).
19 Hall, A. Rho family GTPases. Biochemical Society transactions 40, 1378-1382, doi:10.1042/BST20120103 (2012).
20 O'Brien, L. E. et al. Rac1 orientates epithelial apical polarity through effects on basolateral laminin assembly. Nature cell biology 3, 831-838, doi:10.1038/ncb0901-831 (2001).
21 Yu, W. et al. Beta1-integrin orients epithelial polarity via Rac1 and laminin. Molecular biology of the cell 16, 433-445, doi:10.1091/mbc.E04-05-0435 (2005).
22 Overeem, A. W., Bryant, D. M. & van, I. S. C. Mechanisms of apical-basal axis orientation and epithelial lumen positioning. Trends in cell biology 25, 476-485, doi:10.1016/j.tcb.2015.04.002 (2015).
23 Andrew, D. J. & Ewald, A. J. Morphogenesis of epithelial tubes: Insights into tube formation, elongation, and elaboration. Dev Biol 341, 34-55, doi:10.1016/j.ydbio.2009.09.024 (2010).
24 Roper, K. Integration of cell-cell adhesion and contractile actomyosin activity during morphogenesis. Curr Top Dev Biol 112, 103-127, doi:10.1016/bs.ctdb.2014.11.017 (2015).
25 Jaffe, A. B., Kaji, N., Durgan, J. & Hall, A. Cdc42 controls spindle orientation to position the

apical surface during epithelial morphogenesis. The Journal of cell biology 183, 625-633, doi:10.1083/jcb.200807121 (2008).
26 Rojas, R., Ruiz, W. G., Leung, S. M., Jou, T. S. & Apodaca, G. Cdc42-dependent modulation of tight junctions and membrane protein traffic in polarized Madin-Darby canine kidney cells. Molecular biology of the cell 12, 2257-2274 (2001).
27 Ueyama, T. et al. Maintenance of stereocilia and apical junctional complexes by Cdc42 in cochlear hair cells. Journal of cell science 127, 2040-2052, doi:10.1242/jcs.143602 (2014).
28 Etienne-Manneville, S. Cdc42--the centre of polarity. Journal of cell science 117, 1291-1300, doi:10.1242/jcs.01115 (2004).
29 Yang, H. W., Collins, S. R. & Meyer, T. Locally excitable Cdc42 signals steer cells during chemotaxis. Nature cell biology 18, 191-201, doi:10.1038/ncb3292 (2016).
30 O'Neill, P. R., Kalyanaraman, V. & Gautam, N. Subcellular optogenetic activation of Cdc42 controls local and distal signaling to drive immune cell migration. Molecular biology of the cell 27, 1442-1450, doi:10.1091/mbc.E15-12-0832 (2016).
31 Bryant, D. M. et al. A molecular network for de novo generation of the apical surface and lumen. Nature cell biology 12, 1035-1045, doi:10.1038/ncb2106 (2010).
32 Zihni, C. et al. Dbl3 drives Cdc42 signaling at the apical margin to regulate junction position and apical differentiation. The Journal of cell biology 204, 111-127, doi:10.1083/jcb.201304064 (2014).
33 Raaijmakers, J. H. & Bos, J. L. Specificity in Ras and Rap signaling. The Journal of biological chemistry 284, 10995-10999, doi:10.1074/jbc.R800061200 (2009).
34 Goldstein, B. & Macara, I. G. The PAR proteins: fundamental players in animal cell polarization. Developmental cell 13, 609-622, doi:10.1016/j.devcel.2007.10.007 (2007).
35 Hurov, J. B., Watkins, J. L. & Piwnica-Worms, H. Atypical PKC phosphorylates PAR-1 kinases to regulate localization and activity. Current biology : CB 14, 736-741, doi:10.1016/j.cub.2004.04.007 (2004).
36 Suzuki, A. et al. aPKC acts upstream of PAR-1b in both the establishment and maintenance of mammalian epithelial polarity. Current biology : CB 14, 1425-1435, doi:10.1016/j.cub.2004.08.021 (2004).
37 Benton, R. & St Johnston, D. Drosophila PAR-1 and 14-3-3 inhibit Bazooka/PAR-3 to establish complementary cortical domains in polarized cells. Cell 115, 691-704 (2003).
38 Martin-Belmonte, F. et al. PTEN-mediated apical segregation of phosphoinositides controls epithelial morphogenesis through Cdc42. Cell 128, 383-397, doi:10.1016/j.cell.2006.11.051 (2007).
39 Li, Z. et al. Regulation of PTEN by Rho small GTPases. Nature cell biology 7, 399-404, doi:10.1038/ncb1236 (2005).
40 Nakamura, N. et al. Phosphorylation of ERM proteins at filopodia induced by Cdc42. Genes to cells : devoted to molecular & cellular mechanisms 5, 571-581 (2000).
41 Ren, L. et al. The actin-cytoskeleton linker protein ezrin is regulated during osteosarcoma metastasis by PKC. Oncogene 28, 792-802, doi:10.1038/onc.2008.437 (2009).
42 Wu, C. F. & Lew, D. J. Beyond symmetry-breaking: competition and negative feedback in GTPase regulation. Trends in cell biology 23, 476-483, doi:10.1016/j.tcb.2013.05.003 (2013).
43 Goryachev, A. B. & Pokhilko, A. V. Dynamics of Cdc42 network embodies a Turing-type mechanism of yeast cell polarity. FEBS letters 582, 1437-1443, doi:10.1016/j.febslet.2008.03.029 (2008).
44 Rodriguez-Boulan, E., Kreitzer, G. & Musch, A. Organization of vesicular trafficking in epithelia. Nature reviews. Molecular cell biology 6, 233-247, doi:10.1038/nrm1593 (2005).
45 Apodaca, G., Gallo, L. I. & Bryant, D. M. Role of membrane traffic in the generation of epithelial cell asymmetry. Nature cell biology 14, 1235-1243, doi:10.1038/ncb2635 (2012).
46 Dhekne, H. S. et al. Myosin Vb and rab11a regulate ezrin phosphorylation in enterocytes. Journal of cell science, doi:10.1242/jcs.137273 (2014).
47 Golachowska, M. R., Hoekstra, D. & van, I. S. C. Recycling endosomes in apical plasma membrane domain formation and epithelial cell polarity. Trends in cell biology 20, 618-626, doi:10.1016/j.tcb.2010.08.004 (2010).
48 Harris, K. P. & Tepass, U. Cdc42 and Par proteins stabilize dynamic adherens junctions in the Drosophila neuroectoderm through regulation of apical endocytosis. The Journal of cell biology 183, 1129-1143, doi:10.1083/jcb.200807020 (2008).

49 Muller, T. et al. MYO5B mutations cause microvillus inclusion disease and disrupt epithelial cell polarity. Nature genetics 40, 1163-1165, doi:10.1038/ng.225 (2008).
50 Melendez, J. et al. Cdc42 Coordinates Proliferation, Polarity, Migration, and Differentiation of Small Intestinal Epithelial Cells in Mice. Gastroenterology, doi:10.1053/j.gastro.2013.06.021 (2013).
51 Kovacs, E. M., Verma, S., Thomas, S. G. & Yap, A. S. Tuba and N-WASP function cooperatively to position the central lumen during epithelial cyst morphogenesis. Cell Adhesion & Migration 5, 344-350, doi:10.4161/cam.5.4.16717 (2014).
52 Mohammadi, S. & Isberg, R. R. Cdc42 interacts with the exocyst complex to promote phagocytosis. The Journal of cell biology 200, 81-93, doi:10.1083/jcb.201204090 (2013).
53 Zuo, X., Fogelgren, B. & Lipschutz, J. H. The small GTPase Cdc42 is necessary for primary ciliogenesis in renal tubular epithelial cells. The Journal of biological chemistry 286, 22469-22477, doi:10.1074/jbc.M111.238469 (2011).
54 Choi, S. Y. et al. Cdc42 deficiency causes ciliary abnormalities and cystic kidneys. J Am Soc Nephrol 24, 1435-1450, doi:10.1681/ASN.2012121236 (2013).
55 Elias, B. C. et al. Cdc42 regulates epithelial cell polarity and cytoskeletal function in kidney tubule development. Journal of cell science, doi:10.1242/jcs.164509 (2015).
56 Harris, K. P. & Tepass, U. Cdc42 and vesicle trafficking in polarized cells. Traffic 11, 1272-1279, doi:10.1111/j.1600-0854.2010.01102.x (2010).
57 Schuh, M. An actin-dependent mechanism for long-range vesicle transport. Nature cell biology 13, 1431-1436, doi:10.1038/ncb2353 (2011).
58 Mangan, A. J. et al. Cingulin and actin mediate midbody-dependent apical lumen formation during polarization of epithelial cells. Nature communications 7, 12426, doi:10.1038/ncomms12426 (2016).
59 Zihni, C., Mills, C., Matter, K. & Balda, M. S. Tight junctions: from simple barriers to multifunctional molecular gates. Nature reviews. Molecular cell biology 17, 564-580, doi:10.1038/nrm.2016.80 (2016).
60 Citi, S., Guerrera, D., Spadaro, D. & Shah, J. Epithelial junctions and Rho family GTPases: the zonular signalosome. Small GTPases 5, 1-15, doi:10.4161/21541248.2014.973760 (2014).
61 Otani, T., Ichii, T., Aono, S. & Takeichi, M. Cdc42 GEF Tuba regulates the junctional configuration of simple epithelial cells. The Journal of cell biology 175, 135-146, doi:10.1083/jcb.200605012 (2006).
62 Oda, Y., Otani, T., Ikenouchi, J. & Furuse, M. Tricellulin regulates junctional tension of epithelial cells at tricellular contacts through Cdc42. Journal of cell science 127, 4201-4212, doi:10.1242/jcs.150607 (2014).
63 Elbediwy, A. et al. Epithelial junction formation requires confinement of Cdc42 activity by a novel SH3BP1 complex. The Journal of cell biology 198, 677-693, doi:10.1083/jcb.201202094 (2012).
64 Wells, C. D. et al. A Rich1/Amot complex regulates the Cdc42 GTPase and apical-polarity proteins in epithelial cells. Cell 125, 535-548, doi:10.1016/j.cell.2006.02.045 (2006).
65 Hayase, J. et al. The WD40 protein Morg1 facilitates Par6-aPKC binding to Crb3 for apical identity in epithelial cells. The Journal of cell biology 200, 635-650, doi:10.1083/jcb.201208150 (2013).
66 Fogg, V. C., Liu, C. J. & Margolis, B. Multiple regions of Crumbs3 are required for tight junction formation in MCF10A cells. Journal of cell science 118, 2859-2869, doi:10.1242/jcs.02412 (2005).
67 Shen, Y., Hirsch, D. S., Sasiela, C. A. & Wu, W. J. Cdc42 regulates E-cadherin ubiquitination and degradation through an epidermal growth factor receptor to Src-mediated pathway. The Journal of biological chemistry 283, 5127-5137, doi:10.1074/jbc.M703300200 (2008).
68 Wu, X. et al. Cdc42 is crucial for the establishment of epithelial polarity during early mammalian development. Developmental dynamics : an official publication of the American Association of Anatomists 236, 2767-2778, doi:10.1002/dvdy.21309 (2007).
69 Georgiou, M., Marinari, E., Burden, J. & Baum, B. Cdc42, Par6, and aPKC regulate Arp2/3-mediated endocytosis to control local adherens junction stability. Current biology : CB 18, 1631-1638, doi:10.1016/j.cub.2008.09.029 (2008).
70 Leibfried, A., Fricke, R., Morgan, M. J., Bogdan, S. & Bellaiche, Y. Drosophila Cip4

and WASp define a branch of the Cdc42-Par6-aPKC pathway regulating E-cadherin endocytosis. Current biology : CB 18, 1639-1648, doi:10.1016/j.cub.2008.09.063 (2008).
71 Selamat, W., Tay, P. L., Baskaran, Y. & Manser, E. The Cdc42 Effector Kinase PAK4 Localizes to Cell-Cell Junctions and Contributes to Establishing Cell Polarity. PloS one 10, e0129634, doi:10.1371/journal.pone.0129634 (2015).
72 Huo, L. et al. Cdc42-dependent formation of the ZO-1/MRCKbeta complex at the leading edge controls cell migration. The EMBO journal 30, 665-678, doi:10.1038/emboj.2010.353 (2011).
73 Blasky, A. J., Mangan, A. & Prekeris, R. Polarized Protein Transport and Lumen Formation During Epithelial Tissue Morphogenesis. Annu Rev Cell Dev Biol 31, 575-591, doi:10.1146/annurev-cellbio-100814-125323 (2015).
74 Pruyne, D. W., Schott, D. H. & Bretscher, A. Tropomyosin-containing actin cables direct the Myo2p-dependent polarized delivery of secretory vesicles in budding yeast. The Journal of cell biology 143, 1931-1945 (1998).
75 Slaughter, B. D., Smith, S. E. & Li, R. Symmetry breaking in the life cycle of the budding yeast. Cold Spring Harbor perspectives in biology 1, a003384, doi:10.1101/cshperspect.a003384 (2009).
76 Irazoqui, J. E., Gladfelter, A. S. & Lew, D. J. Scaffold-mediated symmetry breaking by Cdc42p. Nature cell biology 5, 1062-1070, doi:10.1038/ncb1068 (2003).
77 Kovacs, E. M. et al. N-WASP regulates the epithelial junctional actin cytoskeleton through a non-canonical post-nucleation pathway. Nature cell biology 13, 934-943, doi:10.1038/ncb2290 (2011).
78 Knoblich, J. A. Asymmetric cell division: recent developments and their implications for tumour biology. Nature reviews. Molecular cell biology 11, 849-860, doi:10.1038/nrm3010 (2010).
79 Bryant, D. M. & Mostov, K. E. From cells to organs: building polarized tissue. Nature reviews. Molecular cell biology 9, 887-901, doi:10.1038/nrm2523 (2008).
80 Goulas, S., Conder, R. & Knoblich, J. A. The par complex and integrins direct asymmetric cell division in adult intestinal stem cells. Cell stem cell 11, 529-540, doi:10.1016/j.stem.2012.06.017 (2012).
81 Siller, K. H. & Doe, C. Q. Spindle orientation during asymmetric cell division. Nature cell biology 11, 365-374, doi:10.1038/ncb0409-365 (2009).
82 Campinho, P. et al. Tension-oriented cell divisions limit anisotropic tissue tension in epithelial spreading during zebrafish epiboly. Nature cell biology 15, 1405-1414, doi:10.1038/ncb2869 (2013).
83 Leung, C. T. & Brugge, J. S. Outgrowth of single oncogene-expressing cells from suppressive epithelial environments. Nature, doi:10.1038/nature10826 (2012).
84 Druso, J. E. et al. An Essential Role for Cdc42 in the Functioning of the Adult Mammary Gland. The Journal of biological chemistry 291, 8886-8895, doi:10.1074/jbc.M115.694349 (2016).
85 Kieserman, E. K. & Wallingford, J. B. In vivo imaging reveals a role for Cdc42 in spindle positioning and planar orientation of cell divisions during vertebrate neural tube closure. Journal of cell science 122, 2481-2490, doi:10.1242/jcs.042135 (2009).
86 Anttonen, T. et al. Cdc42-dependent structural development of auditory supporting cells is required for wound healing at adulthood. Sci Rep 2, 978, doi:10.1038/srep00978 (2012).
87 Hao, Y. et al. Par3 controls epithelial spindle orientation by aPKC-mediated phosphorylation of apical Pins. Current biology : CB 20, 1809-1818, doi:10.1016/j.cub.2010.09.032 (2010).
88 Durgan, J., Kaji, N., Jin, D. & Hall, A. Par6B and atypical PKC regulate mitotic spindle orientation during epithelial morphogenesis. The Journal of biological chemistry 286, 12461-12474, doi:10.1074/jbc.M110.174235 (2011).
89 Qin, Y., Meisen, W. H., Hao, Y. & Macara, I. G. Tuba, a Cdc42 GEF, is required for polarized spindle orientation during epithelial cyst formation. The Journal of cell biology 189, 661-669, doi:10.1083/jcb.201002097 (2010).
90 Galli, M. et al. aPKC phosphorylates NuMA-related LIN-5 to position the mitotic spindle during asymmetric division. Nature cell biology 13, 1132-1138, doi:10.1038/ncb2315 (2011).
91 Zheng, Z. et al. LGN regulates mitotic spindle orientation during epithelial morphogenesis. The Journal of cell biology 189, 275-288, doi:10.1083/jcb.200910021 (2010).
92 Rodriguez-Fraticelli, A. E. et al. The Cdc42 GEF Intersectin 2 controls mitotic spindle orientation to form the lumen during epithelial morphogenesis. The Journal of cell biology 189, 725-738,

doi:10.1083/jcb.201002047 (2010).
93 Mitsushima, M., Toyoshima, F. & Nishida, E. Dual role of Cdc42 in spindle orientation control of adherent cells. Molecular and cellular biology 29, 2816-2827, doi:10.1128/MCB.01713-08 (2009)
94 Yasuda, S. et al. Cdc42 and mDia3 regulate microtubule attachment to kinetochores. Nature 428, 767-771, doi:10.1038/nature02452 (2004).
95 Oceguera-Yanez, F. et al. Ect2 and MgcRacGAP regulate the activation and function of Cdc42 in mitosis. The Journal of cell biology 168, 221-232, doi:10.1083/jcb.200408085 (2005).
96 Bornens, M. Organelle positioning and cell polarity. Nature reviews. Molecular cell biology 9, 874-886, doi:10.1038/nrm2524 (2008).
97 Gomes, E.R., Jani, S. & Gundersen, G.G. Nuclear movement regulated by Cdc42, MRCK, myosin, and actin flow establishes MTOC polarization in migrating cells. Cell 121, 451-463, doi:10.1016/j.cell.2005.02.022 (2005).
98 Osmani, N., Vitale, N., Borg, J. P. & Etienne-Manneville, S. Scrib controls Cdc42 localization and activity to promote cell polarization during astrocyte migration. Current biology : CB 16, 2395-2405, doi:10.1016/j.cub.2006.10.026 (2006).
99 Etienne-Manneville, S. Microtubules in cell migration. Annu Rev Cell Dev Biol 29, 471-499, doi:10.1146/annurev-cellbio-101011-155711 (2013).
100 Palazzo, A. F. et al. Cdc42, dynein, and dynactin regulate MTOC reorientation independent of Rho-regulated microtubule stabilization. Current biology : CB 11, 1536-1541 (2001).
101 Etienne-Manneville, S. & Hall, A. Cdc42 regulates GSK-3beta and adenomatous polyposis coli to control cell polarity. Nature 421, 753-756, doi:10.1038/nature01423 (2003).
102 Manneville, J. B., Jehanno, M. & Etienne-Manneville, S. Dlg1 binds GKAP to control dynein association with microtubules, centrosome positioning, and cell polarity. The Journal of cell biology 191, 585-598, doi:10.1083/jcb.201002151 (2010).
103 Gundersen, G. G. & Worman, H. J. Nuclear positioning. Cell 152, 1376-1389, doi:10.1016/j.cell.2013.02.031 (2013).
104 Hartsock, A. & Nelson, W. J. Adherens and tight junctions: structure, function and connections to the actin cytoskeleton. Biochimica et biophysica acta 1778, 660-669, doi:10.1016/j.bbamem.2007.07.012 (2008).
105 Yin, H., Pruyne, D., Huffaker, T. C. & Bretscher, A. Myosin V orientates the mitotic spindle in yeast. Nature 406, 1013-1015, doi:10.1038/35023024 (2000).
106 Wang, T., Yanger, K., Stanger, B. Z., Cassio, D. & Bi, E. Cytokinesis defines a spatial landmark for hepatocyte polarization and apical lumen formation. Journal of cell science 127, 2483-2492, doi:10.1242/jcs.139923 (2014).
107 Gloerich, M. et al. Rap2A links intestinal cell polarity to brush border formation. Nature cell biology 14, 793-801, doi:10.1038/ncb2537 (2012).
108 Crawley, S. W., Mooseker, M. S. & Tyska, M. J. Shaping the intestinal brush border. The Journal of cell biology 207, 441-451, doi:10.1083/jcb.201407015 (2014).
109 Viswanatha, R., Ohouo, P. Y., Smolka, M. B. & Bretscher, A. Local phosphocycling mediated by LOK/SLK restricts ezrin function to the apical aspect of epithelial cells. The Journal of cell biology 199, 969-984, doi:10.1083/jcb.201207047 (2012).
110 Osmani, N., Peglion, F., Chavrier, P. & Etienne-Manneville, S. Cdc42 localization and cell polarity depend on membrane traffic. The Journal of cell biology 191, 1261-1269, doi:10.1083/jcb.201003091 (2010).
111 Brandman, O. & Meyer, T. Feedback loops shape cellular signals in space and time. Science 322, 390-395, doi:10.1126/science.1160617 (2008).
112 Mitrophanov, A. Y. & Groisman, E. A. Positive feedback in cellular control systems. Bioessays 30, 542-555, doi:10.1002/bies.20769 (2008).
113 Klunder, B., Freisinger, T., Wedlich-Soldner, R. & Frey, E. GDI-mediated cell polarization in yeast provides precise spatial and temporal control of Cdc42 signaling. PLoS computational biology 9, e1003396, doi:10.1371/journal.pcbi.1003396 (2013).
114 Howell, A. S. et al. Negative feedback enhances robustness in the yeast polarity establishment circuit. Cell 149, 322-333, doi:10.1016/j.cell.2012.03.012 (2012).
115 Johnson, J. M., Jin, M. & Lew, D. J. Symmetry breaking and the establishment of cell polarity in budding yeast. Current opinion in genetics & development 21, 740-746, doi:10.1016/j.

gde.2011.09.007 (2011).
116 Martin, S. G. Spontaneous cell polarization: Feedback control of Cdc42 GTPase breaks cellular symmetry. Bioessays 37, 1193-1201, doi:10.1002/bies.201500077 (2015).
117 Vicente-Manzanares, M., Newell-Litwa, K., Bachir, A.I., Whitmore, L.A. & Horwitz, A.R. Myosin IIA/IIB restrict adhesive and protrusive signaling to generate front-back polarity in migrating cells. The Journal of cell biology 193, 381-396, doi:10.1083/jcb.201012159 (2011).
118 Kang, P. J., Lee, M. E. & Park, H. O. Bud3 activates Cdc42 to establish a proper growth site in budding yeast. The Journal of cell biology 206, 19-28, doi:10.1083/jcb.201402040 (2014).
119 Li, R. & Bowerman, B. Symmetry breaking in biology. Cold Spring Harbor perspectives in biology 2, a003475, doi:10.1101/cshperspect.a003475 (2010).
120 Huang, S. Where to Go: Breaking the Symmetry in Cell Motility. PLoS biology 14, e1002463, doi:10.1371/journal.pbio.1002463 (2016).
121 Munro, E. & Bowerman, B. Cellular symmetry breaking during Caenorhabditis elegans development. Cold Spring Harbor perspectives in biology 1, a003400, doi:10.1101/cshperspect.a003400 (2009).
122 Fivaz, M., Bandara, S., Inoue, T. & Meyer, T. Robust neuronal symmetry breaking by Ras-triggered local positive feedback. Current biology : CB 18, 44-50, doi:10.1016/j.cub.2007.11.051 (2008).
123 Hebert, A. M., DuBoff, B., Casaletto, J. B., Gladden, A. B. & McClatchey, A. I. Merlin/ERM proteins establish cortical asymmetry and centrosome position. Genes & development 26, 2709-2723, doi:10.1101/gad.194027.112 (2012).
124 Kozubowski, L. et al. Symmetry-breaking polarization driven by a Cdc42p GEF-PAK complex. Current biology : CB 18, 1719-1726, doi:10.1016/j.cub.2008.09.060 (2008).
125 Bonazzi, D. et al. Symmetry breaking in spore germination relies on an interplay between polar cap stability and spore wall mechanics. Developmental cell 28, 534-546, doi:10.1016/j.devcel.2014.01.023 (2014).
126 Leibfried, A., Muller, S. & Ephrussi, A. A Cdc42-regulated actin cytoskeleton mediates Drosophila oocyte polarization. Development 140, 362-371, doi:10.1242/dev.089250 (2013).
127 Altschuler, S. J., Angenent, S. B., Wang, Y. & Wu, L. F. On the spontaneous emergence of cell polarity. Nature 454, 886-889, doi:10.1038/nature07119 (2008).
128 Turing, A. M. The Chemical Basis of Morphogenesis. Philosophical Transactions of the Royal Society of London B: Biological Sciences 237, 37-72 (1952).
129 Howard, J., Grill, S. W. & Bois, J. S. Turing's next steps: the mechanochemical basis of morphogenesis. Nature reviews. Molecular cell biology 12, 392-398, doi:10.1038/nrm3120 (2011).
130 Raspopovic, J., Marcon, L., Russo, L. & Sharpe, J. Modeling digits. Digit patterning is controlled by a Bmp-Sox9-Wnt Turing network modulated by morphogen gradients. Science 345, 566-570, doi:10.1126/science.1252960 (2014).
131 Sheth, R. et al. Hox genes regulate digit patterning by controlling the wavelength of a Turing-type mechanism. Science 338, 1476-1480, doi:10.1126/science.1226804 (2012).
132 Blagodatski, A., Sergeev, A., Kryuchkov, M., Lopatina, Y. & Katanaev, V. L. Diverse set of Turing nanopatterns coat corneae across insect lineages. Proceedings of the National Academy of Sciences of the United States of America 112, 10750-10755, doi:10.1073/pnas.1505748112 (2015).
133 Watanabe, M. & Kondo, S. Is pigment patterning in fish skin determined by the Turing mechanism? Trends Genet 31, 88-96, doi:10.1016/j.tig.2014.11.005 (2015).
134 Payne, R. J. & Grierson, C. S. A theoretical model for ROP localisation by auxin in Arabidopsis root hair cells. PloS one 4, e8337, doi:10.1371/journal.pone.0008337 (2009).
135 Inagaki, N., Toriyama, M. & Sakumura, Y. Systems biology of symmetry breaking during neuronal polarity formation. Dev Neurobiol 71, 584-593, doi:10.1002/dneu.20837 (2011).
136 Meitinger, F. et al. A memory system of negative polarity cues prevents replicative aging. Cell 159, 1056-1069, doi:10.1016/j.cell.2014.10.014 (2014).
137 Park, H. O. & Bi, E. Central roles of small GTPases in the development of cell polarity in yeast and beyond. Microbiol Mol Biol Rev 71, 48-96, doi:10.1128/MMBR.00028-06 (2007).
138 Kang, P. J., Sanson, A., Lee, B. & Park, H. O. A GDP/GTP exchange factor involved in linking a spatial landmark to cell polarity. Science 292, 1376-1378, doi:10.1126/science.1060360 (2001).

139 Wedlich-Soldner, R., Altschuler, S., Wu, L. & Li, R. Spontaneous cell polarization through actomyosin-based delivery of the Cdc42 GTPase. Science 299, 1231-1235, doi:10.1126/science.1080944 (2003).
140 Rose, L. & Gonczy, P. Polarity establishment, asymmetric division and segregation of fate determinants in early C. elegans embryos. WormBook : the online review of C. elegans biology, 1-43, doi:10.1895/wormbook.1.30.2 (2014).
141 Munro, E., Nance, J. & Priess, J. R. Cortical flows powered by asymmetrical contraction transport PAR proteins to establish and maintain anterior-posterior polarity in the early C. elegans embryo. Developmental cell 7, 413-424, doi:10.1016/j.devcel.2004.08.001 (2004).
142 Freisinger, T. et al. Establishment of a robust single axis of cell polarity by coupling multiple positive feedback loops. Nature communications 4, 1807, doi:10.1038/ncomms2795 (2013).
143 Ambravaneswaran, V., Wong, I. Y., Aranyosi, A. J., Toner, M. & Irimia, D. Directional decisions during neutrophil chemotaxis inside bifurcating channels. Integrative biology : quantitative biosciences from nano to macro 2, 639-647, doi:10.1039/c0ib00011f (2010).
144 Houk, A.R. et al. Membrane Tension Maintains Cell Polarity by Confining Signals to the Leading Edge during Neutrophil Migration. Cell 148, 175-188, doi:10.1016/j.cell.2011.10.050 (2012).
145 Lieber, A. D., Yehudai-Resheff, S., Barnhart, E. L., Theriot, J. A. & Keren, K. Membrane tension in rapidly moving cells is determined by cytoskeletal forces. Current biology : CB 23, 1409-1417, doi:10.1016/j.cub.2013.05.063 (2013).
146 Wu, C. F. et al. Role of competition between polarity sites in establishing a unique front. Elife 4, doi:10.7554/eLife.11611 (2015).
147 Caviston, J. P., Tcheperegine, S. E. & Bi, E. Singularity in budding: a role for the evolutionarily conserved small GTPase Cdc42p. Proceedings of the National Academy of Sciences of the United States of America 99, 12185-12190, doi:10.1073/pnas.182370299 (2002).
148 Howell, A. S. et al. Singularity in polarization: rewiring yeast cells to make two buds. Cell 139, 731-743, doi:10.1016/j.cell.2009.10.024 (2009).
149 Bendezu, F. O. et al. Spontaneous Cdc42 Polarization Independent of GDI-Mediated Extraction and Actin-Based Trafficking. PLoS biology 13,e1002097,doi:10.1371/journal.pbio.1002097(2015)
150 Das, A. et al. Flippase-mediated phospholipid asymmetry promotes fast Cdc42 recycling in dynamic maintenance of cell polarity. Nature cell biology 14, 304-310,doi:10.1038/ncb2444(2012)
151 Slaughter, B. D. et al. Non-uniform membrane diffusion enables steady-state cell polarization via vesicular trafficking. Nature communications 4, 1380, doi:10.1038/ncomms2370 (2013).
152 Marco, E., Wedlich-Soldner, R., Li, R., Altschuler, S. J. & Wu, L. F. Endocytosis optimizes the dynamic localization of membrane proteins that regulate cortical polarity. Cell 129, 411-422, doi:10.1016/j.cell.2007.02.043 (2007).
153 Fairn, G. D., Hermansson, M., Somerharju, P. & Grinstein, S. Phosphatidylserine is polarized and required for proper Cdc42 localization and for development of cell polarity. Nature cell biology 13, 1424-1430, doi:10.1038/ncb2351 (2011).
154 Cole, R. A. & Fowler, J. E. Polarized growth: maintaining focus on the tip. Curr Opin Plant Biol 9, 579-588, doi:10.1016/j.pbi.2006.09.014 (2006).
155 Carol, R. J. et al. A RhoGDP dissociation inhibitor spatially regulates growth in root hair cells. Nature 438, 1013-1016, doi:10.1038/nature04198 (2005).
156 Das, M. et al. Oscillatory dynamics of Cdc42 GTPase in the control of polarized growth. Science 337, 239-243, doi:10.1126/science.1218377 (2012).
157 Das, M. et al. Phosphorylation-dependent inhibition of Cdc42 GEF Gef1 by 14-3-3 protein Rad24 spatially regulates Cdc42 GTPase activity and oscillatory dynamics during cell morphogenesis. Molecular biology of the cell 26, 3520-3534, doi:10.1091/mbc.E15-02-0095 (2015).
158 Caceres, A., Ye, B. & Dotti, C. G. Neuronal polarity: demarcation, growth and commitment. Current opinion in cell biology 24, 547-553, doi:10.1016/j.ceb.2012.05.011 (2012).
159 Asnacios, A. & Hamant, O. The mechanics behind cell polarity. Trends in cell biology 22, 584-591, doi:10.1016/j.tcb.2012.08.005 (2012).
160 Goehring, N. W. & Grill, S. W. Cell polarity: mechanochemical patterning. Trends in cell biology 23, 72-80, doi:10.1016/j.tcb.2012.10.009 (2013).
161 Keren, K. et al. Mechanism of shape determination in motile cells. Nature 453, 475-480, doi:10.1038/nature06952 (2008).

162 Weiner, O. D., Marganski, W. A., Wu, L. F., Altschuler, S. J. & Kirschner, M. W. An actin-based wave generator organizes cell motility. PLoS biology 5, e221, doi:10.1371/journal.pbio.0050221 (2007).
163 Diz-Munoz, A. et al. Membrane Tension Acts Through PLD2 and mTORC2 to Limit Actin Network Assembly During Neutrophil Migration. PLoS biology 14, e1002474, doi:10.1371/journal.pbio.1002474 (2016).
164 Nejsum, L. N. & Nelson, W. J. A molecular mechanism directly linking E-cadherin adhesion to initiation of epithelial cell surface polarity. The Journal of cell biology 178, 323-335, doi:10.1083/jcb.200705094 (2007).
165 Roignot, J., Peng, X. & Mostov, K. Polarity in mammalian epithelial morphogenesis. Cold Spring Harbor perspectives in biology 5, doi:10.1101/cshperspect.a013789 (2013).
166 Baas, A. F. et al. Complete polarization of single intestinal epithelial cells upon activation of LKB1 by STRAD. Cell 116, 457-466 (2004).
167 Gon, H., Fumoto, K., Ku, Y., Matsumoto, S. & Kikuchi, A. Wnt5a signaling promotes apical and basolateral polarization of single epithelial cells. Molecular biology of the cell 24, 3764-3774, doi:10.1091/mbc.E13-07-0357 (2013).
168 Cohen, D., Brennwald, P. J., Rodriguez-Boulan, E. & Musch, A. Mammalian PAR-1 determines epithelial lumen polarity by organizing the microtubule cytoskeleton. The Journal of cell biology 164, 717-727, doi:10.1083/jcb.200308104 (2004).
169 Langlois, M. J. et al. The PTEN phosphatase controls intestinal epithelial cell polarity and barrier function: role in colorectal cancer progression. PloS one 5, e15742, doi:10.1371/journal.pone.0015742 (2010).
170 Verhulst, P. M. et al. A flippase-independent function of ATP8B1, the protein affected in familial intrahepatic cholestasis type 1, is required for apical protein expression and microvillus formation in polarized epithelial cells. Hepatology (Baltimore, Md.) 51, 2049-2060, doi:10.1002/hep.23586 (2010).
171 Bryant, D. M. et al. A molecular switch for the orientation of epithelial cell polarization. Developmental cell 31, 171-187, doi:10.1016/j.devcel.2014.08.027 (2014).
172 Debnath, J. & Brugge, J. S. Modelling glandular epithelial cancers in three-dimensional cultures. Nature reviews. Cancer 5, 675-688, doi:10.1038/nrc1695 (2005).
173 Rizki, A. et al. A human breast cell model of preinvasive to invasive transition. Cancer research 68, 1378-1387, doi:10.1158/0008-5472.CAN-07-2225 (2008).
174 Petersen, O. W., Ronnov-Jessen, L., Howlett, A. R. & Bissell, M. J. Interaction with basement membrane serves to rapidly distinguish growth and differentiation pattern of normal and malignant human breast epithelial cells. Proceedings of the National Academy of Sciences of the United States of America 89, 9064-9068 (1992).
175 Mailleux, A. A., Overholtzer, M. & Brugge, J. S. Lumen formation during mammary epithelial morphogenesis: insights from in vitro and in vivo models. Cell cycle 7, 57-62, doi:10.4161/cc.7.1.5150 (2008).

II

ATP8B1-mediated spatial organization of Cdc42 signaling maintains singularity during enterocyte polarization

Lucas J.M. Bruurs, Lisa Donker, Susan Zwakenberg,
Fried J. Zwartkruis, Harry Begthel, A.S. Knisely, George Posthuma,
Stan F.J. van de Graaf, Coen C. Paulusma, Johannes L. Bos

Published in:
The Journal of Cell Biology.
2015 Sep 28;210(7):1055-63.

Abstract
During yeast cell polarization localization of the small GTPase Cdc42 is clustered to ensure the formation of a single bud. Here we show that the disease-associated flippase ATP8B1 enables Cdc42 clustering during enterocyte polarization. Loss of this regulation results in increased apical membrane size with scattered apical recycling endosomes and permits the formation of more than one apical domain, resembling the singularity defect observed in yeast.

Mechanistically, we show that to become apically clustered, Cdc42 requires the interaction between its polybasic region and negatively charged membrane lipids provided by ATP8B1. Disturbing this interaction, either by ATP8B1 depletion or by introduction of a Cdc42 mutant defective in lipid binding, increases Cdc42 mobility and results in apical membrane enlargement. Re-establishing Cdc42 clustering, by tethering it to the apical membrane or lowering its diffusion, restores normal apical membrane size in ATP8B1-depleted cells.

We therefore conclude that singularity regulation by Cdc42 is conserved between yeast and man and that this regulation is required to maintain healthy tissue architecture.

Introduction

The generation of polarized epithelial cells is paramount to proper tissue development and homeostasis. Seminal in the establishment and maintenance of stable polarity is tight spatial regulation of the small GTPase Cdc42[1,2]. During polarity establishment in budding yeast, Cdc42 functions as a pioneer factor, since its clustered activation suffices to recruit all downstream signaling components required for bud formation[3]. To prevent ectopic bud formation, Cdc42 localization is therefore strictly governed by multiple feedback mechanisms that allow accumulation of Cdc42 at the apical membrane and ensure singularity by depleting Cdc42 elsewhere in the cell[4,5].

By remodeling the apical plasma membrane phospholipid flippase complexes can modulate Cdc42 signaling during yeast bud formation[6,7]. Nevertheless, it is unknown to what extent this mechanism contributes to polarity establishment in mammalian cells. Human phospholipid flippases of the type 4 subfamily of P-type ATPases (P4-ATPases) have been implicated in various human disorders. Most notably, mutations in the phosphatidylserine (PS) flippase ATP8B1 underlie progressive familial intrahepatic cholestasis type 1 (PFIC1), a disease hallmarked by the development of cholestasis ultimately causing liver failure. In addition, ATP8B1 mutations impose various extrahepatic symptoms including diarrhea[8]. These symptoms reflect the tissue distribution of ATP8B1, which is expressed only at the apical surfaces of polarized epithelial cells such as hepatocytes and enterocytes[9,10]. Although it is well established that mutations in ATP8B1 cause PFIC1, it is largely unknown which signaling pathways are affected by ATP8B1 loss and how this contributes to pathogenesis in PFIC1.

Results

To investigate the mechanistic consequences of ATP8B1 loss we generated small intestinal organoid cultures derived from an ATP8B1$^{G308V/G308V}$ mouse ("PFIC organoids"). The G308V mutation destabilizes the ATP8B1 protein resulting in its functional loss (Fig. 1c)[11,12].

In PFIC organoids we observed structural defects in the apical membranes of the enterocytes that form the central lumen. Whereas wild type organoids form a sphere-shaped lumen with a smooth continuous apical brush border, PFIC organoids have unstructured lumina with larger apical membranes and irregularly shaped brush borders (Fig. 1a, b). These structural abnormalities are not observed in the crypts of PFIC organoids (Fig. 1d), which is in agreement with the limitation in intestinal expression of ATP8B1 to differentiated enterocytes[10].

Apical membrane generation is critically governed by recycling endosomes that deliver signaling proteins to the nascent apical membrane[13,14]. We found that concomitant with the defects in lumen architecture in PFIC organoids, the

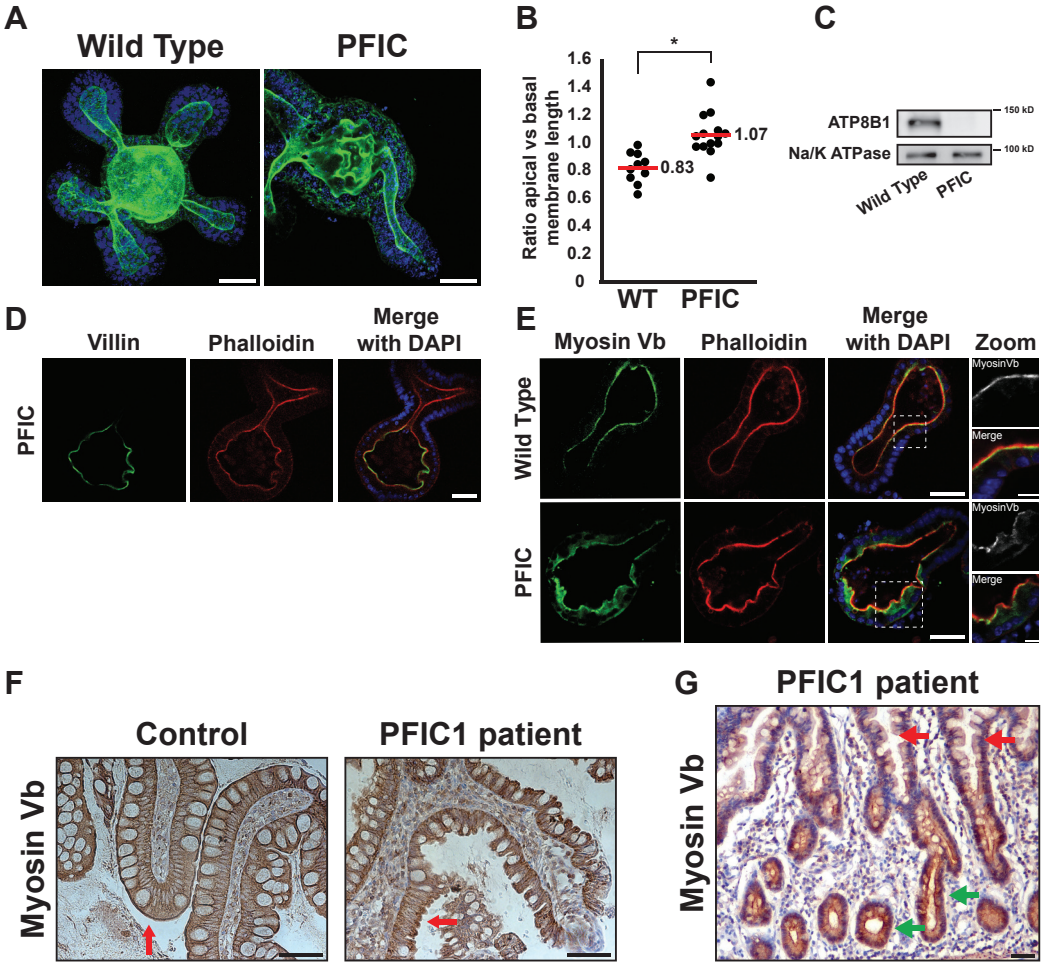

Figure 1: Pathogenic mutations in ATP8B1 cause cell-autonomous defects in intestinal lumen formation.
(**a**) Maximum intensity projections of wild type and PFIC small intestinal organoids, fixed and stained with phalloidin (green) and DAPI (blue). Bars, 35 µm (**b**) Ratio of apical vs. basal membrane length of wild type (n=11) and PFIC organoids (n=15). * $p < 0.0002$. (**c**) Western blot of lysates from wild type and PFIC organoids, probed for ATP8B1 and Na/K ATPase. (**d**) PFIC organoid staining for the enterocyte marker villin, phalloidin and DAPI. Bar, 35 µm (**e**) Wild type and PFIC organoids stained for the apical endosomal marker Myosin Vb. Bars, 35 µm; in zoom 10 µm (**f**) Control and PFIC1 patient ileum samples stained for Myosin Vb. Red arrows highlight apical Myosin Vb staining. Bars, 25 µm (**g**) Ileal sample from PFIC1 patient immunostained for Myosin Vb. Red arrows highlight villi and green arrows highlight crypts. Bar, 25 µm

global distribution of apical endosomes was diffusely scattered, as determined by Myosin Vb staining (Fig. 1e). Importantly, in PFIC organoids the apical membrane marker phosphorylated Ezrin/Radixin/Moesin (pERM) and the basolateral marker CD71 segregated normally and apical tight junction were present, as judged by ZO-1 staining, demonstrating that overall polarity is intact in PFIC organoids (Fig. S1a, b, c).

To demonstrate further that ATP8B1 loss causes diffuse localization of apical endosomes we stained biopsy specimens from healthy and PFIC1 small intestine mucosa for Myosin Vb. We found that apical accumulation of Myosin Vb is diminished and observed irregularities in apical membrane organization in PFIC1 patient enterocytes, similar to what was found in mouse PFIC organoids (Fig. 1f). Furthermore, Myosin Vb was normally enriched at the luminal membrane in the crypts of PFIC1 mucosa (Fig. 1g). Evidence that ATP8B1 functions *in vivo* to control apical membrane size and lumen formation is additionally provided by the findings that ATP8B1$^{G308V/G308V}$ mice, which do not develop cholestasis[11], do form enlarged bile canalicular lumina (Fig. S1d, e) and that PFIC1 patients have altered bile canalicular lumen morphology[15], additionally demonstrating that this effect is not limited to the intestine.

To study the molecular mechanism via which ATP8B1 deficiency affects apical membrane formation we used the Ls174T:W4 cell line as a model system for enterocyte polarization. In W4 cells, doxycycline-induced expression of STRAD drives the cytosolic activation of LKB1, which is sufficient to polarize these cells in the absence of cell-cell contacts[16]. During W4 cell polarization, an apical brush border is formed and ATP8B1 localization is restricted to the apical domain (Fig. S2a).

In W4 cells with stable knockdown of ATP8B1, doxycycline-induced polarization resulted in appearance of microvilli over a larger part of the cell than in W4 cells that expressed control shRNA (Fig. 2a, b, c). These microvilli stained positive for villin, demonstrating the formation a *bona fide* brush border, and other polarity markers segregated normally compared to control W4 cells (Fig. S2b, c, d). As in PFIC organoids, depletion of ATP8B1 from W4 cells resulted in multiple foci of Rab11-positive recycling endosomes (Fig 2d). The dispersal of recycling endosomes spanned the enlarged brush border in ATP8B1-depleted cells and thus correlated with apical membrane size.

Next to apical membrane enlargement and Rab11 endosome dispersal, knockdown of ATP8B1 in the W4 cells also caused the formation of multiple, discrete apical membrane patches in a fraction of cells, indicative of a singularity defect (Fig. 2e, f). In yeast, singularity in budding is ensured by spatial confinement of the small GTPase Cdc42 into a single cluster at the incipient bud site[3,4]. To test whether Cdc42 is also important to ensure singularity in apical membrane generation during W4 cell polarization we used CRISPR/Cas9-mediated gene disruption to generate W4 cells that have no endogenous Cdc42 (W4:NEC). These Cdc42 knockout cells retained the ability to generate an apical brush border (Fig. 3c). Nevertheless, W4:NEC cells violated singularity as demonstrated by the appearance of multiple foci of recycling endosomes and the presence of many cells that formed multiple brush borders (Fig 3a, b). This singularity defect could

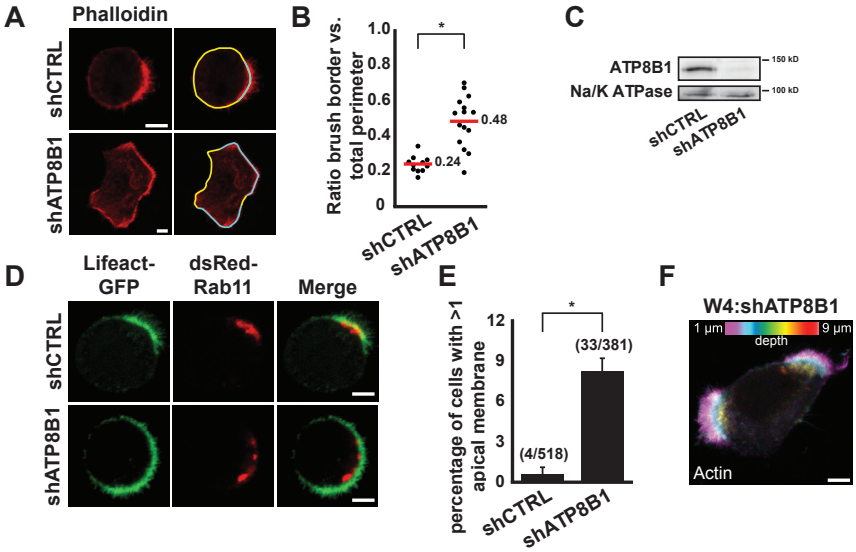

Figure 2: Loss of ATP8B1 in polarized Ls174T:W4 cells results in the formation of an enlarged apical membrane and causes loss of singularity.
(**a**) Polarized Ls174T:W4 cells infected with control short hairpin or shATP8B1 stained with phalloidin to visualize the actin cytoskeleton. (**b**) Apical membrane size quantified by determining the fraction of the plasma membrane bearing microvilli as visualized by actin staining. * $p <$ 0.00002 (**c**) Western blot of W4 cell and ATP8B1-depleted W4 cell lysates, probed for ATP8B1 and Na/K ATPase. (**d**) Localization of the apical recycling endosomal marker dsRed-Rab11 in control- and ATP8B1-depleted W4 cells. (**e**) Quantification of cells with multiple brush borders in polarized control or ATP8B1-depleted W4 cells. Numbers between parentheses indicate total number of cells with multiple apical membranes in three independent experiments. Error bars are s.e.m. * $p < 0.0003$ (**f**) Example of ATP8B1-depleted cell that has formed two discrete brush border patches. Bars, 5 µm

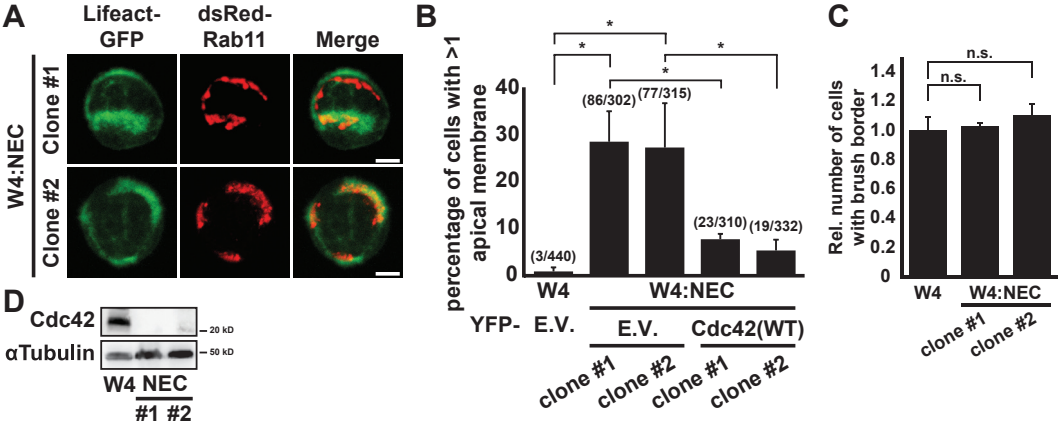

Figure 3: Cdc42 knockout cells form multiple brush borders and have dispersed recycling endosome localization
(**a**) Maximum intensity projections of polarized W4:NEC cells expressing dsRed-Rab11 and Lifeact-GFP. (**b**) Quantification of cells with multiple brush borders in polarized W4 cells or W4:NEC cells expressing YFP or YFP-Cdc42. Numbers between parentheses indicate total number of cells with multiple apical membranes during three independent experiments. Error bars are s.e.m from three experiments. * $p < 0.003$ (**c**) Western blot of W4 cell or W4:NEC cell lysates, probed for Cdc42 and alpha-tubulin. Bars, 5 µm

be rescued by re-introducing YFP-Cdc42, excluding potential CRISPR/Cas9 off-target effects (Fig 3b). Therefore, we conclude that Cdc42 is required for ensure the formation of a single apical membrane during W4 cell polarization.

In order to maintain singularity during yeast budding Cdc42 is subjected to strict spatial regulation[4,17]. We thus questioned whether the singularity defect observed in ATP8B1-depleted W4 cells originated from altered Cdc42 localization. Indeed whereas in W4 cells YFP-Cdc42 is enriched at the clustered apical membrane, in ATP8B1-depleted W4 cells Cdc42 localization is dispersed and is poorly enriched at the apical membrane (Fig. 4a, b).

Next, using the Cdc42(D185) mutant, we investigated whether the dispersed localization of Cdc42 in ATP8B1-depleted W4 cells caused apical membrane enlargement. By introducing a negative charge into the polybasic region of Cdc42, the S185D mutation abrogates electrostatic interaction with negatively charged membrane lipids: whereas wild type Cdc42 can interact with phosphatidylserine (PS) and phosphatidic acid (PA) *in vitro*, the Cdc42(D185) mutant has lost the ability to bind these lipids (Fig. 4d). When expressed in polarized W4 cells, YFP-Cdc42(D185) was dispersed, like wild type Cdc42 in ATP8B1-depleted W4 cells (Fig. 4a). Importantly, expression of YFP-Cdc42(D185) in W4 cells resulted in failure of apical membrane clustering like that in ATP8B1-depleted W4 cells (Fig. 4c). We therefore conclude that dispersed localization of Cdc42 causes apical membrane enlargement in polarized W4 cells.

To demonstrate that improper clustering of Cdc42 at the apical membrane causes apical membrane enlargement in ATP8B1-depleted cells, we replaced the C-terminal hypervariable region (HVR) of Cdc42 with the pleckstrin homology (PH) domain of phospholipase Cδ (PLCδ), which binds $PI(4,5)P_2$. This apically enriched membrane lipid is localized independently of ATP8B1 and thus provides an alternative apical localization signal[18,19]. Indeed, this fusion protein completely recued the enlarged apical membrane in ATP8B1-depleted cells (Fig. 4f, g).

The dispersed localization of Cdc42 in ATP8B1-depleted W4 cells suggests that ATP8B1 functions to tether Cdc42 at the apical membrane which is required for Cdc42 to direct apical membrane clustering and maintain singularity. To measure apical membrane association of Cdc42, we fused the HVR of Cdc42, either wild type or D185, with the photoconvertible Dendra fluorescent protein. Upon expression of these probes in polarized W4 cells, local green-to-red photoconversion in the brush border is followed by gradual loss of red signal from this region as a result of diffusion (Fig. 5a). Therefore, the rate of signal decline from the converted region reflects the ability of these probes to be maintained at the apical plasma membrane. As full length Cdc42(D185) induces apical

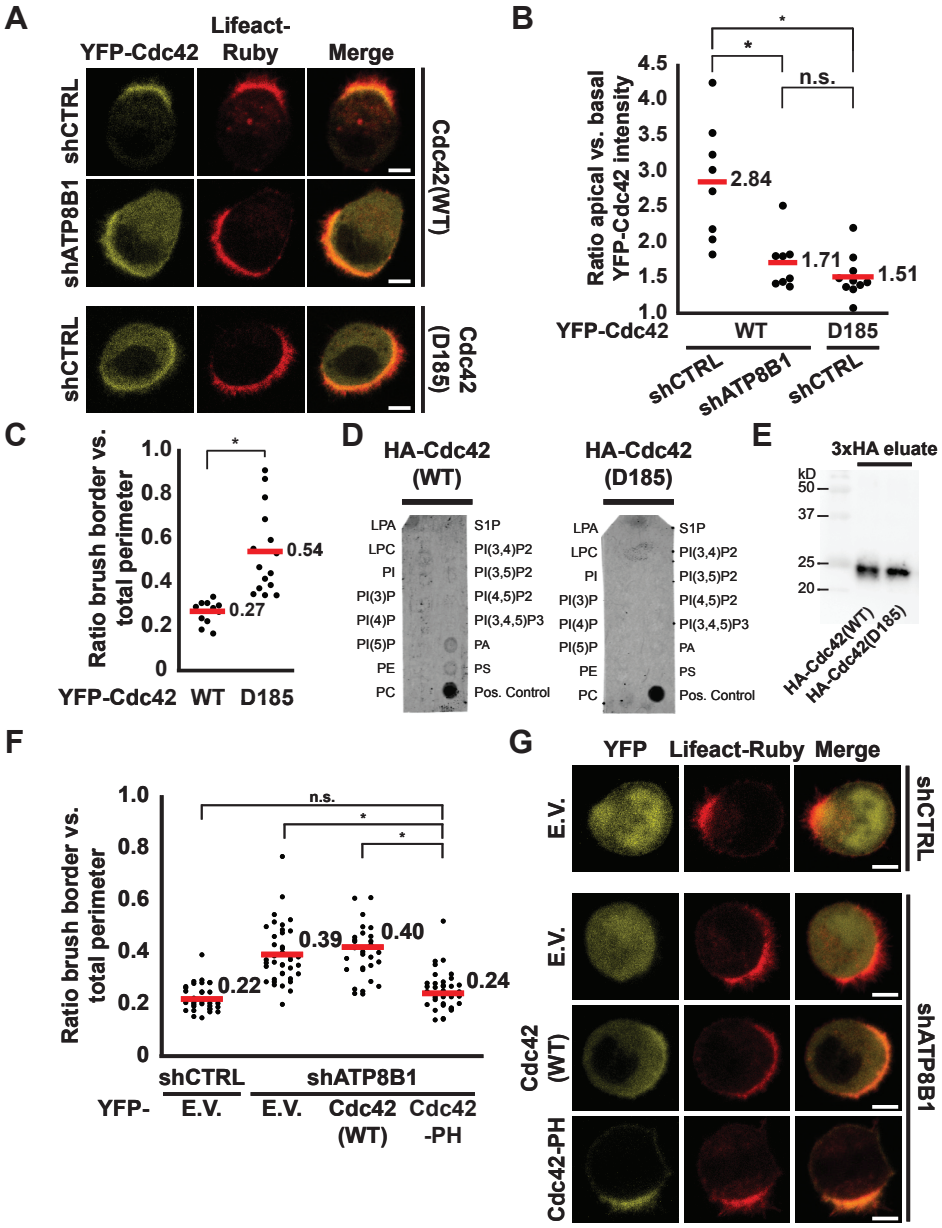

Figure 4: Loss of clustered Cdc42 localization causes apical membrane enlargement downstream from ATP8B1.

(**a**) Localization of YFP-Cdc42, wild type or D185, in polarized control- or ATP8B1-depleted W4 cells. (**b**) Quantification of apical enrichment of YFP-Cdc42 in polarized W4 cells. Quantified as the ratio of the average signal intensity between apical and basal membrane localized YFP-Cdc42. * $p < 0.005$ (**c**) Quantification of apical membrane size in polarized W4 cells expressing YFP-Cdc42 WT or D185. * $p < 0.0002$, n.s. $p > 0{,}05$ (**d**) HA-Cdc42 and HA-Cdc42(D185) binding profile to membrane-spotted phospholipids. (**e**) Western blot for HA-tag of IP eluates that were added to the lipid-spotted membranes in d, demonstrating that equal amounts of HA-Cdc42 were allowed to bind. (**f**) Quantification of apical membrane size in control W4 cells or ATP8B1-depleted W4 cells expressing YFP, YFP-Cdc42(WT) or YFP-Cdc42-PH. * $p < 0{,}00001$, n.s. $p > 0{,}05$ (**g**) Representative images of polarized W4 cells, control or ATP8B1-depleted, expressing YFP, YFP-Cdc42(WT) or YFP-Cdc42-PH in combination with the actin marker Lifeact-Ruby. Bars, 5 µm

membrane enlargement, we used the isolated hypervariable regions to monitor intrinsic membrane association without disturbing cell morphology.
Averages of normalized decline traces revealed that the D185 mutant was lost from the apical membrane more rapidly than the wild type probe (average half-life 132.5 vs. 81.1s.) (Fig. 5b, c, d). The wild type probe was evicted from the apical membrane more rapidly in ATP8B1-depleted cells than in control W4 cells, at a rate similar to the D185 mutant in control W4 cells (93.3s. and 81.1s. respectively) (Fig. 5b, c, d). In contrast, the eviction rate of Dendra-Rap2A(HVR), which does not contain a polybasic region but requires palmitoylation for plasma membrane association, was unaffected by ATP8B1 knockdown (Fig. S3a, b).

The increased mobility of Cdc42 in ATP8B1-depleted cells critically impedes the ability of Cdc42 to maintain a clustered apical membrane, because Cdc42 mutants that have stronger membrane association, resulting from introduction of additional basic residues, could restore normal apical membrane size in ATP8B1-depleted cells (Fig. 5e, f, S3c).

Discussion

We have established that loss of the mammalian flippase ATP8B1 results in defects in apical membrane architecture and abolishes singularity in recycling endosomal directionality. These defects are likely to contribute to the pathogenesis of PFIC1 in a bile acid-independent, cell-autonomous manner. Depletion of ATP8B1 causes a singularity defect as demonstrated by the appearance of cells that have multiple apical domains, but also as illustrated by the multiple clusters of Rab11 recycling endosomes in ATP8B1-depleted cells. The enlarged apical membrane in ATP8B1-depleted cells may mask potential multiplicity and likely explains why multiple brush borders are only observed in a fractions of cells.

We and others have demonstrated that Cdc42, the master regulator of singularity during yeast budding, interacts with phosphatidylserine[20], thus linking ATP8B1 via its preferred lipid substrate to Cdc42 localization[21-23]. Flippase-mediated modulation of Cdc42 membrane association also occurs during yeast budding[6,7]. Nevertheless, in contrast to ATP8B1, these flippases function to promote Cdc42 membrane dissociation and have not been implicated in singularity regulation. Therefore, our work demonstrates for the first time that membrane remodeling by lipid flippases is crucial for Cdc42 to enforce singularity in apical membrane generation.

We show that ATP8B1 loss results in a higher mobility of Cdc42 at the apical membrane. Various mechanisms may account for Cdc42 loss from the apical cluster, including GDI-mediated extraction and lateral diffusion. These mechanisms are likely interconnected as impaired function of the polybasic region both weakens membrane association and increases GDI binding[6,24].

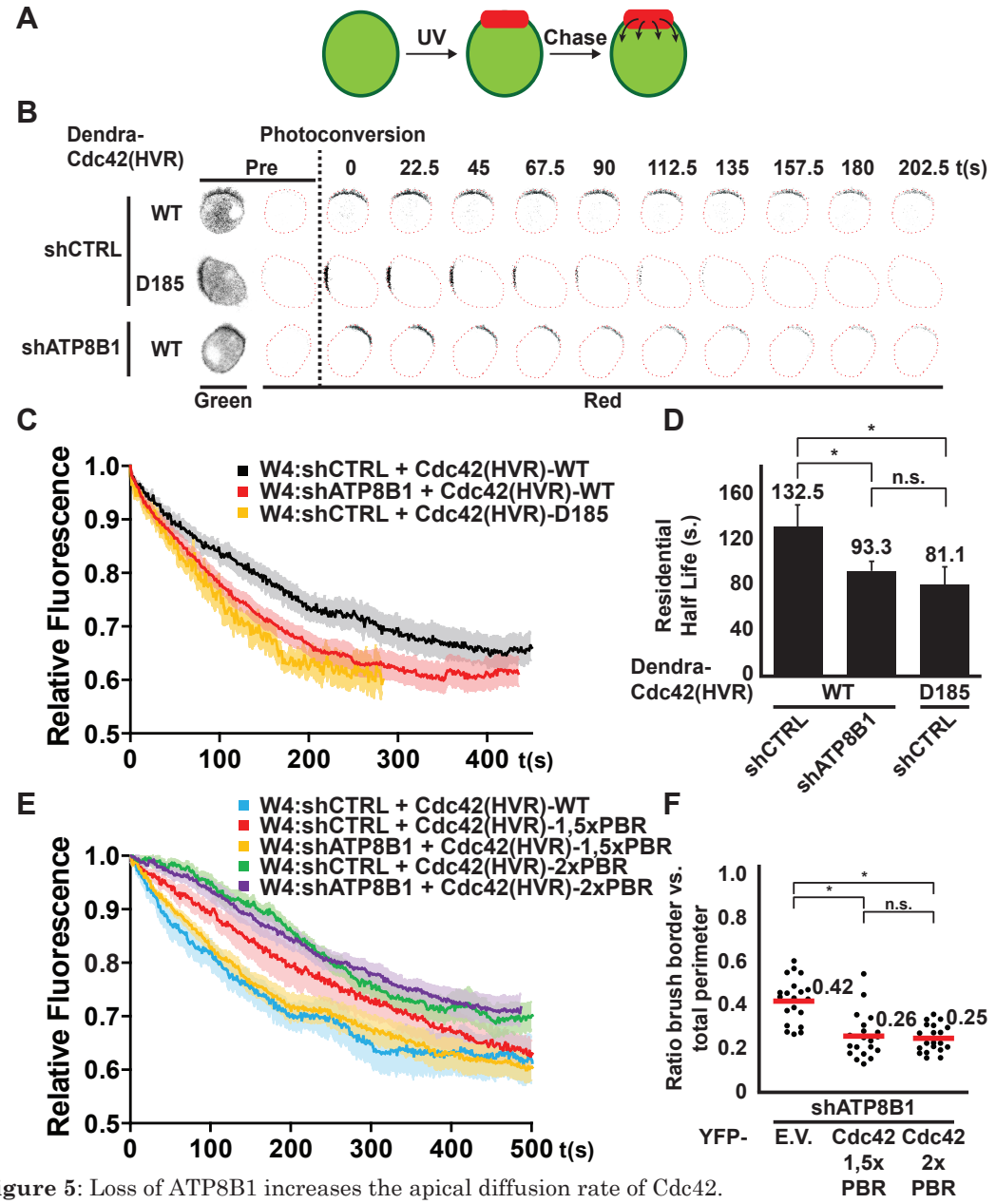

Figure 5: Loss of ATP8B1 increases the apical diffusion rate of Cdc42. (**a**) Schematic representation of the experimental setup used to determine the apical membrane diffusion rate. (**b**) Still images from representative photoconversion movies based on which the dissociation traces in c were generated. (**c**) Average normalized dissociation traces for control W4 cells expressing Dendra-Cdc42(HVR) wild type (n = 11), Dendra-Cdc42(HVR) D185 (n = 6), or ATP8B1-depleted cells expressing Dendra-Cdc42(HVR) wild type (n = 17). Light areas indicate s.e.m. (**d**) Residential half-lifes determined from average decay traces shown in c using curve fitting. Statistics were performed using half-lifes from individual cell traces. Error bars represent s.e.m. * $p < 0,05$, n.s. $p > 0,05$ (**e**) Average normalized dissociation traces for control or ATP8B1-depleted W4 cells expressing Dendra-Cdc42(HVR) wild type (n = 6), 1,5xPBR (shCTRL n = 7, shATP8B1 n = 9) or 2xPBR (shCTRL n = 12, shATP8B1 n = 8) Light areas indicate s.e.m. (**f**) Apical membrane size in ATP8B1-depleted W4 cells expressing YFP, YFP-Cdc42(1,5xPBR), or YFP-Cdc42(2xPBR). * $p < 0.00002$, n.s. $p > 0,05$, red bars indicate average

By using the C-terminal fragments of Cdc42, which are not bound by GDIs, the mobility observed during photoconversion experiments is GDI-independent and demonstrates that ATP8B1 affects Cdc42 membrane association independent of GDP/GTP loading or GDI binding. Nevertheless, GDI-mediated extraction may act in concert to impose the diffuse localization of full length Cdc42 in ATP8B1-depleted cells.
The ATP8B1-mediated decrease in Cdc42 mobility at the apical membrane critically affects the ability of Cdc42 to maintain singularity. Our data thus provide experimental evidence, in a mammalian context, for mathematical models of singularity in yeast that stress the importance of apical membrane diffusion as a key determinant in the establishment of a single apical domain[17,25-28].

Importantly, tight and adherens junctions are normally formed in intact tissue when ATP8B1 is lost and no ectopic lumina are formed, indicating that junction formation is dominant in apico-basal membrane segregation. However, the structural defects in apical membrane organization demonstrate that pathogenic loss of ATP8B1 affects lumen formation in a multicellular context and suggest a function for the evolutionary conserved process of singularity in maintaining healthy tissue architecture.

Materials & Methods

Cell culture & plasmids

Ls174T:W4 cells were cultured in RPMI1640 (Lonza) supplemented with 10% tetracycline-free FBS (Lonza) and antibiotics. To induce polarization, W4 cells were cultured in medium containing 1 µg/ml doxycycline (Sigma) for at least 16h. For transient transfection, W4 cells were transfected using X-tremeGene9 (Roche) according to the manufacturer's guidelines.

N-terminally tagged YFP- or HA-tagged Cdc42 proteins were generated using Gateway recombination (Invitrogen) in pcDNA3 and pMT2 backbones respectively and under control of a CMV promotor. The Cdc42 S185D mutation was introduced by site-directed mutagenesis. For the C-terminal Cdc42 mutants (PH fusion and PBR extensions) first a unique EcoR1 site was introduced after amino acid 174. This site was subsequently used to introduce the PH domain (amino acid 21 -130) PCR fragment, derived from PLCδ, or the modified polybasic regions, generated by annealing the corresponding oligonucleotides, using In-Fusion cloning reactions (Clontech). For photoconversion experiments, the region encoding the Cdc42 hypervariable region (corresponding to amino acid residues 175 – 191) or Rap2A hypervariable region (amino acid residues 167 – 183) was N-terminally fused to Dendra in pDendra-C2 under control of a CMV promotor. Lifeact-Ruby and Lifeact-GFP in pmRFP-Ruby-N1 and pEGFP-N1 under control of a CMV promotor was provided by R. Wedlich-Soldner and dsRed-Rab11 in pdsRed-N1 under control of a CMV promotor was provided by J.P. Ten Klooster.

Antibodies

The following antibodies were used for immunofluorescence: rabbit anti-Myosin Vb (Novus Biologicals, 1:1000), mouse anti-villin (1D2C3, Santa Cruz, 1:500), mouse anti-CD66 (BD Biosciences, 1:500), mouse anti-CD71 (H68.4, Life Technologies, 1:1000), rabbit anti-phospho Ezrin (Thr567)/Radixin (Thr564)/Moesin (Thr558) (Cell Signaling, 1:250), and mouse anti-ZO-1 (1A12, Life Technologies, 1:500) The following antibodies were used for Western blots: rabbit anti-ATP8B1 (H-91, Santa Cruz, 1:1000), rabbit anti-Cdc42 (11A11, Cell Signaling), mouse anti-Na/K ATPase (Millipore, 1:5000), mouse anti-HA (12CA5, Roche, 1:5000) and mouse anti-alpha-Tubulin (DM1A, Calbiochem, 1:10000)

Lentiviral knockdown

Ls174T-W4 cells were infected for two successive days with lentiviral shRNA constructs (Mission library, Sigma). Infected cells were selected for puromycin resistance (10 µg/ml) for at least three days. For stable knockdown of ATP8B1 three hairpins were used (target sequence shRNA #1: 5'-CGGAAGCGAATGTCTATCATT-3', shRNA #2: 5'-CCGATGGTCTTACATAAGGAT-3', shRNA #3: 5'-CCACTATCTTATTGAGCAAAT-3') and for Cdc42 five hairpins were used (target sequence shRNA #1: 5'-CCCTCTACTATTGAGAAACTT-3', shRNA #2: 5'-CGGAATATGTACCGACTGTTT-3', shRNA #3: 5'-CAGATGTATTTCTAGTCTGTT-3', shRNA #4: 5'- GACTCTGTAACAGACTAATTG-3', shRNA #4: 5'-CCTGATATCCTACACAACAAA-3', shRNA #5: 5'-CCAAGAACAAACAGAAGCCTA-3')

Generation of Cdc42-deficient W4 cells using CRISPR/Cas9

W4 cells were transiently transfected with pSpCas9(BB)-2A-GFP (PX458), encoding an sgRNA (GAAGCCTTTATACTTACAGT) targeting the first coding exon of Cdc42. Single GFP-positive cells were sorted to individual wells of a 96-wells plate using a BD FACS AriaII flow cytometer. Genomic DNA from expanded clones was isolated using the QIAamp DNA Micro Kit. The targeted genomic region was amplified by PCR (forward primer: GAATAGCCAGGGATCAGAAAC; reverse primer TTGAGACCACCACTCGTTAG), cloned into pGEMT (Promega), and sequenced. Absence of Cdc42 was demonstrated by Western blotting. The two clones presented are independent clonal lines generated using the same sgRNA.

Live cell imaging

Transfected W4 cells were split and seeded onto glass-bottom dishes (WillCo Wells) in the presence of doxycycline (1µg/ml). Before imaging, medium was removed and replaced with HEPES-buffered (pH = 7.4) Leibovitz's L-15 medium (Invitrogen). Cells were imaged at 37 ºC using an Axioskop2 LSM510 scanning confocal microscope (Zeiss) with a 63x magnification oil objective (PLAN Apochromat, NA 1,4) using Zen image acquisition software. Apical membrane

size was determined using ImageJ software by measuring the total perimeter of the cell and the length of the membrane bearing microvilli. Average apical membrane sizes were compared using independent samples t-test in SPSS with a *p*-value <0.05 as a cutoff for significance. Quantification of apical enrichment of YFP-Cdc42 was performed by making a line scan through the apical and basal membrane and determining the ratio between average apical and basal membrane pixel intensities using ImageJ. Average enrichment ratios were compared using independent samples t-test in SPSS with a *p*-value <0.05 as a cutoff for significance.

Intestinal organoid cultures

Wild type and PFIC organoids were cultured as described previously[29]. Briefly, crypts from an ATP8B1$^{G308V/G308V}$ mouse were isolated in PBS/EDTA (2mM). Crypts were pelleted and resuspended in Matrigel (BD Bioscience) and plated in 24-well plates. Organoids were cultured in advanced DMEM/F12 (Life Technologies) supplemented with B27 supplement (Life Technologies), mEGF (Life Technologies), 5% R-Spondin-conditioned medium, 10% Noggin-conditioned medium and N-acetyl-cysteine. Organoids were passaged every 5 days by mechanical dissociation using a Pasteur pipette.

Immunofluorescence staining on organoids

For immunofluorescence, organoids were seeded on glass-bottom dishes (WillCo Wells) after passaging. Four days after passaging, organoids were fixed in 4% formaldehyde for 15 min. at 4ºC. After gentle washing with PBS, organoids were permeabilized in PBD-2T buffer (1% BSA, 10% DMSO, 2% Triton X-100 all in PBS) for at least 4h at 4ºC. PBD-2T buffer containing primary antibody was added to permeabilized organoids and incubated overnight at 4ºC. After washing with PBD-2T buffer, Alexa488-coupled secondary antibody diluted in PBD-2T buffer together with DAPI and phalloidin-Alexa568 was added and incubated overnight at 4ºC. After washing with PBD-2T three times for 10 minutes, the organoids were washed twice with PBS and were stored at 4ºC in PBS. Organoids were imaged using an Axioskop2 LSM510 scanning confocal microscope (Zeiss) with a 40x magnification oil objective (EC PLAN-Neofluar, NA 1,3) using Zen image acquisition software. Apical membrane size was quantified by determining the ratio of apical and basal membrane at the center of the lumen using ImageJ software. Average apical membrane sizes were compared using independent samples t-test in SPSS with a *p*-value <0.05 as a cutoff for significance.

Lipid-overlay assay

HEK293T cells were transfected with HA-Cdc42(WT) of HA-Cdc42(D185). After three days, cells were lysed in IPP buffer (50mM Tris pH 7.5, 5mM EDTA, 0,1% Tween-20, 350mM NaCl) and cleared by centrifugation at 4ºC. Protein A beads were pre-coupled with anti-HA antibody and used to precipitate HA-Cdc42 from

lysates for 3h at 4ºC. After washing, HA-Cdc42 was eluted from the beads using HA peptide (Sigma) (0.5 mg/ml in BC300 buffer: 20mM Tris pH 7.9, 20% glycerol, 300mM KCl) by shaking for 1h at room temperature. 10% of both eluates was loaded onto a gel for SDS-PAGE to evaluate protein recovery. PIP-Strips (Echelon Biosciences) were blocked in PIP-Strip buffer (20mM Tris pH 7.5, 150mM NaCl, 3% BSA, 0,1% Tween-20) for 1h at room temperature. HA-Cdc42 eluates were added to the PIP-Strips and incubated for 16h at 4ºC. After washing, PIP-Strips were probed with anti-HA antibody and Alexa-690 coupled secondary antibody before detection with a LICOR Odyssey imaging system.

Apical membrane eviction rates

To determine apical membrane eviction rates, W4 cells were transfected with Dendra-Cdc42(HVR), polarized and imaged at 37ºC in HEPES-buffered (pH = 7.4) Leibovitz's L-15 medium (Invitrogen). Photoconversion and imaging were performed using a Leica SP8x microscope equipped with a temperature- and CO_2-controlled chamber using a 63x objective (HC PL APO 63x/1.40 oil) with Leica LAS AF image acquisition software. Photoconversion of the Dendra fluorophore was done with a pulse of 405nm laser and imaging was done with a 1.5s frame rate. To generate a fluorescent decay trace, the ratio of photoconverted (red) signal in the brush border and the total amount of red signal in the cell were determined for each time point. Moving regions-of-interest were drawn to correct for cell movements during imaging. Ratios were normalized and multiple traces were averaged to generate an average fluorescence decay trace. Single exponential curve fitting was performed on the average decay traces using Matlab software with the general formula: f(x) = a * e^(-b*x) + c. An average half-life was determined using the fitted curve. For statistical analyses, half-lifes of the individual decay traces were determined and compared using independent samples t-test in SPSS with a *p*-value < 0,05 as a cutoff for significance.

Acknowledgements

We thank Bas Ponsioen for assistance in microscopy and data analysis, Hugo Snippert for help in organoid culture establishment, Cilia de Heus for technical assistance with electron microscopy, Kees Hoeben for quantification of canalicular lumen area, Johan Offerhaus for histopathologic evaluation of patient biopsy materials, and J. van Velzen and P. van der Burght for technical assistance with FACS sorting. We thank Martijn Gloerich for comments on the manuscript and all members of the Bos lab for continuous support and discussion. The authors declare no competing financial interests.

References

1 Bryant, D. M. & Mostov, K. E. From cells to organs: building polarized tissue. Nature reviews. Molecular cell biology 9, 887-901, doi:10.1038/nrm2523 (2008).
2 Rodriguez-Boulan, E. & Macara, I. G. Organization and execution of the epithelial polarity programme. Nature reviews. Molecular cell biology 15, 225-242, doi:10.1038/nrm3775 (2014).
3 Caviston, J. P., Tcheperegine, S. E. & Bi, E. Singularity in budding: a role for the evolutionarily conserved small GTPase Cdc42p. Proceedings of the National Academy of Sciences of the United States of America 99, 12185-12190, doi:10.1073/pnas.182370299 (2002).
4 Slaughter, B. D., Smith, S. E. & Li, R. Symmetry breaking in the life cycle of the budding yeast. Cold Spring Harbor perspectives in biology 1, a003384, doi:10.1101/cshperspect. a003384 (2009).
5 Wedlich-Soldner, R., Altschuler, S., Wu, L. & Li, R. Spontaneous cell polarization through actomyosin-based delivery of the Cdc42 GTPase. Science 299, 1231-1235, doi:10.1126/science. 1080944 (2003).
6 Das, A. et al. Flippase-mediated phospholipid asymmetry promotes fast Cdc42 recycling in dynamic maintenance of cell polarity. Nature cell biology 14, 304-310, doi:10.1038/ ncb2444(2012)
7 Saito, K. et al. Transbilayer phospholipid flipping regulates Cdc42p signaling during polarized cell growth via Rga GTPase-activating proteins. Developmental cell 13, 743-751, doi:10.1016/ j.devcel.2007.09.014 (2007).
8 van der Woerd, W. L. et al. Familial cholestasis: progressive familial intrahepatic cholestasis, benign recurrent intrahepatic cholestasis and intrahepatic cholestasis of pregnancy. Best practice & research. Clinical gastroenterology 24, 541-553, doi:10.1016/j.bpg.2010.07.010 (2010).
9 Bull, L. N. et al. A gene encoding a P-type ATPase mutated in two forms of hereditary cholestasis. Nature genetics 18, 219-224, doi:10.1038/ng0398-219 (1998).
10 van Mil, S. W. et al. Fic1 is expressed at apical membranes of different epithelial cells in the digestive tract and is induced in the small intestine during postnatal development of mice. Pediatric research 56, 981-987, doi:10.1203/01.PDR.0000145564.06791.D1 (2004).
11 Paulusma, C. C. et al. Atp8b1 deficiency in mice reduces resistance of the canalicular membrane to hydrophobic bile salts and impairs bile salt transport. Hepatology 44, 195-204, doi:10.1002/hep.21212 (2006).
12 Pawlikowska, L. et al. A mouse genetic model for familial cholestasis caused by ATP8B1 mutations reveals perturbed bile salt homeostasis but no impairment in bile secretion. Human molecular genetics 13, 881-892, doi:10.1093/hmg/ddh100 (2004).
13 Bryant, D. M. et al. A molecular network for de novo generation of the apical surface and lumen. Nature cell biology 12, 1035-1045, doi:10.1038/ncb2106 (2010).
14 Dhekne, H. S. et al. Myosin Vb and rab11a regulate ezrin phosphorylation in enterocytes. Journal of cell science, doi:10.1242/jcs.137273 (2014).
15 Bull, L. N. et al. Genetic and morphological findings in progressive familial intrahepatic cholestasis (Byler disease [PFIC-1] and Byler syndrome): evidence for heterogeneity. Hepatology 26, 155-164, doi:10.1002/hep.510260121 (1997).
16 Baas, A. F. et al. Complete polarization of single intestinal epithelial cells upon activation of LKB1 by STRAD. Cell 116, 457-466 (2004).
17 Howell, A. S. et al. Singularity in polarization: rewiring yeast cells to make two buds. Cell 139, 731-743, doi:10.1016/j.cell.2009.10.024 (2009).
18 Martin-Belmonte, F. et al. PTEN-mediated apical segregation of phosphoinositides controls epithelial morphogenesis through Cdc42. Cell 128, 383-397,doi:10.1016/j.cell.2006.11.051 (2007)
19 Gervais, L., Claret, S., Januschke, J., Roth, S. & Guichet, A. PIP5K-dependent production of PIP2 sustains microtubule organization to establish polarized transport in the Drosophila oocyte. Development 135, 3829-3838, doi:10.1242/dev.029009 (2008).
20 Finkielstein, C. V., Overduin, M. & Capelluto, D. G. Cell migration and signaling specificity is determined by the phosphatidylserine recognition motif of Rac1. The Journal of biological chemistry 281, 27317-27326, doi:10.1074/jbc.M605560200 (2006).
21 Cai, S. Y. et al. ATP8B1 deficiency disrupts the bile canalicular membrane bilayer structure in hepatocytes, but FXR expression and activity are maintained. Gastroenterology 136, 1060-

1069, doi:10.1053/j.gastro.2008.10.025 (2009).
22 Paulusma, C.C. et al. ATP8B1 requires an accessory protein for endoplasmic reticulum exit and plasma membrane lipid flippase activity. Hepatology 47, 268-278, doi:10.1002/hep.21950 (2008).
23 Ujhazy, P. et al. Familial intrahepatic cholestasis 1: studies of localization and function. Hepatology 34, 768-775, doi:10.1053/jhep.2001.27663 (2001).
24 Forget, M. A., Desrosiers, R. R., Gingras, D. & Beliveau, R. Phosphorylation states of Cdc42 and RhoA regulate their interactions with Rho GDP dissociation inhibitor and their extraction from biological membranes. Biochem J 361, 243-254 (2002).
25 Goryachev, A. B. & Pokhilko, A. V. Dynamics of Cdc42 network embodies a Turing-type mechanism of yeast cell polarity. FEBS letters 582, 1437-1443, doi:10.1016/j.febslet.2008.03.029 (2008).
26 Klunder, B., Freisinger, T., Wedlich-Soldner, R. & Frey, E. GDI-mediated cell polarization in yeast provides precise spatial and temporal control of Cdc42 signaling. PLoS computational biology 9, e1003396, doi:10.1371/journal.pcbi.1003396 (2013).
27 Marco, E., Wedlich-Soldner, R., Li, R., Altschuler, S. J. & Wu, L. F. Endocytosis optimizes the dynamic localization of membrane proteins that regulate cortical polarity. Cell 129, 411-422, doi:10.1016/j.cell.2007.02.043 (2007).
28 Slaughter, B. D. et al. Non-uniform membrane diffusion enables steady-state cell polarization via vesicular trafficking. Nature communications 4, 1380, doi:10.1038/ncomms2370 (2013).
29 Sato, T. et al. Single Lgr5 stem cells build crypt-villus structures in vitro without a mesenchymal niche. Nature 459, 262-265, doi:10.1038/nature07935 (2009).

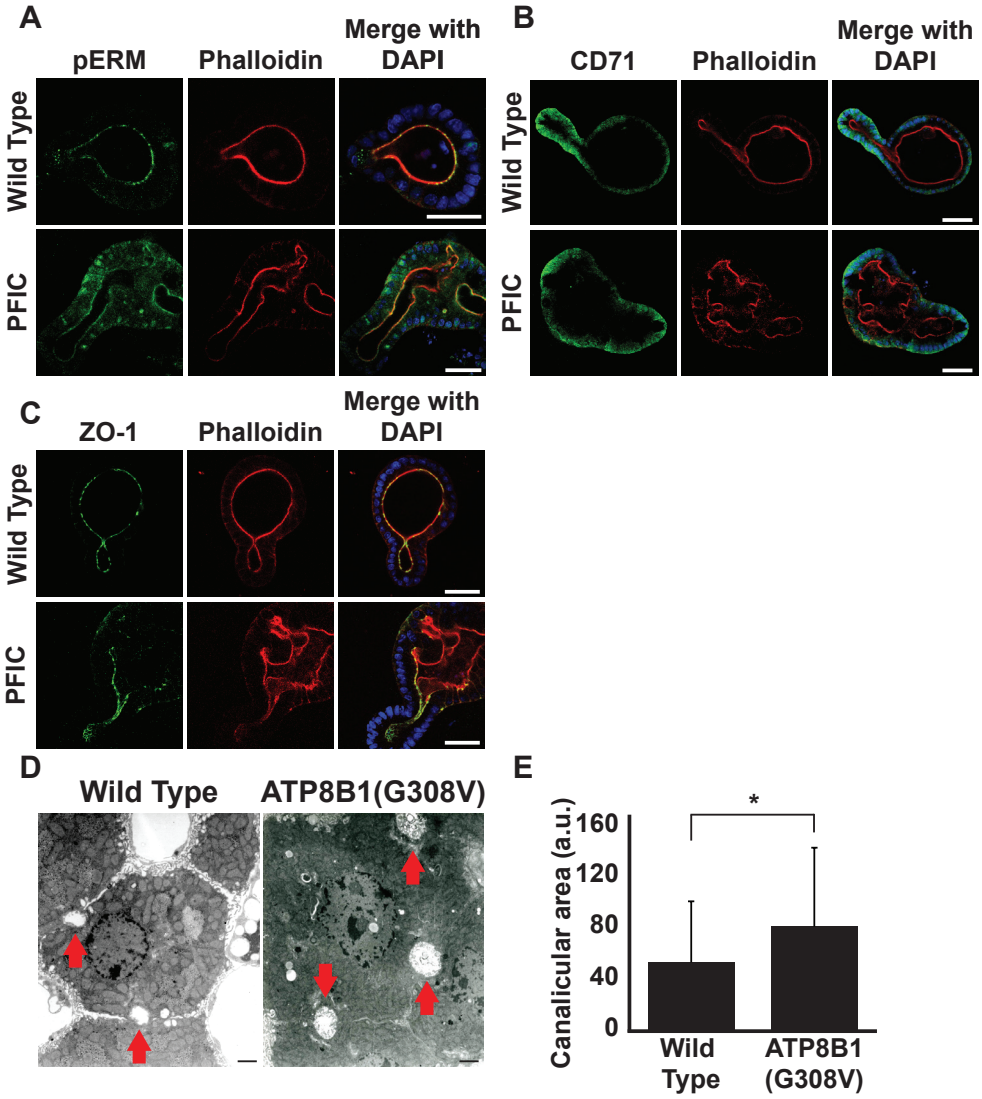

Supplementary Figure 1: ATP8B1 mutations affect lumen morphology in the intestine and liver.

(**a**) Localization of the apical marker phosphorylated Ezrin/Radixin/Moesin (pERM), basolateral marker CD71 (**b**), and apical tight junction marker ZO-1 (**c**) in wild type and PFIC organoids. (**d**) Transmission electron micrographs of liver sections from wild type or ATP8B1$^{G308V/G308V}$ mice. Red arrows highlights bile canaliculi. Bars, 500 nm (**e**) Quantification of bile canalicular lumen size in wild type or ATP8B1$^{G308V/G308V}$ mice. Wild type n = 138, ATP8B1$^{G308V/G308V}$ n = 146 (total number of canaliculi from 2 different mice per genotype). Error bars are s.d. * $p < 0{,}00003$ Bars, 35 µm

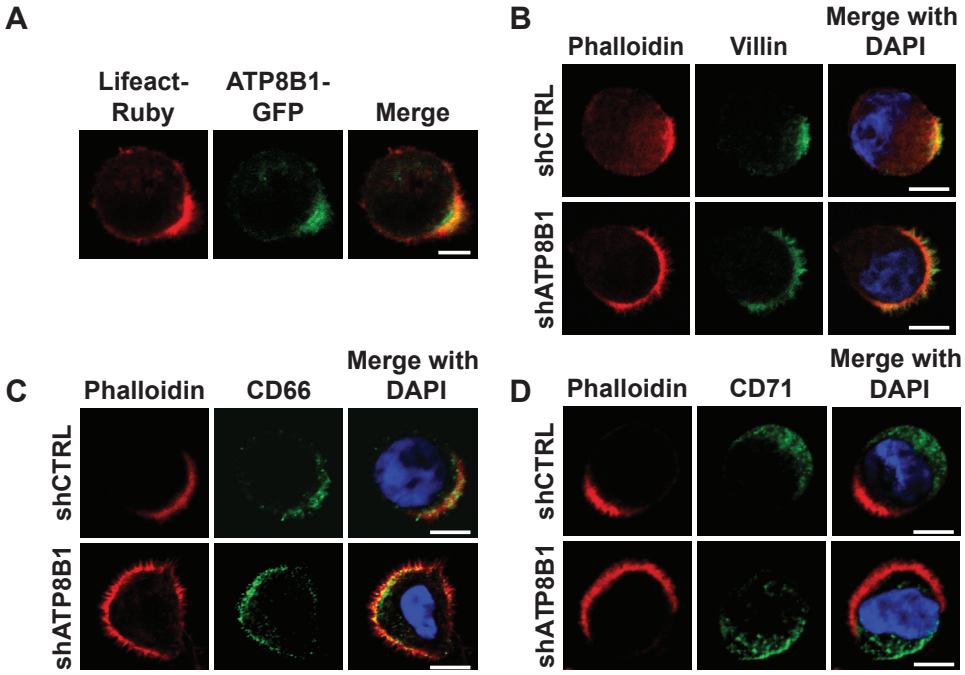

Supplementary Figure 2: Polarity markers distribute normally in ATP8B1-depleted W4 cells. (**a**) W4 cell expressing ATP8B1-GFP and the actin marker Lifeact-Ruby. (**b**) Control or ATP8B1-depleted W4 cells immunostained for the brush border marker villin. Immunofluorescence staining in polarized control or ATP8B1-depleted W4 cells demonstrates normal segregation of apical and basolateral markers (CD66, (**c**) and CD71, (**d**) respectively). Bars, 5 µm

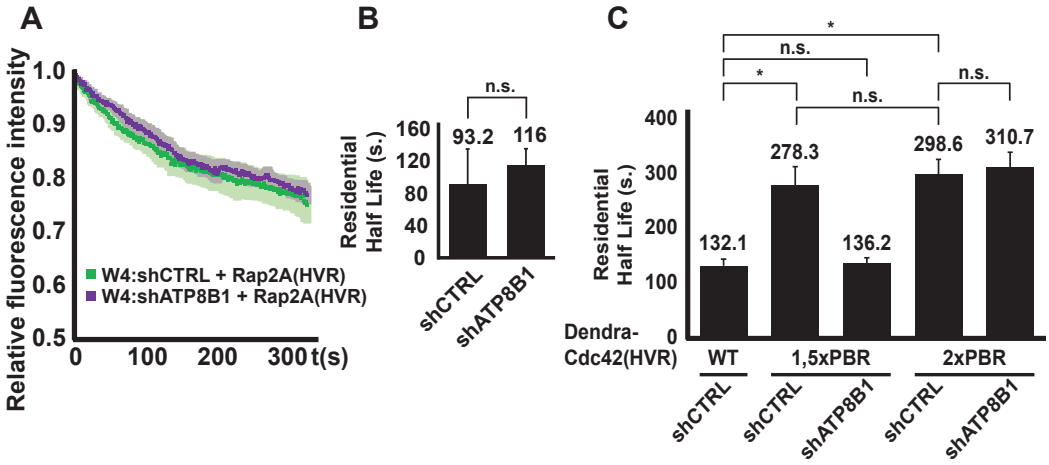

Supplementary Figure 3: ATP8B1 knockdown does not affect apical membrane diffusion of Dendra-Rap2A(HVR).
(**a**) Average normalized dissociation traces for control (n = 9) or ATP8B1 depleted (n = 9) W4 cells expressing Dendra-Rap2A(HVR). Light areas indicate s.e.m. (**b**) Residential half-lifes determined from average decay traces shown in (**a**) using curve fitting. Statistics were performed using the half-lifes from individual cell traces. Error bars represent s.e.m. n.s. $p > 0{,}05$ (**c**) Residential half-lifes determined from average decay traces shown in fig. 4e using curve fitting. Statistics were performed using the half-lifes from individual cell traces. Error bars represent s.e.m. * $p < 0.02$, n.s. $p > 0{,}05$

2

III

A two-tiered mechanism enables localized Cdc42 signaling during enterocyte polarization

Lucas J.M. Bruurs, Susan Zwakenberg, Fried J. Zwartkruis, Johannes L. Bos

Manuscript under review

Abstract
Signaling by the small GTPase Cdc42 governs a diverse set of cellular processes that contribute to tissue morphogenesis. Since these processes often require highly localized signaling, Cdc42 activity must be clustered in order to prevent ectopic signaling. During cell polarization, apical Cdc42 signaling directs the positioning of the nascent apical membrane. However, the molecular mechanisms that drive Cdc42 clustering during polarity establishment are largely unknown.

Here we demonstrate that during cell polarization localized Cdc42 signaling is enabled via activity-dependent control of Cdc42 mobility. By performing photoconversion experiments, we show that inactive Cdc42-GDP is 30-fold more mobile compared to active Cdc42-GTP. This switch in apical mobility originates from a dual mechanism involving RhoGDI-mediated membrane dissociation of Cdc42-GDP and Tuba-mediated immobilization of Cdc42-GTP. Interference with either mechanism affects Cdc42 clustering and as a consequence impairs Cdc42-mediated apical membrane clustering.

We therefore identify a molecular network, comprised of a Cdc42, the GEF Tuba and RhoGDI, that enables differential diffusion of inactive and active Cdc42 and is required to establish localized Cdc42 signaling during enterocyte polarization.

Introduction

Cdc42 signaling controls multiple aspects of tissue morphogenesis by regulating processes such as junction formation and cell polarization[1]. As these processes are often localized to a specific part of the cell, Cdc42 activity must be confined in a local cluster to prevent ectopic signaling. During cell polarization, Cdc42 is recruited to the nascent apical membrane where it governs the positioning of the apical domain[1,2]. As a consequence, loss of Cdc42 results in the formation of multiple apical domains in a single cell model for enterocyte polarization and in the formation of multiple lumina in 3D cyst cultures[3,4].

In order to restrict apical membrane formation to a single site, Cdc42 itself must be confined into a single cluster. We previously demonstrated that an inability to restrict Cdc42 localization results in the formation of an enlarged apical membrane and consequently in the formation of an aberrantly shaped lumen[3]. Despite the importance of Cdc42 clustering, little is known about the molecular mechanisms that drive Cdc42 cluster formation during cell polarization.

Cdc42 dynamics have been extensively studied in the context of yeast cell polarization[5-10]. Clustered Cdc42 activity is required for yeast cell polarization but it also ensures that only one polarization site is established[5,11]. As a consequence, interference with Cdc42 mobility affects the apical accumulation of Cdc42 and may give rise to yeast cells with multiple bud sites[5,9,12]. These findings in yeast therefore indicate that control over Cdc42 dynamics is crucial for Cdc42 clustering and signaling. However, it remains unclear whether regulation of Cdc42 mobility is of similar relevance during mammalian cell polarization.

Here we show that during enterocyte polarization, Cdc42 mobility is regulated in an activity-dependent manner, with inactive Cdc42-GDP being highly mobile and active Cdc42-GTP being relatively immobile. This striking difference in mobility is enabled via selective membrane dissociation of Cdc42-GDP by RhoGDI and immobilization of Cdc42-GTP by the Cdc42-specific GEF Tuba. We show that this switch-like diffusive behavior is critical for Cdc42 function as interfering with either mechanism impedes spatial confinement of Cdc42 signaling resulting in an inability to establish a clustered apical membrane.

Results

Previously, we reported that during enterocyte polarization Cdc42 is apically concentrated to ensure clustering of the apical membrane[3]. To study the mechanisms that drive Cdc42 clustering in this process we made use of Ls174T:W4 cells. These cells can polarize in absence of cell-cell contacts by means of forced LKB1 activation, prompted by doxycycline-induced STRAD expression[13]. To determine its mobility we expressed Cdc42, equipped with the photoconvertible Dendra fluorophore, in polarized Ls174T:W4 cells and locally

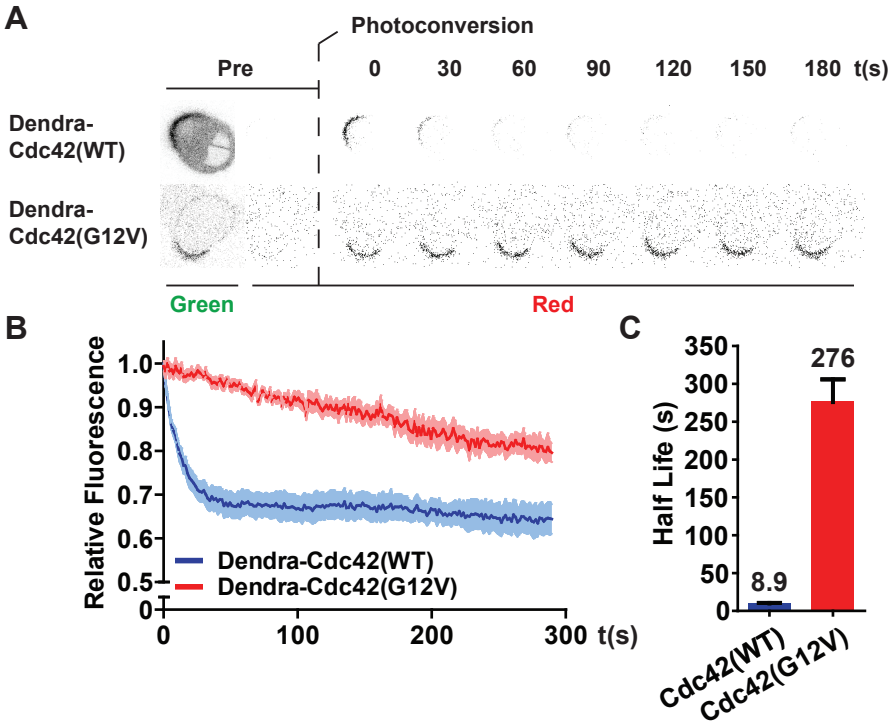

Figure 1: Apical mobility of Cdc42 is regulated in an activity-dependent manner.
(**a**) Images from photoconversion experiments in polarized Ls174T:W4 cells expressing Dendra-Cdc42(WT) or (G12V). (**b**) Average normalized fluorescence decay traces after photoconversion of cells expressing Dendra-Cdc42(WT) (blue line, n = 11) and (G12V) (red line, n = 14). Light-colored areas reflect s.e.m. (**c**) Eviction half-lives determined from average decay traces shown in b using curve fitting. Error bars represent the 95% confidence interval of the fit.

converted Dendra-Cdc42 in the apical brush border. Subsequent loss of red signal from the converted region was used to determine an eviction half life, which reflects Cdc42's mobility at the apical plasma membrane.
Using this strategy, we compared the mobility of constitutively activated Dendra-Cdc42(G12V) with wild type Cdc42 and found a striking difference in mobility: whereas wild type Cdc42 is highly mobile at the apical plasma membrane, Cdc42(G12V) is relatively immobile with an approximately 30-fold longer eviction half life (8.9 s. vs. 276 s. respectively) (Fig. 1). Since the immobilization of active Cdc42 is likely to drive the establishment of localized Cdc42 signaling we set out to identify the molecular mechanisms responsible for Cdc42 immobilization upon GTP-loading.

RhoGDIs bind small GTPases of the Rho family and facilitate their dissociation from the plasma membrane[14,15]. Although RhoGDI has similar affinities for Cdc42-GDP and Cdc42-GTP in solution, when Cdc42 is inserted in an artificial bilayer RhoGDI has a higher affinity for Cdc42-GDP[15]. Therefore, RhoGDIs may selectively increase the mobility of Cdc42-GDP.
Indeed, in Ls174T:W4 cells with stable knockdown of RhoGDIα the mobility of

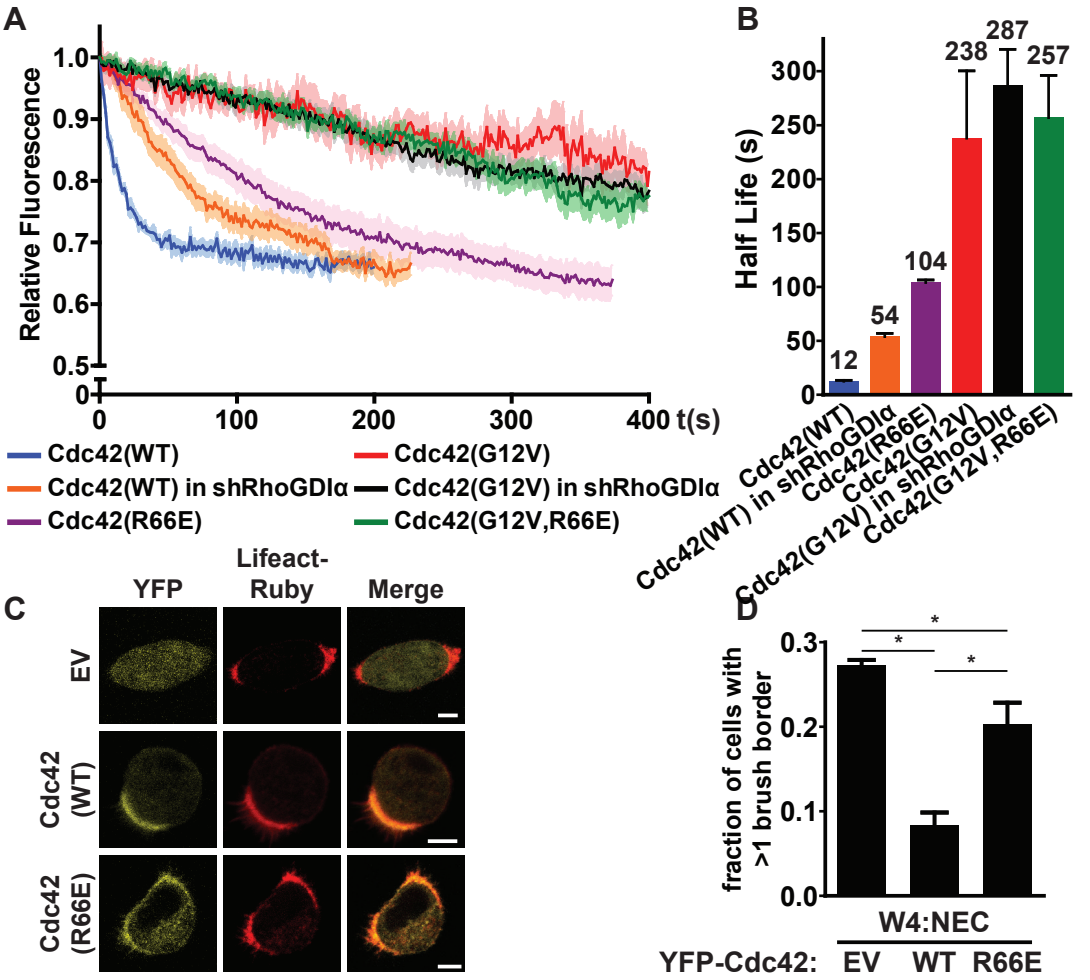

Figure 2: RhoGDI selectively increases mobility of inactive Cdc42 and is required for Cdc42 clustering.
(**a**) Average normalized fluorescence decay traces of Dendra-Cdc42(WT) in W4 cells (blue line, n = 11), Dendra-Cdc42(WT) in W4:shRhoGDIα cells (orange line, n = 11), Dendra-Cdc42(R66E) in W4 cells (purple line, n = 12), Dendra-Cdc42(G12V) in W4 cells (red line, n = 16), Dendra-Cdc42(G12V) in W4:shRhoGDIα cells (black line, n = 17), and Dendra-Cdc42(G12V, R66E) in W4 cells (green line, n = 13). Light-colored areas reflect s.e.m. (**b**) Eviction half-lives determined from average decay traces shown in a using curve fitting. Error bars represent the 95% confidence interval of the fit. (**c**) NEC cells expressing the actin marker lifeact-ruby in combination with YFP, YFP-Cdc42(WT), or YFP-Cdc42(R66E). Scale bars indicate 5µm. (**d**) Quantification of cells with multiple brush borders in W4:NEC cells expressing YFP, YFP-Cdc42(WT), or YFP-Cdc42(R66E). Error bars are s.e.m. (n = 3) * $p < 0.05$ using independent samples t-test.

wild type Cdc42 was reduced (eviction half life 53.8 s.) (Fig. 2a, b). In addition, Cdc42(R66E), which is unable to interact with RhoGDIs, displays an even slower apical mobility (half life 104 s.) (Fig 2a, b). Importantly, the R66E mutation does not affect the global GTP-loading or posttranslational lipid modification of Cdc42 (Supp. Fig. 1). The observed difference in half life between RhoGDIα knockdown and Cdc42(R66E) may be of technical origin: knockdown of RhoGDIα impairs

brush border formation and since mobility is only assessed in cells with a brush border, these cells are likely to have only moderate knockdown (Supp. Fig. 2). In addition, since efficient knockdown of all three RhoGDI isoforms could not be realized, this difference may also be explained by the effects of RhoGDIß and ɣ. Importantly, membrane dissociation by RhoGDI selectively acts on Cdc42-GDP as the mobility of constitutively active Cdc42 is not affected by introduction the R66E mutation or RhoGDIα knockdown (Fig. 2a, b).

To assess the functional contribution of RhoGDI-mediated membrane dissociation of Cdc42-GDP we tested whether Cdc42(R66E) was able to restore singularity in apical membrane formation in Ls174T:W4 cells that have no endogenous Cdc42 (W4:NEC cells). We previously reported that these Cdc42 knockout cells retain the ability to form a brush border, but are nonetheless unable to ensure that polarization is restricted to a single site[3]. Whereas the singularity defect in the W4:NECs is rescued by reintroduction of YFP-Cdc42, expression of YFP-Cdc42(R66E) could not restore singularity, indicating that the interaction with RhoGDIs is required to concentrate Cdc42 into a single cluster and is therefore required for Cdc42 function (Fig. 2c, d).

Although RhoGDI-dependent membrane dissociation of Cdc42-GDP contributes to the high mobility of inactive Cdc42, it can only in part explain the immobilization of Cdc42 upon GTP-loading. To find the mechanism that is responsible for the additional immobilization of Cdc42-GTP we focused on the GEF for Cdc42, reasoning that RhoGEFs often act as a scaffold for the complexation of Cdc42-GTP with its effector and that this complexation could limit the mobility of activated Cdc42.

Tuba (also known as DNMBP or ArhGEF36) is a Cdc42-specific GEF that has been implicated in regulating Cdc42 signaling in polarizing MDCK cysts and during zebrafish development[2,16-19]. We therefore tested whether Tuba, like Cdc42, is involved in apical membrane clustering in polarized Ls174T:W4 cells. Surprisingly, Tuba knockout cells showed a decreased ability to generate a brush border and to polarize, as judged by the distribution of apical (CD66) and basolateral (CD71) markers (Fig 3a, b, c, d). This phenotype can not be attributed to loss of Cdc42 signaling because Cdc42 knockout cells are unaffected in their ability to form brush borders[3].

Therefore, in order to specifically address the Cdc42-depedent effects of Tuba, we reintroduced either wild type Tuba or a mutant lacking the GEF domain (TubaΔDH) in Tuba knockout cells. Re-expression of wild type Tuba rescued the brush border formation defect and resulted in brush borders of normal size, excluding potential off-target effects of the CRISPR/Cas9 procedure used to generate the knockout cells (Fig. 3b, e, f). In contrast, whereas expression of

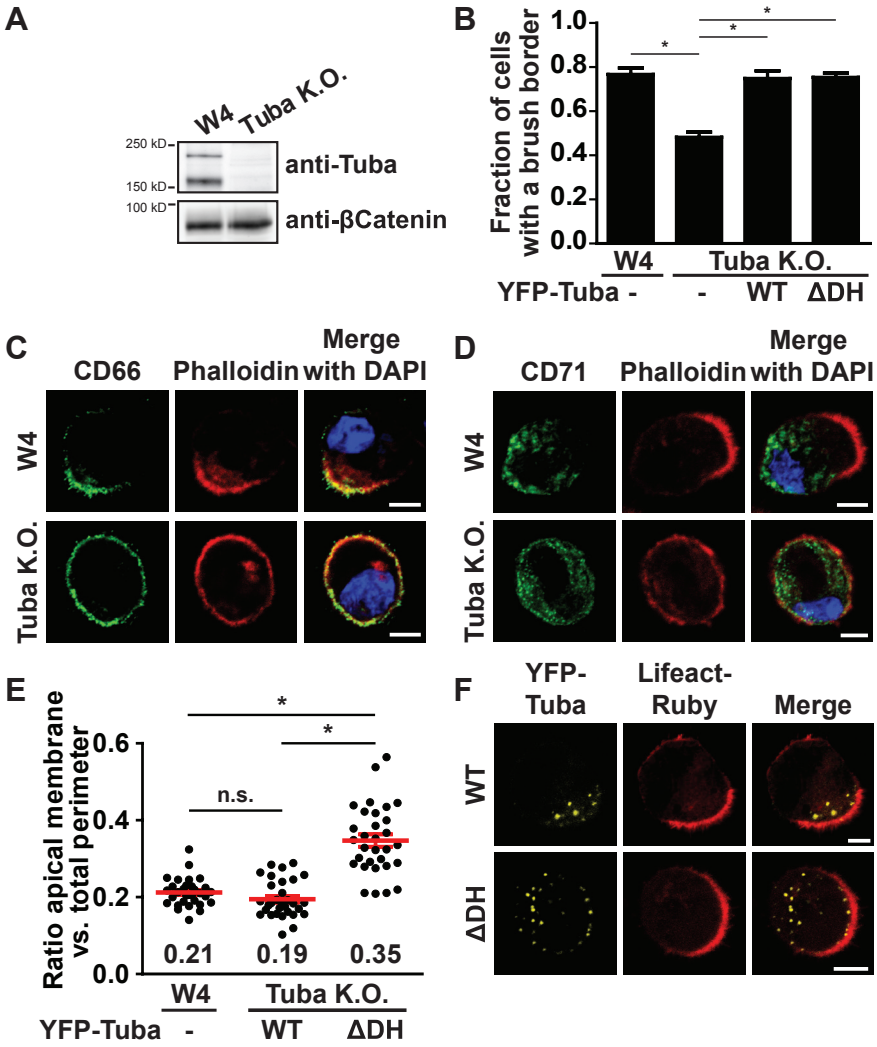

Figure 3: Tuba has a Cdc42 dependent and independent function during enterocyte polarization. (**a**) Western blot of W4 and W4:Tuba k.o. cell lysate, probed for Tuba and ßCatenin. (**b**) Quantification of brush border formation in W4 cells or Tuba k.o. cells expressing lifeact-ruby alone or in combination with YFP-Tuba(WT) or YFP-Tuba(ΔDH). Error bars are s.e.m. (n = 3) * $p < 0.05$ using independent samples t-test. (**c,d**) Immunofluorescence of W4 or Tuba k.o. cells stained for the apical membrane marker CD66 (**c**) and the basolateral marker (**d**). Scale bars indicate 5µm. (**e**) Quantification of brush border size in W4 cells expressing lifeact-ruby and Tuba k.o. cells expressing lifeact-ruby in combination with YFP-Tuba(WT) or YFP-Tuba(ΔDH). Red lines indicate the average and s.e.m (n = 30 in 3 independent experiments). * $p < 0.05$ using independent samples t-test. n.s. not significant (p > 0,05) (**f**) Representative images of Tuba k.o. cells expressing lifeact-ruby and YFP-Tuba(WT) or YFP-Tuba(ΔDH). Scale bars indicate 5µm.

Tuba(ΔDH) was able to restore brush border formation, it resulted in the formation of brush borders that were larger in size, the phenotype associated with defective Cdc42 clustering in Ls174T:W4 cells (Fig. 3b, e, f). This therefore demonstrates that Tuba, next to a Cdc42-independent function in cell polarization, is required for apical membrane clustering in polarized Ls174T:W4 cells.

Next we addressed whether Tuba contributes to the diffusive behavior of Cdc42 in polarized Ls174T:W4 cells. For this we determined the apical eviction half life of wild type Cdc42 and Cdc42(G12V) in polarized Ls174T:W4 cells and in the fraction of Tuba knockout cells that were polarized. We found that the mobility of wild type Cdc42 is minimally affected by Tuba loss (10.3 s. in W4 cells vs. 8.4 s. in Tuba knockout cells) (Fig. 4a, b). In contrast, Cdc42(G12V) was more rapidly lost from the apical membrane in Tuba knockout cells (220 s. vs. 157 s.), demonstrating that Tuba selectively affects the mobility of active Cdc42 (Fig. 4c, d).

In order to test whether the effect of Tuba on Cdc42 mobility is dependent on Tuba's GEF activity towards Cdc42 we assessed the mobility of Cdc42 in Ls174T:W4 cells stably overexpressing either wild type Tuba or catalytically inactive Tuba(ΔDH) (Supp. Fig. 3). As any promiscuous Cdc42GEF may decrease the mobility of wild type Cdc42 by increasing the fraction of RhoGDI-resistant Cdc42-GTP, we used Cdc42(R66E) to address whether Tuba is able to immobilize Cdc42 in a RhoGDI-independent manner. Indeed, we find that overexpression of wild type Tuba is able to decrease the mobility of Cdc42(R66E) at the apical membrane (Fig. 4e, f). This effect is dependent on the GEF activity of Tuba because overexpression of Tuba(ΔDH) did not lead to a similar deceleration of Cdc42(R66E) (Fig. 4e, f). Therefore, these data demonstrate that Tuba selectively immobilizes activated Cdc42 and is thus required to enable differential mobility between GDP- and GTP-bound Cdc42.

Finally, we tested whether Tuba-mediated immobilization of Cdc42 affects Cdc42 clustering at the apical membrane. In agreement with previous reports we find that YFP-Cdc42 accumulates poorly at the apical membrane in polarized Tuba knockout cells demonstrating a crucial role for Tuba in establishing localized Cdc42 signaling[17] (Fig. 4g, h).

Discussion

Here we show that during enterocyte polarization the mobility of Cdc42 at the apical membrane is governed via a two-faced mechanism: on the one hand RhoGDI-mediated membrane dissociation results in selective mobilization of inactive Cdc42, whereas on the other hand activated Cdc42 is selectively immobilized by the Cdc42GEF Tuba. The combined effect of this dual regulation is a switch-like behavior in Cdc42 mobility resulting in an over 30-fold decrease in Cdc42 mobility upon activation. This switch-like diffusive behavior ensures that upon GTP-loading Cdc42 signaling remains spatially restricted and may therefore be important for many biological processes which involve localized Cdc42 signaling. Indeed, we show that interference with the mechanisms that enable differential Cdc42 mobility impedes local Cdc42 signaling during enterocyte polarization resulting in an inability to cluster the apical membrane.

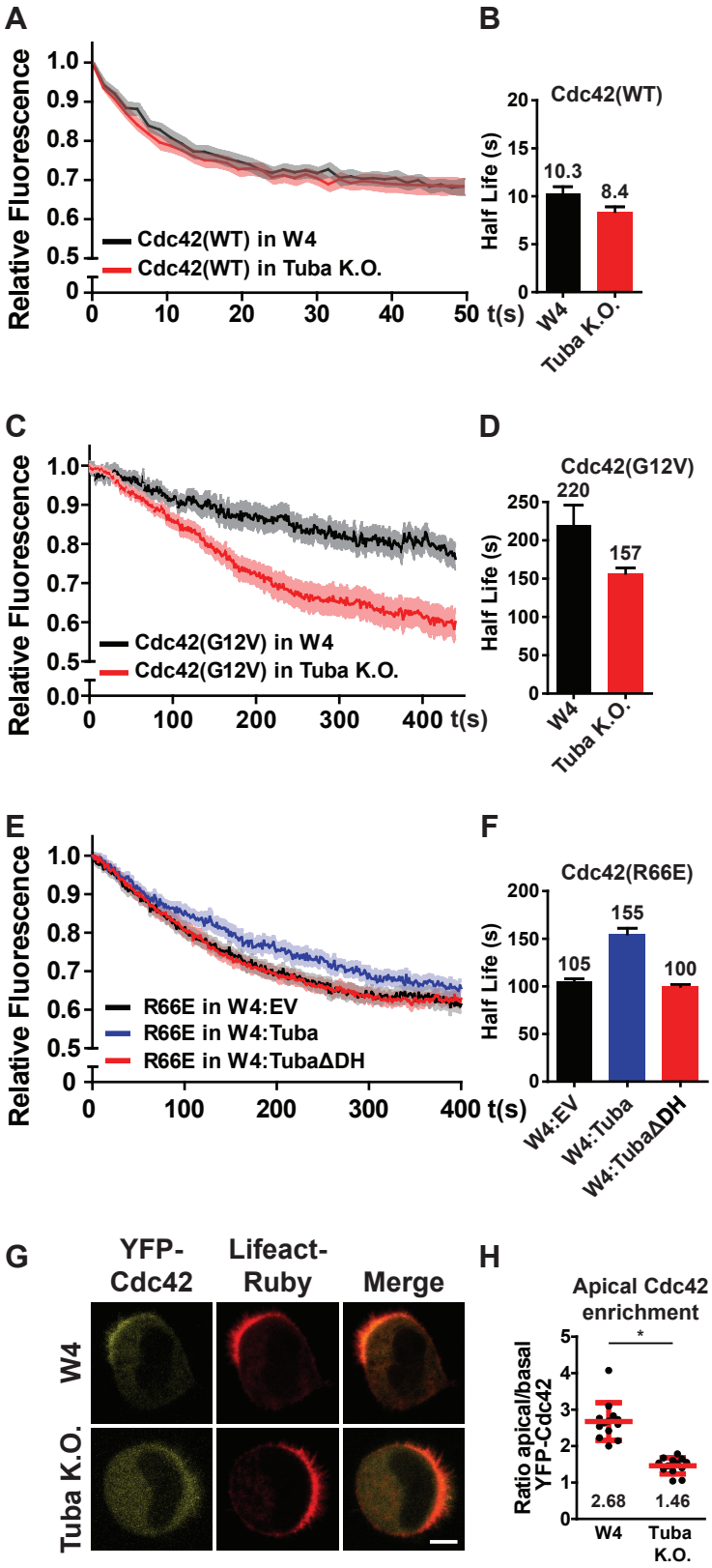

Figure 4: Tuba selectively immobilizes activated Cdc42 at the apical membrane. (**a**) Average normalized fluorescence decay traces of Dendra-Cdc42(WT) in W4 cells (black line, n = 8) and Dendra-Cdc42(WT) in Tuba k.o. cells (red line, n = 11). (**b**) Eviction half-lives for Dendra-Cdc42(WT) in W4 and Tuba k.o. cells determined from average decay traces shown in a using curve fitting. (**c**) Average normalized fluorescence decay traces of Dendra-Cdc42(G12V) in W4 cells (black line, n = 14) and Dendra-Cdc42(G12V) in Tuba k.o. cells (red line, n = 16). (**d**) Eviction half-lives for Dendra-Cdc42(G12V) in W4 and Tuba k.o. cells determined from average decay traces shown in c using curve fitting. (**e**) Average normalized fluorescence decay traces of Dendra-Cdc42(R66E) in W4:EV cells (black line, n = 20), in Tuba overexpressing cells (blue line, n = 17), and Tuba(ΔDH) overexpressing cells (black line, n = 20). (**f**) Eviction half-lives for Dendra-Cdc42(R66E) in W4:EV, Tuba overexpressing, or Tuba(ΔDH) overexpressing cells determined from average decay traces shown in e using curve fitting. Light areas in a, c and e reflect s.e.m. Error bars in b, d and f represent the 95% confidence interval of the fit. (**g**) Localization of YFP-Cdc42 in W4 and Tuba k.o. cells in combination with lifeact-ruby. Scale bars indicate 5µm. (**h**) Quantification of apical membrane enrichment of YFP-Cdc42 in polarized W4 or Tuba k.o. cells. Red lines indicate the average and s.d. (W4: n = 13; Tuba k.o. n = 13; in 3 independent experiments). * $p < 0.05$ using independent samples t-test.

We show that the Cdc42-specific GEF Tuba is required for apical membrane clustering, in a manner dependent on its catalytic GEF domain. However, we also notice that Tuba knockout cells have reduced brush border formation capacity, a phenotype that is not dependent on Cdc42. We therefore reveal that Tuba has a dual function during cell polarization: one Cdc42-dependent function in apical membrane clustering and a second Cdc42-independent function in apical membrane formation. The notion that Tuba has a function in cell polarization independent of its GEF activity can explain recent findings in zebrafish where Tuba knockdown results in a set of phenotypes that are not fully phenocopied by Cdc42 depletion[18]. The molecular mechanism of Tuba's Cdc42-independent polarity function remains elusive, but it has been reported that Tuba binds many actin modulators that are important during cell polarization[20].

An important consequence of our finding that Tuba is able to specifically immobilize activated Cdc42 is that Tuba not only provides temporal control but also spatial control over Cdc42 signaling. By generating a pool of immobile, active Cdc42 molecules Tuba enables clustering of active Cdc42. Indeed, we found that Cdc42 enrichment at the apical membrane is decreased in Tuba knockout cells, in agreement with previous findings in MDCK cysts[17]. This poses the question how Tuba itself becomes localized during cell polarization. We speculate that, analogous to yeast cell polarization, this may involve recruitment by activated Cdc42, thereby establishing a positive feedback mechanism for Cdc42 clustering. In support of this idea, we find that whereas localization of wild type Tuba is mostly restricted to the apical domain, TubaΔDH localization is more scattered and not exclusively apical.

Although Tuba-mediated activation of Cdc42 enables differential mobility by both immobilizing Cdc42-GTP and by generating RhoGDI-resistant Cdc42-GTP, RhoGDI-mediated membrane dissociation of Cdc42-GDP is required for clustered Cdc42 signaling. We find that RhoGDI is required to maximize the differential mobility because whereas in the absence of RhoGDI Tuba allows for only a 2,5-fold reduction in Cdc42 mobility upon GTP loading, the presence of RhoGDI results in a 30-fold deceleration of Cdc42 upon activation. Therefore, our findings suggest that RhoGDI is required for Cdc42 clustering by maximizing the difference between mobility of inactive and active Cdc42.

Differential diffusion of an inactive and active signaling molecule is one of the central requirements for a Turing-like reaction-diffusion system[21]. Interestingly, it has been shown that the dynamics of Cdc42 clustering during yeast cell polarization can be described by a Turing-type model, where Cdc42-GDP and Cdc42-GTP meet the requirements for a Turing type "inhibitor" and "activator" respectively[22]. Therefore, we speculate that Cdc42 dynamics during enterocyte polarization may also be governed by a Turing-type reaction-diffusion system.

What makes this interesting from a biological perspective is that a Turing-type clustering mechanism can mathematically account for complex biological phenomena such as symmetry breaking and ensuring singularity in apical membrane formation[22,23].

In summary, we show how differential diffusion of active and inactive Cdc42 is enabled by a molecular network comprised of a small GTPase, GEF and GDI. Because of this simple network organization it is expected that similar regulation of diffusive behavior occurs in wide range of biological processes involving localized signaling by small GTPases.

Materials and Methods

Cell culture and plasmids

Ls174T:W4 cells were cultured in RPMI1640 (Sigma) supplemented with 10% FBS (Lonza) and antibiotics. Polarization was induced by culturing Ls174T:W4 cells in medium containing 1 μg/ml doxycycline (Sigma) for at least 16h. For transient expression of DNA constructs, cells were transfected using XtremeGene9 (Roche) according to the manufacturer's guidelines.

Dendra-Cdc42 constructs were generated by introducing a Cdc42 PCR product in pDendra2-C2 using In-Fusion (Clontech). G12V and R66E mutations were introduced by site-directed mutagenesis. pcDNA-HA-Tuba was provided by Pietro di Camilli. This construct served a template to generate full length Tuba or TubaΔDH entry clones which were subsequently N-terminally tagged with YFP using Gateway cloning (Invitrogen). miniTol2 constructs for stable overexpression of untagged Tuba were generated by introducing full length or TubaΔDH PCR products in miniTol2-EF1α-MCS-PGK-PuroR using In-Fusion. pCMV-Transposase was provided by Stephen Ekker and Lifeact-Ruby was provided by R. Wedlich-Soldner.

Antibodies

The following antibodies were used for immunofluorescence: mouse anti-CD66 (BD Biosciences, 1:500), mouse anti-CD71 (H68.4, Life Technologies, 1:1000). For Western blotting the following antibodies were used: rabbit anti-DNMBP (Sigma, 1:2000), mouse anti-ßCatenin (BD biosciences, 1:5000), mouse anti-GFP (clones 7.1 and 13.1, Roche, 1:5000), mouse anti-V5 (Invitrogen, 1:5000) and mouse anti-αTubulin (Calbiochem, 1:5000).

Generation of RhoGDIα knockdown, Tuba knockout and Tuba overexpression cell lines

For stable knockdown of RhoGDIα, Ls174T-W4 cells were infected for two successive days with lentiviral shRNA constructs (Mission library, Sigma) and subsequently selected for puromycin resistance. To stably deplete RhoGDIα five pooled short hairpins were used with the following targeting sequences: shRNA#1

5'-AGCTTCAAGAAGCAGTCGTTT-3', shRNA#2 5'-CGTCTAACCATGATGCCT-TAA-3', shRNA#3 5'-CAAGATTGACAAGACTGACTA-3', shRNA#4 5'-CCGCT-TCACAGACGACGACAA-3', shRNA#5 5'-GACTACATGGTAGGCAGCTAT-3'. Tuba knockout Ls174T:W4 cells were generated using CRISPR/Cas9-mediated gene disruption as previously reported3. Briefly, Ls174T:W4 cells were transfected with pSpCas9(BB)-2A-GFP (PX458), encoding an sgRNA (AAGAGACTACAT-TCGGGATC) targeting the exon encoding the DH domain of Tuba. GFP-positive cells were sorted and clonally expanded. Genomic DNA of candidate clones was sequenced and absence of Tuba protein was confirmed by Western blotting.

For stable overexpression of untagged Tuba, Ls174T:W4 were transiently cotransfected with miniTol2-Tuba constructs and Tol2 transposase in a 2:1 ratio. Three days after transfection cells were selected for puromycin resistance and continuously cultured in the presence of puromycin (10μg/ml). Monoclonal cell lines were established by serial dilution and presence of Tuba was assessed by Western blotting.

Live cell imaging

Two days after transfection, Ls174T:W4 were trypsinized and plated onto glass-bottom dishes (WillCo Wells) in the presence of doxycycline. Before imaging, medium was replaced with HEPES-buffered (pH = 7.4) Leibovitz's L-15 medium (Invitrogen). Cells were imaged at 37 ºC using an Axioskop2 LSM510 scanning confocal microscope (Zeiss) with a 63x magnification oil objective (PLAN Apochromat, NA 1.4) using Zen image acquisition software. To determine apical membrane size, the fraction of cell membrane that was covered with microvilli was determined using ImageJ software. Average apical membrane sizes were compared using independent samples t-test in SPSS with a p-value <0.05 as a cutoff for significance.

Apical enrichment of YFP-Cdc42 was quantified by making a line plot through the apical and basal membrane using ImageJ and subsequently determining the ratio between average apical and basal membrane pixel intensities. Average enrichment ratios were compared using independent samples t-test in SPSS with a p-value <0.05 as a cutoff for significance.

Apical membrane eviction rates

To determine apical mobility of Cdc42 cells were transfected with Dendra-Cdc42. After two days, cells were split and seeded onto glass-bottom dishes in the presence of doxycycline. Before imaging, medium was replaced with HEPES-buffered (pH = 7.4) Leibovitz's L-15 medium. Photoconversion experiments were performed on a Leica SP8x microscope equipped with a temperature- and CO_2-controlled chamber using a 63x oil objective (HC PL APO 63x/1.40) with Leica LAS AF image acquisition software. Local Dendra photoconversion in the brush border was done using a pulse of 405 nm laser light. Cells were subsequently

imaged at a frame rate of 1.5s. To determine the average decay rate, the ratio of the average intensity of red signal in the brush border and the average intensity of red signal in the whole cell was determined. Moving regions-of-interest were used to correct for cell movements during imaging. For each cell ratios were normalized and traces were averaged to generate an average fluorescence decay trace. Using Matlab software, these curves were fitted with the general formula: f(x) = a * e^(-b*x) + c. An average half-life was determined from the fitted curve and expressed with the 95% CI of the fit.

Immunofluorescence

Cells were seeded on glass cover slips in the presence of doxycycline and subsequently fixed in 4% methanol-free formaldehyde (Electron Microscopy Sciences) for 30 min, permeabilized in 2% Trition X-100 in PBS for 10 min and blocked in 0,2% BSA in PBS for 1h. Slides were then incubated with primary antibody for at least 16h, washed three times with PBS and incubated with Alexa-488 coupled secondary antibody in the presence of DAPI and Phalloidin-Alexa568 (ThermoFisher) for at least 4h. After PBS washes slides were mounted and imaged using an Axioskop2 LSM510 scanning confocal microscope (Zeiss) with a 63x magnification oil objective (PLAN Apochromat, NA 1.4) using Zen image acquisition software.

Immunoprecipitation

HEK293T cells were cultured in DMEM (Sigma) containing 10% FBS (Sigma) and antibiotics. Two days after transfection, cells were lysed in RAL buffer (1% Nonidet P-40 substitute; 10% glycerol; 50 mM Tris-HCl pH 7.4; 2.0 mM MgCl2; 200 mM NaCl; protease and phosphatase inhibitors) on ice. Lysates were cleared by centrifugation and incubated with GFP-binding protein (GBP)-agarose beads for 2h at 4ºC while rotating. Beads were washed with RAL buffer for three times and eluted in sample buffer.

Cdc42-GTP was precipitated using PAK1-PBD-agarose beads (Millipore) according to the manufacturer's instructions. To assess geranylgeranylation, transfected cells were incubated in medium containing 50µM geranylgeranyl alcohol azide (Life Technologies) for 24h. Labeled YFP-Cdc42 was precipitated from cleared lysates and functionalized with alkyne cyanine-718 (Sigma) using Copper(I)-catalyzed azide-alkyne cycloaddition. For this beads were resuspended in 94µl PBS and 6µl of click reaction mix was added, containing 10µM alkyne cyanine-718, 1mM tris(2-carboxyethyl)phosphine (TCEP), 100µM tris[(1-benzyl-1H-1,2,3-triazol-4-yl)methyl]amine (TBTA), and 1mM $CuSO_4$. Beads incubated for 2h at room temperature while rotating, washed three times with 1% Nonidet P-40 substitute in PBS and eluted in sample buffer. Samples were subjected to SDS-PAGE and cyanine-718 labeling was detected by in-gel fluorescence imaging using a LICOR Odyssey system.

Quantitative PCR

RNA was isolated from cells using the RNeasy mini kit (Qiagen) according to the manufacturer's instructions. 1.5µg of total RNA was used for cDNA synthesis using the iScript cDNA synthesis kit (Biorad) and subjected to quantitative PCR using the Faststart universal SYBR green master mix (Roche). cDNA was amplified on a C1000 Thermal Cycler (Bio-Rad) using the following primers: ARHGDIA_fw 5'-CGAACCCTCCGGTGTCC-3' and ARHGDIA_rv 5'-TTGTAGTTGACCGAGTGCTCATC-3'. Expression levels were normalized to GAPDH and HPRT1 mRNA levels. The data presented is the average of three biological replicates which each contained three technical replicates.

Acknowledgments

We thank Bas Ponsioen for assistance in microscopy data analysis. We would like to thank all members of our lab for continuous support and discussion.

References

1 Etienne-Manneville, S. Cdc42--the centre of polarity. Journal of cell science 117, 1291-1300, doi:10.1242/jcs.01115 (2004).
2 Bryant, D. M. et al. A molecular network for de novo generation of the apical surface and lumen. Nature cell biology 12, 1035-1045, doi:10.1038/ncb2106 (2010).
3 Bruurs, L. J. et al. ATP8B1-mediated spatial organization of Cdc42 signaling maintains singularity during enterocyte polarization. J Cell Biol 210, 1055-1063, doi:10.1083/jcb.201505118 (2015).
4 Jaffe, A. B., Kaji, N., Durgan, J. & Hall, A. Cdc42 controls spindle orientation to position the apical surface during epithelial morphogenesis. J Cell Biol 183, 625-633, doi:10.1083/jcb.200807121 (2008).
5 Wu, C. F. et al. Role of competition between polarity sites in establishing a unique front. Elife 4, doi:10.7554/eLife.11611 (2015).
6 Slaughter, B. D., Das, A., Schwartz, J. W., Rubinstein, B. & Li, R. Dual modes of cdc42 recycling fine-tune polarized morphogenesis. Developmental cell 17, 823-835, doi:10.1016/j.devcel.2009.10.022 (2009).
7 Ozbudak, E. M., Becskei, A. & van Oudenaarden, A. A system of counteracting feedback loops regulates Cdc42p activity during spontaneous cell polarization. Developmental cell 9, 565-571, doi:10.1016/j.devcel.2005.08.014 (2005).
8 Klunder, B., Freisinger, T., Wedlich-Soldner, R. & Frey, E. GDI-mediated cell polarization in yeast provides precise spatial and temporal control of Cdc42 signaling. PLoS computational biology 9, e1003396, doi:10.1371/journal.pcbi.1003396 (2013).
9 Bendezu, F. O. et al. Spontaneous Cdc42 Polarization Independent of GDI-Mediated Extraction and Actin-Based Trafficking. PLoS Biol 13, e1002097, doi:10.1371/journal.pbio.1002097 (2015).
10 Freisinger, T. et al. Establishment of a robust single axis of cell polarity by coupling multiple positive feedback loops. Nat Commun 4, 1807, doi:10.1038/ncomms2795 (2013).
11 Woods, B., Kuo, C. C., Wu, C. F., Zyla, T. R. & Lew, D. J. Polarity establishment requires localized activation of Cdc42. The Journal of Cell Biology 211, 19-26, doi:10.1083/jcb.201506108 (2015).
12 Howell, A. S. et al. Singularity in polarization: rewiring yeast cells to make two buds. Cell 139, 731-743, doi:10.1016/j.cell.2009.10.024 (2009).
13 Baas, A. F. et al. Complete polarization of single intestinal epithelial cells upon activation of LKB1 by STRAD. Cell 116, 457-466 (2004).
14 Leonard, D. et al. The identification and characterization of a GDP-dissociation inhibitor (GDI) for the CDC42Hs protein. J Biol Chem 267, 22860-22868 (1992).
15 Johnson, J. L., Erickson, J. W. & Cerione, R. A. New insights into how the Rho guanine nucleotide dissociation inhibitor regulates the interaction of Cdc42 with membranes. J Biol

Chem 284, 23860-23871, doi:10.1074/jbc.M109.031815 (2009).
16 Kovacs, E. M., Verma, S., Thomas, S. G. & Yap, A. S. Tuba and N-WASP function cooperatively to position the central lumen during epithelial cyst morphogenesis. Cell Adhesion & Migration 5, 344-350, doi:10.4161/cam.5.4.16717 (2014).
17 Qin, Y., Meisen, W. H., Hao, Y. & Macara, I. G. Tuba, a Cdc42 GEF, is required for polarized spindle orientation during epithelial cyst formation. J Cell Biol 189, 661-669, doi:10.1083/jcb.201002097 (2010).
18 Baek, J. I. et al. Dynamin Binding Protein (Tuba) Deficiency Inhibits Ciliogenesis and Nephrogenesis in Vitro and in Vivo. J Biol Chem 291, 8632-8643, doi:10.1074/jbc.M115.688663 (2016).
19 Otani, T., Ichii, T., Aono, S. & Takeichi, M. Cdc42 GEF Tuba regulates the junctional configuration of simple epithelial cells. J Cell Biol 175, 135-146, doi:10.1083/jcb.200605012 (2006).
20 Salazar, M. A. et al. Tuba, a novel protein containing bin/amphiphysin/Rvs and Dbl homology domains, links dynamin to regulation of the actin cytoskeleton. J Biol Chem 278, 49031-49043, doi:10.1074/jbc.M308104200 (2003).
21 Turing, A. M. The Chemical Basis of Morphogenesis. Philosophical Transactions of the Royal Society of London B: Biological Sciences 237, 37-72 (1952).
22 Goryachev, A. B. & Pokhilko, A. V. Dynamics of Cdc42 network embodies a Turing-type mechanism of yeast cell polarity. FEBS letters 582, 1437-1443, doi:10.1016/j.febslet.2008.03.029 (2008).
23 Wu, C. F. & Lew, D. J. Beyond symmetry-breaking: competition and negative feedback in GTPase regulation. Trends in cell biology 23, 476-483, doi:10.1016/j.tcb.2013.05.003 (2013).

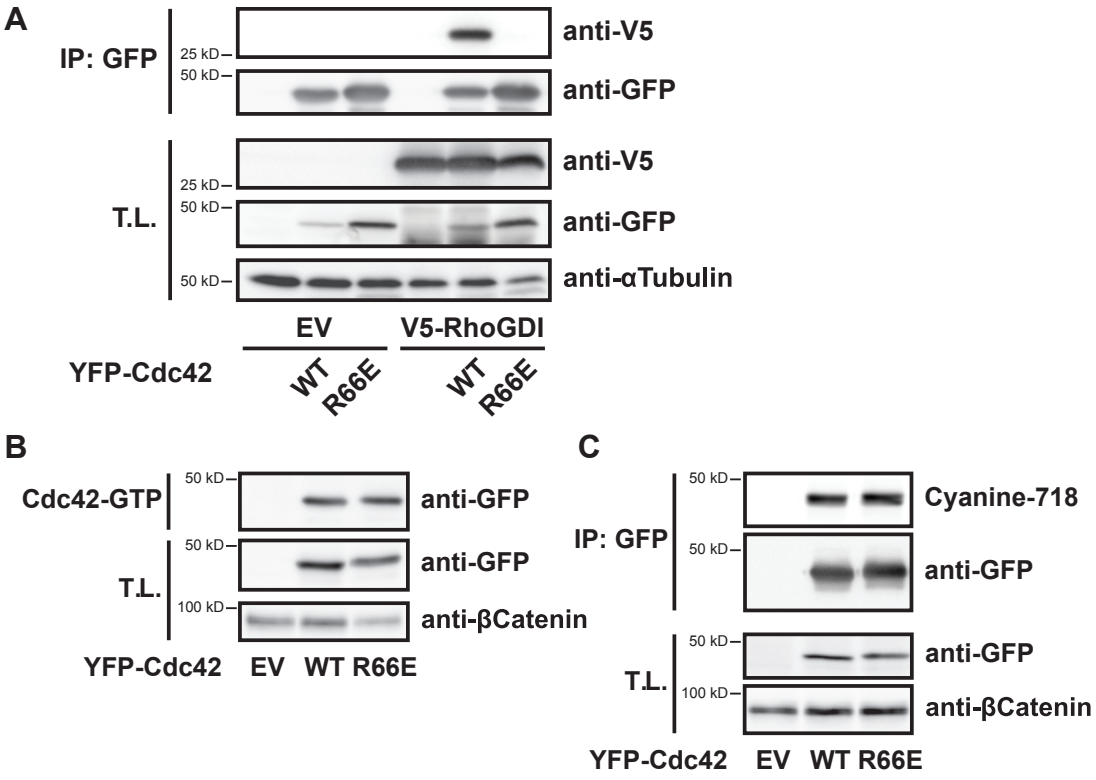

Supplementary Figure 1: Cdc42(R66E) abrogates RhoGDI binding without affecting global GTP loading or lipid modification.
(**a**) Co-immunoprecipitation of YFP-Cdc42(WT) or YFP-Cdc42(R66E) with V5-RhoGDI in HEK293T cells. (**b**) Cdc42-GTP pulldown of YFP-Cdc42(WT) or YFP-Cdc42(R66E) from HEK293T lysates. (**c**) Cyanine-718 labeling of geranylgeranylated YFP-Cdc42(WT) or YFP-Cdc42(R66E) in HEK293T cells.

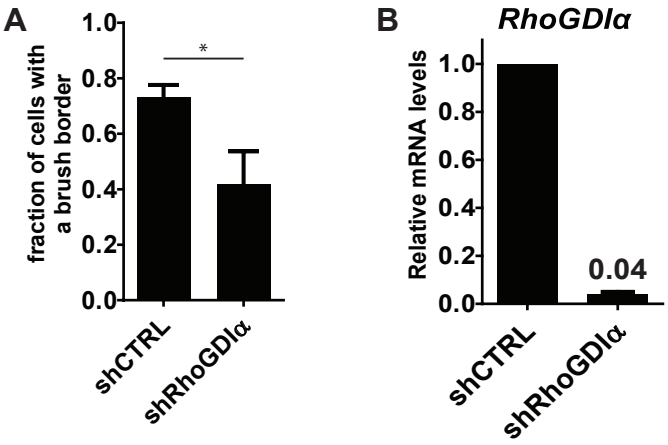

Supplementary Figure 2: Knockdown of RhoGDIα inhibits brush border formation.
(**a**) Quantification of brush border formation in W4:shCTRL and W4:shRhoGDIα cells. Error bars indicate s.e.m. (n = 3). * $p < 0.05$ using independent samples t-test. (**b**) Relative mRNA levels of RhoGDIα in W4:shCTRL and W4:shRhoGDIα cells as determined by QPCR. Error bars indicate s.e.m. (n = 3).

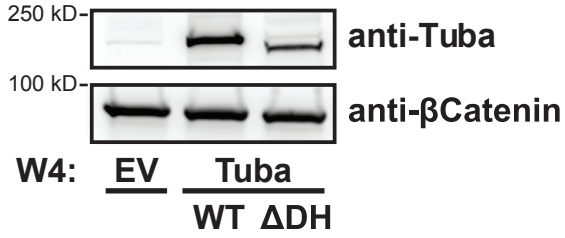

Supplementary Figure 3: Stable overexpression of Tuba or Tuba(ΔDH)
Western blot of W4:EV, W4:Tuba and W4:Tuba(ΔDH) cell lysates probed for Tuba and ßCatenin.

IV

4

Apical membrane clustering requires interacting phosphatases PTEN and PTPL1

Lucas J.M. Bruurs, Mirjam C. van der Net, Susan Zwakenberg, Axel Rosendahl Huber, Maaike Y. Kapteijn, Anneke Post, Fried J. Zwartkruis, Johannes L. Bos

Abstract
PTEN is a tumor suppressor that is frequently lost in epithelial malignancies. Part of the tumor suppressive properties of PTEN is attributed to its function in cell polarization and consequently its role in maintaining epithelial tissue integrity. Nevertheless, surprisingly little is known about the function and regulation of PTEN during epithelial cell polarization.

We used CRISPR/Cas9-mediated gene disruption to delete PTEN in polarized Ls174T:W4 cells. We show that PTEN knockout Ls174T:W4 cells form a brush border that covers the entire plasma membrane. Therefore we demonstrate that PTEN is not required for the formation of an apical membrane but instead is required for apical membrane clustering in polarized Ls174T:W4 cells. For this PTEN binds the tumor suppressor PTPL1, a PDZ domain containing protein phosphatase that is located at the apical membrane and which itself is also required for apical membrane clustering. We show that the interaction between PTEN and PTPL1 is necessary to ensure apical membrane enrichment of PTEN and is therefore required for clustering of the apical domain.

From these findings we conclude that PTEN is necessary for apical membrane clustering and that this requires spatial regulation of PTEN by PTPL1. Since disruption of cell polarity and tissue integrity are hallmarks of cancer, regulation of apical membrane clustering by PTEN may be relevant for tumorigenesis and might contribute to the tumor suppressive properties of PTEN and PTPL1.

Introduction

Control over cell polarization contributes to the maintenance of epithelial tissue integrity and thereby provides a barrier in tumorigenesis[1-3]. The tumor suppressor PTEN is frequently lost in epithelial malignancies and loss of PTEN often coincides with loss of epithelial tissue integrity[4,5]. PTEN is a lipid phosphatase that is primarily implicated in the conversion of phosphatidylinositol-3,4,5 triphosphate ($PI3,4,5P_3$) to phosphatidylinositol-4,5 bisphosphate ($PI4,5P_2$), thereby counteracting the activity of phosphatidylinositol 3-kinase (PI3K)[6,7]. Furthermore, PTEN also has protein phosphatase activity and can function as a scaffold in a phosphatase-independent manner[4].

In addition to its well-documented function in antagonizing PI3K/PKB signaling, PTEN has a role in the regulation of cell polarization via which it contributes to epithelial tissue integrity[8-14]. Nonetheless, the role of PTEN during polarity establishment is subject to debate: Martin-Belmonte et al. reported that PTEN is required for the formation of an apical plasma membrane and is therefore necessary for lumen formation in MDCK cyst cultures[14]. Similar results were subsequently reported using 3D mammary gland cultures and CaCO2 cysts[10,15]. In contrast, recent findings in (inducible) PTEN knockout mice demonstrated that although lumen morphology is altered, apical membrane formation is not impaired in epithelial cells that have lost PTEN[8,9]. Therefore, it remains unclear how PTEN is involved in epithelial cell polarization and via which mechanisms PTEN is regulated in this process.

We studied the role of PTEN in cell polarization in the Ls174T:W4 colon carcinoma cell line[16]. These cells can polarize in the absence of cell-cell junctions by forced activation of LKB1, induced by doxycycline-controlled expression of its coactivator STRADα[16]. We show that loss of PTEN in Ls174T:W4 cells results in the formation of an apical brush border that covers the entire cell perimeter, thereby revealing a role for PTEN in apical membrane clustering. We find a similar clustering defects in cells depleted for PTPL1 (or PTPN13, PTP-BAS, FAP1), a protein tyrosine phosphatase that binds PTEN and a putative tumor suppressive protein. Furthermore, we demonstrate that the interaction between PTPL1 and PTEN is required to enrich PTEN at the apical plasma membrane and is therefore required for apical membrane clustering. Our results therefore demonstrate a crucial role for PTEN in controlling apical membrane clustering and identify PTPL1 as a PTEN-binding partner required in this process.

Results

To study the function of PTEN during epithelial cell polarization, we established PTEN knockout Ls174T:W4 cells using CRISPR/Cas9 mediated gene disruption (Fig. 1a). In general, doxycycline-induced polarization of Ls174T:W4 cells results in the formation of a basolateral domain and a microvilli-covered apical domain.

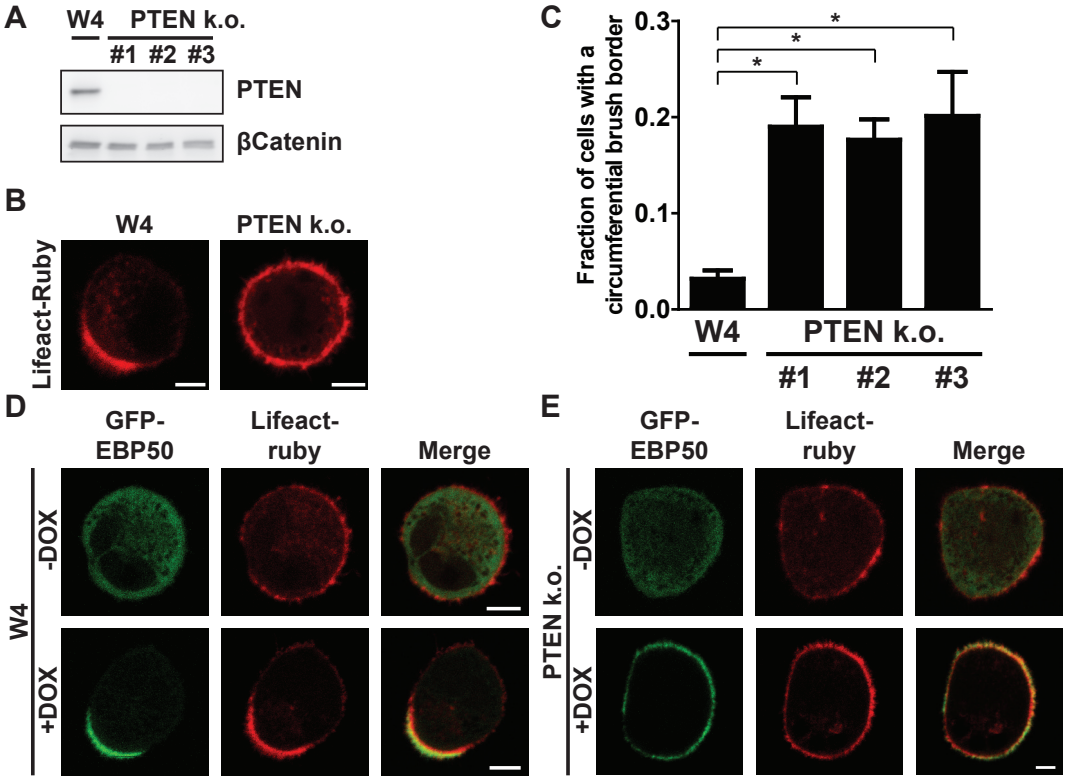

Figure 1: PTEN knockout W4 cells can not restrict apical membrane formation
(**a**) Western blot of W4 cell and PTEN k.o. cell lysates probed for PTEN and ßCatenin. (**b**) Localization of the actin marker Lifeact-Ruby in polarized W4 cells and PTEN k.o. cells. Scale bars indicate 5µm. (**c**) Quantification of the fraction of cells that form an actin cap that covers the entire cell perimeter in W4 cells and PTEN knockout cells. Error bars represent s.e.m. in three experiments (n > 100 cells per experiment). * $p < 0,05$ using independent samples t-test. (**d**) Localization of the brush border marker GFP-EBP50 and Lifeact-Ruby in unpolarized (-DOX) and polarized (+DOX) W4 cells and PTEN k.o. cells. Scale bars indicate 5µm. DOX = doxycycline

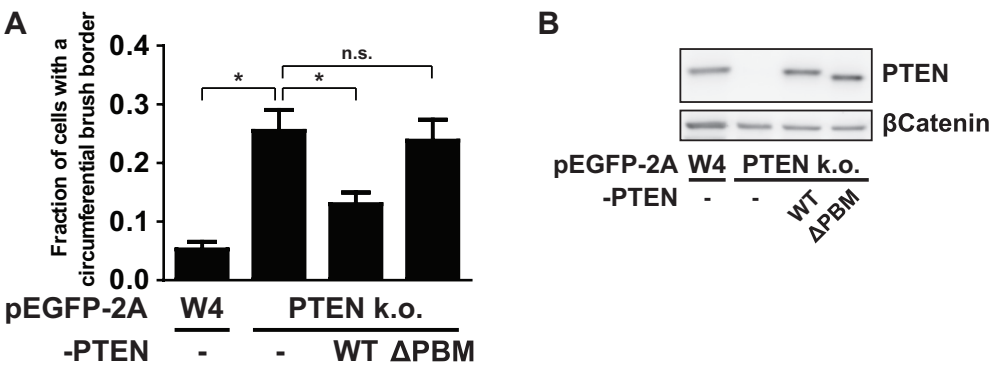

Figure 2: The PDZ binding motif of PTEN is required for apical membrane clustering
(**a**) Quantification of the fraction of cells that form a brush border that covers the entire cell perimeter in W4 cells and PTEN knockout cells expressing PTEN wt or ΔPBM. Error bars represent s.e.m. in three experiments (n > 100 cells per experiment). * $p < 0,05$ using independent samples t-test. n.s. not significant ($p > 0,05$) (**b**) Western blot of W4 cells and PTEN knockout cells expressing PTEN wt or ΔPBM probed for PTEN and ßCatenin.

In contrast, doxycycline-stimulated PTEN knockout cells were often completely covered with microvilli, as judged by the localization of the actin marker lifeact-ruby, suggesting that these cells only form an apical plasma membrane (Fig. 1b, c).

To demonstrate that the microvilli in PTEN knockout cells indeed represent a *bona fide* apical membrane we assessed the distribution of the brush border marker GFP-EBP50 in these cells[17]. Whereas GFP-EBP50 localizes uniformly cytosolic in unpolarized cells, it is almost exclusively located in the brush border of polarized W4 cells (Fig. 1d). Similarly, in unstimulated PTEN knockout cells GFP-EBP50 is mostly cytosolic, but upon doxycycline stimulation GFP-EBP50 is recruited to entire the plasma membrane (Fig. 1d). Therefore, these findings show that PTEN knockout cells form a dispersed apical plasma membrane that covers the entire surface of the cell.

Next we tested whether the C-terminal PDZ binding motif (PBM) of PTEN is important for PTENs' ability to control apical membrane size. For this, we re-expressed either wild type PTEN or PTENΔPBM in PTEN knockout cells and quantified the fraction of cells that formed an apical membrane that covered the complete cell perimeter. Whereas, re-expression of wild type PTEN resulted in a partial rescue of the PTEN knockout phenotype, PTENΔPBM expression did not lead to a similar decrease in the fraction of cells with a circumferential brush border (Fig. 2a, b). Therefore we conclude that PTEN regulation via its C-terminal PDZ binding motif is required for PTEN dependent apical membrane clustering.

Having demonstrated that the PDZ binding motif of PTEN is crucial for the function of PTEN in limiting apical membrane formation to a confined domain, we next focused on possible interaction partners that may be important for this function of PTEN. PTPL1 is a large multidomain protein tyrosine phosphatase that localizes to the apical membrane of polarized epithelial cells and is able to bind PTEN *in vitro* via its second PDZ domain[18,19]. Co-immunoprecipitation of PTPL1 with PTEN revealed that the full length proteins interact and this binding was lost when the PDZ binding motif of PTEN was deleted (Fig. 3a).

To assess the consequence of the interaction between PTEN and PTPL1 we determined the localization of YFP-PTEN and YFP-PTENΔPBM in polarized Ls174T:W4 cells. We find that whereas YFP-PTEN is concentrated at the apical membrane, YFP-PTENΔPBM does not show a similar enrichment in the brush border (Fig. 3b). Furthermore, in cells stably depleted for PTPL1, localization of YFP-PTEN mimics the diffuse localization of YFP-PTENΔPBM, indicating that PTPL1 binding to PTEN is important for the enrichment of PTEN at the apical plasma membrane (Fig. 3b).

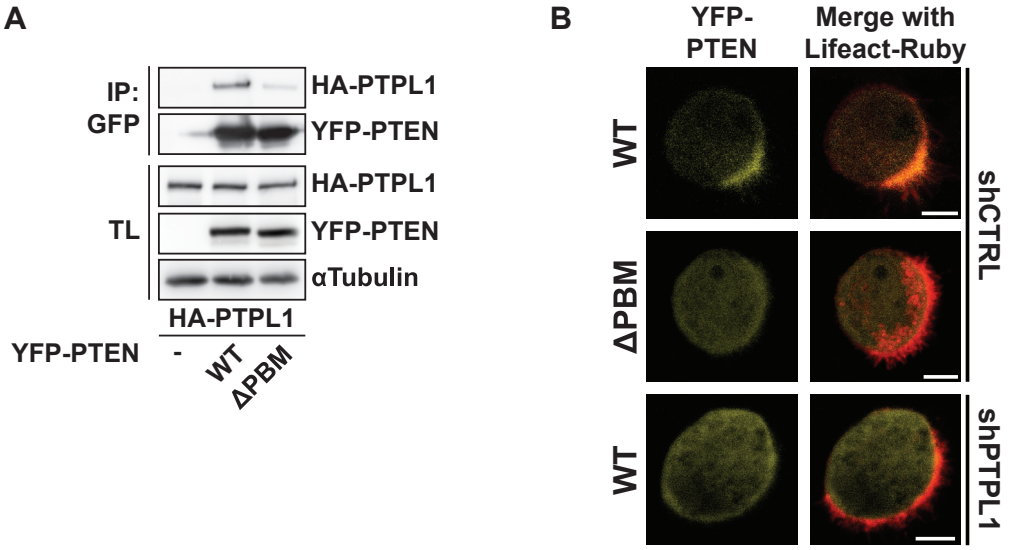

Figure 3: PTPL1 binds PTEN and ensures apical enrichment of PTEN
(**a**) Co-immunoprecipitation of HA-PTPL1 with YFP-PTEN wt and ΔPBM in HEK293T cells. (**b**) Localization of YFP-PTEN wt and ΔPBM in W4:shCTRL cells and YFP-PTEN wt in PTPL1-depleted cells in combination with Lifeact-Ruby. Scale bars indicate 5µm.

Next we tested whether PTPL1 has a function in controlling apical membrane size dimensions similar to PTEN. Although less severe compared to PTEN knockout cells, PTPL1-depleted cells also formed enlarged apical membranes, indicating that both proteins are required for apical membrane clustering (Fig. 4a, b, c). Similar to PTEN knockout cells, the microvilli on PTPL1-depleted cells are positive for the brush border marker GFP-EBP50 demonstrating that they represent a genuine apical membrane (Fig. 4d). In addition, segregation apical and basolateral proteins still occurs in PTPL1-depleted cells as judged by the distribution of apical (CD66) and basolateral (CD71) markers (Fig. 4e, f). These experiments therefore demonstrate that PTPL1 is required for the clustered formation of an apical plasma membrane.

In order to test the hypothesis that PTPL1 controls apical domain size by binding PTEN we generated PTPL1 mutants in which the PDZ domains responsible for PTEN were deleted (Fig. 5a). Although the second PDZ domain of PTPL1 is the only PDZ domain that can bind PTEN *in vitro*[19], deletion of PDZ2 only marginally reduced PTEN binding (Fig. 5b). Therefore, we additionally deleted PDZ1 and the region between PDZ1 and PDZ2 ('interregion'), which modulates PTEN binding *in vitro*[19], resulting in a further reduction in PTEN binding. Only deletion of all five PDZ domains resulted in a near-complete loss of PTEN binding, indicative of redundancy between PDZ domains for PTEN binding (Fig. 5b).

Next we tested whether the PTEN-binding defective PTPL1 mutants could restore normal apical membrane size in Ls174T:W4 cells in which endogenous

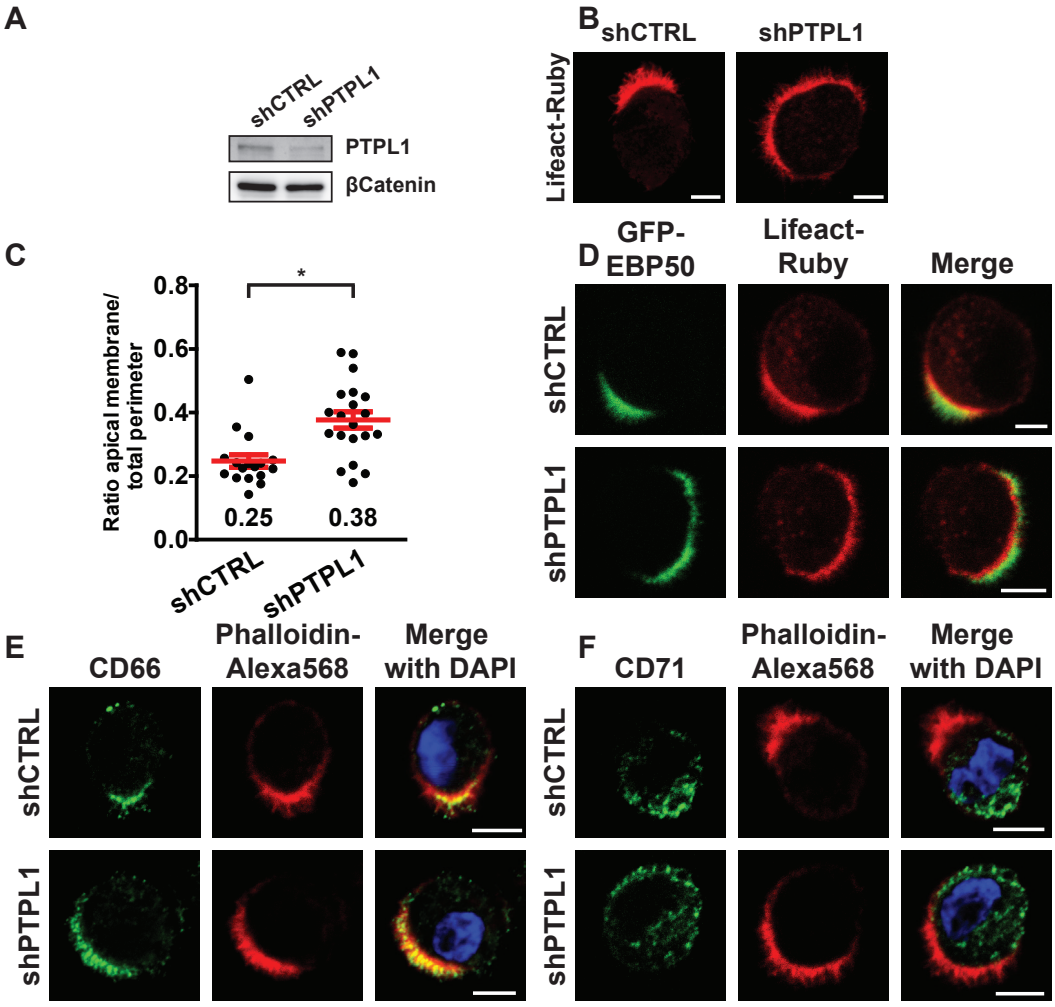

Figure 4: PTPL1 is required for apical membrane clustering
(**a**) Western blot of W4:shCTRL or W4:shPTPL1 lysates probed for PTPL1 and ß-Catenin. (**b**) Localization of Lifeact-Ruby in W4:shCTRL or PTPL1-depleted W4 cells. Scale bars indicate 5µm. (**c**) Quantification of apical membrane size in W4:shCTRL and W4:shPTPL1 cells. Red bars and values in graph represent the average. Red error bars represent s.e.m. ($n > 17$) * $p < 0{,}05$ using independent samples t-test. (**d,e,f**) Localization of the brush border marker GFP-EBP50 (**d**), apical membrane marker CD66 (**e**) and basolateral marker CD71 (**f**) in polarized W4:shCTRL and W4:shPTPL1 cells in combination with the actin markers Lifeact-Ruby or Phalloidin-Alexa568. Scale bars indicate 5µm.

PTPL1 was silenced. We found that the degree of rescue correlated with the ability to bind PTEN: whereas expression PTPL1(ΔPDZ2) restores normal brush border size similar as wild type PTPL1, PTPL1(ΔPDZ1-5) was unable to rescue PTPL1 depletion. Expression of PTPL1(ΔPDZ1-2) resulted in a partial rescue of apical membrane size (Fig. 5c). These findings therefore further support the hypothesis that PTEN binding to PTPL1 is required to control apical membrane size.

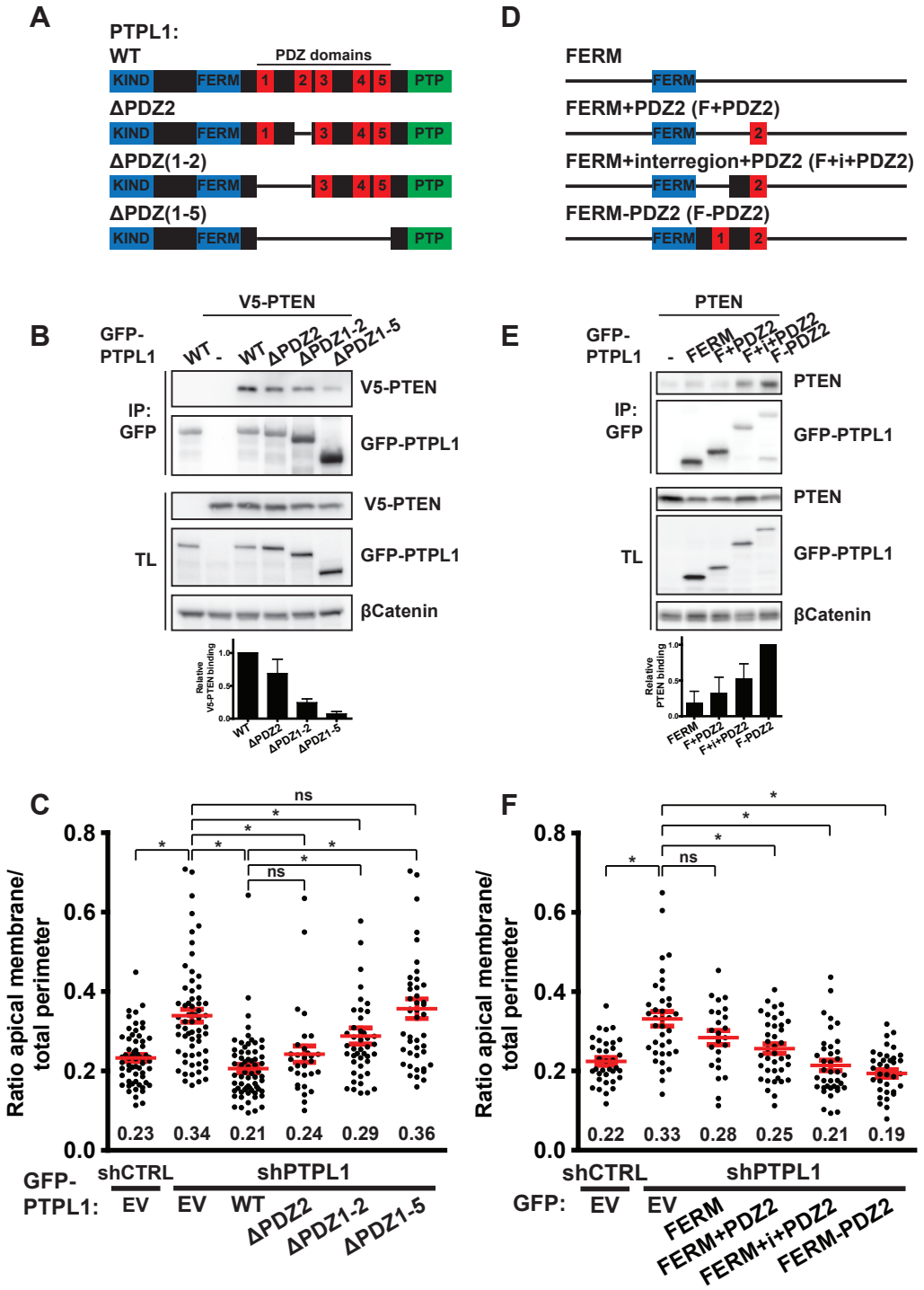

Figure 5: PTPL1 binding is required for PTEN-dependent apical membrane clustering
(**a**) Schematic representation of PTPL1 mutants. KIND = kinase non-catalytic C-lobe domain, FERM = 4.1, Ezrin, Radixin, Moesin domain, PTP = protein tyrosine phosphatase domain. (**b**) Co-immunoprecipitation of V5-PTEN with GFP-PTPL1 wt and PDZ-deletion mutants in HEK293T cells. Bottom: quantification of relative V5-PTEN binding to GFP-PTPL1.

To further test whether the ability to bind PTEN is sufficient for PTPL1 function in controlling apical domain size we generated minimal versions of PTPL1 composed of its localization signal, the FERM domain, and the PDZ domains responsible for PTEN binding (Fig. 5d).
In agreement with the PDZ deletion mutants, PTEN binds poorly to PDZ2 but binding increases when the interregion and PDZ1 are added (Fig. 5e). Expression of these minimal PTPL1 constructs in PTPL1-depleted W4 cells resulted in normalization of apical membrane size in a manner that correlated with the ability to bind PTEN (Fig. 5f). Therefore, these experiments indicate that PTPL1 controls apical membrane size by binding PTEN at the apical plasma membrane.

Discussion

Here we show that PTEN is required for clustering of the apical membrane in polarized Ls174T:W4 cells. For this, PTEN, by means of its PDZ binding motif, binds to the PDZ domains of PTPL1 which in turn ensures apical enrichment of PTEN. Abrogating the interaction between PTEN and PTPL1 results in diffuse PTEN localization and enlargement of the apical plasma membrane. These data therefore support a model were PTPL1 by binding and localizing PTEN to the apical membrane enables PTEN-dependent clustering of the apical domain. This work thus identifies a novel function for PTEN during cell polarization in controlling apical membrane clustering and identifies PTPL1 as a critical PTEN binding partner in this process.

Various conflicting findings have been reported on the role of PTEN during apical membrane and lumen formation[8-14,20]. Specifically, whereas some reports indicate that PTEN is required for the establishment of an apical plasma membrane[11,14,20], other reports find that an apical membrane is normally formed in the absence of PTEN[8,9]. The use of different model systems likely underlies these discrepant findings, since PTEN is only required for apical membrane formation in *in vitro* model systems. Because these system rely on the formation of cell-cell junctions for polarization, the polarization defects observed may be secondary to defective junction formation.

Figure 5 continued

Error bars represent s.e.m. (n = 4) (**c**) Quantification of apical membrane size in W4:shCTRL and W4:shPTPL1 cells expressing EV, GFP-PTPL1 wt or PDZ-deletion mutants. Red bars and values in graph represent the average.Red error bars represent s.e.m. (n > 30 in at least three experiments) * $p < 0,05$ using independent samples t-test. n.s. not significant ($p > 0,05$) (**d**) Schematic representation of minimal PTPL1 mutants. FERM = 4.1, Ezrin, Radixin, Moesin domain (**e**) Co-immunoprecipitation of PTEN with GFP-PTPL1 wt and mutants in HEK293T cells. Bottom: quantification of relative PTEN binding to GFP-PTPL1. Error bars represent s.e.m. (n = 4) (**f**) Quantification of apical membrane size in W4:shCTRL and W4:shPTPL1 cells expressing EV, GFP-PTPL1 wt or mutants. Red bars and values in graph represent the average. Red error bars represent s.e.m. (n > 24 in at least three experiments) * $p < 0,05$ using independent samples t-test. n.s. not significant ($p > 0,05$)

By using Ls174T:W4 cells, which polarize in the absence of cell-cell junctions, we can specifically address the junction-independent role of PTEN in polarization. We show that PTEN knockout Ls174T:W4 cells retain the ability to form an apical membrane but nonetheless fail in restricting the formation of the apical membrane to a fraction of the cell, thus implicating PTEN in the regulation of apical membrane dimensions. Supporting this, Grego-Bessa et al. found that neural plate epithelial cells of PTEN knockout mice can not decrease their apical membrane surface during remodeling of the neural plate, resulting in neural tube closure defects[9]. In addition, deletion of PTEN from the mouse retina results in enlarged cell surfaces and altered retinal architecture[21]. Therefore, these findings indicate that PTEN, instead of being required for apical membrane formation, is necessary for controlling apical plasma membrane dimensions.

We previously found that apical membrane clustering in Ls174T:W4 cells requires the small GTPase Cdc42[22]. This raises the question whether PTEN and Cdc42 operate in a common signaling pathway to control apical membrane clustering. In support of this, PTEN has been linked to Cdc42 by regulating apical $PI(4,5)P_2$ levels, thereby providing a docking site for Annexin2, which in turn binds and localizes Cdc42-GTP to the apical membrane[14]. We however, could not find an apical membrane clustering defect in Ls174T:W4 depleted for Annexin2 (data not shown), indicating that PTEN may regulate an independent process that cooperates with Cdc42 in the regulation of apical membrane clustering.

The PDZ binding motif of PTEN engages in a variety of interactions with PDZ domain containing proteins, including important regulators of cell polarization such as Par3, Dlg1, and MAGI-2[23-25]. We now show that PTPL1 is a functionally relevant interaction partner of PTEN in the process of apical membrane clustering. Whether other PTEN interactors are also involved in this process needs further investigation.

Both PTPL1 and PTEN function as tumor suppressors in colorectal cancer raising the question to what extent their interaction is important for tumorigenesis[4,26]. Interestingly, two findings suggest that PTEN regulation via its PBM is particularly contributing to tumorigenesis. Firstly, $PTEN^{\Delta PBM/\Delta PBM}$ mice develop spontaneous tumors and show higher tumor incidence when combined with various mouse tumor models[24]. Secondly, although rare, oncogenic PTEN mutations that compromise the PBM have been reported and these can not restore normal lumen morphology of PTEN-depleted 3D mammary gland cultures[11]. Therefore, the interaction between PTPL1 and PTEN may be of relevance for cancer progression by controlling epithelial tissue architecture.

Material and Methods

Cell culture and plasmids

Ls174T:W4 cells were cultured in RPMI1640 (Sigma) medium supplemented with 10% FBS (Sigma) and antibiotics. To induce polarization, cells were cultured for at least 16h in presence of 1 μg/ml doxycycline (Sigma). For transient expression of DNA constructs, cells were transfected using XtremeGene9 (Roche) according to the manufacturer's guidelines.

pEGFP-EBP50 was generated by introducing an EBP50 PCR fragment in pEGFP-C2 using In-Fusion (Clontech). Similarly PTPL1 constructs were generated by introducing a PTPL1 PCR product in pEGFP using In-Fusion. PTPL1 mutants were generated by performing the In-Fusion reaction with two PCR fragments, one fragment encoding the upstream sequence and one encoding the sequence downstream of the PDZ domain(s) to be deleted. pEGFP-2A-PTEN wt and the ΔPBM mutant were generated by generating a PCR fragment of PTEN in which PTEN is preceded by the sequence encoding the self-cleaving 2A peptide. This fragment was introduced in pEGFP-C2 using In-Fusion. YFP-PTEN was generated using Gateway cloning (Invitrogen). Lifeact-Ruby was provided by Roland Wedlich-Söldner.

Antibodies

The following antibodies were used for immunofluorescence: mouse anti-CD66 (BD Biosciences, 1:500), mouse anti-CD71 (H68.4, Life Technologies, 1:1000). For Western blotting the following antibodies were used: mouse anti-PTEN (6H2.1, Millipore, 1:5000), mouse anti-βCatenin (BD biosciences, 1:5000), mouse anti-αTubulin (Calbiochem, 1:5000), mouse anti-HA (12CA5, Roche, 1:10000), mouse anti-GFP (clones 7.1 and 13.1, Roche, 1:5000), mouse anti-V5 (Invitrogen, 1:5000) and rabbit anti-Fap1 (H-300, Santa Cruz, 1:2000)

Generation of PTEN knockout and PTPL1 knockdown cell lines

PTEN knockout Ls174T:W4 cells were generated using CRISPR/Cas9 mediated gene disruption. For this, cells were transfected with pSpCas9(BB)-2A-GFP (PX458), encoding an sgRNA (ACCGCCAAATTTAATTGCAG for clone #1 and #2 or GACTGGGAATAGTTACTCCC for clone #3) targeting the fourth and sixth exon of PTEN. GFP-positive cells were expanded monoclonally and knockout clones were identified by sequencing. Absence of PTEN was subsequently demonstrated by Western blotting.

For stable knockdown of PTPL1, cells were transduced with shRNA containing lentiviral particles (Mission shRNA library, Sigma). After two rounds of infection, cells were selected for puromycin resistance (10 μg/ml) and knockdown was confirmed by Western blotting. For PTPL1 knockdown a single shRNA hairpin was used targeting the 3'UTR of PTPL1: 5'- GCATCATCTGTTTGTAATCAT-3'.

Live cell imaging

Transfected cells were split and seeded onto glass bottom dishes (WillCo Wells) in doxycycline-containing medium. Cells were imaged in HEPES-buffered (pH = 7.4) Leibovitz's L-15 medium (Invitrogen) at 37ºC using an Axioskop2 LSM510 scanning confocal microscope (Zeiss) with a 63x magnification oil objective (PLAN Apochromat, NA 1.4) using Zen image acquisition software. Apical membrane size was determined by measuring the fraction of the cell covered with microvilli using ImageJ software. Average apical membrane sizes were compared using independent samples t-test in SPSS with a p-value <0.05 as a cutoff for significance.

Immunofluorescence

Cells were seeded on glass cover slips in the presence of doxycycline. Cells were washed with PBS, fixed in 4% formaldehyde for 30 min, permeabilized with 2% Triton X-100 for 10 min and blocked in 2% BSA for 2h. Slides then incubated with primary antibody for 16h, washed with PBS and incubated with Alexa488-conjugated secondary antibody in the presence of DAPI and Alexa568-coupled phalloidin for at least 4h. After multiple PBS washes, slides were mounted and imaged.

Immunoprecipitation

Transfected HEK293T cells were scraped in ice cold lysis buffer (1% Triton X-100, 50mM Tris-HCl pH 7.5, 150mM NaCl, 5mM MgCl2, supplemented with protease inhibitors) and cleared by centrifugation. Cleared lysates incubated with agarose beads coupled to GFP-binding protein (GBP) for 1h at 4ºC while rotating. Beads were washed three times with lysis buffer and bound proteins were eluted in sample buffer.

References

1 Halaoui, R. & McCaffrey, L. Rewiring cell polarity signaling in cancer. Oncogene 34, 939-950, doi:10.1038/onc.2014.59 (2015).

2 Martin-Belmonte, F. & Perez-Moreno, M. Epithelial cell polarity, stem cells and cancer. Nat Rev Cancer 12, 23-38, doi:10.1038/nrc3169 (2012).

3 McCaffrey, L. M. & Macara, I. G. Epithelial organization, cell polarity and tumorigenesis. Trends Cell Biol 21, 727-735, doi:10.1016/j.tcb.2011.06.005 (2011).

4 Salmena, L., Carracedo, A. & Pandolfi, P. P. Tenets of PTEN tumor suppression. Cell 133, 403-414, doi:10.1016/j.cell.2008.04.013 (2008).

5 Mutter, G. L. Histopathology of genetically defined endometrial precancers. International journal of gynecological pathology : official journal of the International Society of Gynecological Pathologists 19, 301-309 (2000).

6 Myers, M. P. et al. P-TEN, the tumor suppressor from human chromosome 10q23, is a dual-specificity phosphatase. Proceedings of the National Academy of Sciences of the United States of America 94, 9052-9057 (1997).

7 Stambolic, V. et al. Negative regulation of PKB/Akt-dependent cell survival by the tumor suppressor PTEN. Cell 95, 29-39 (1998).

8 Shore, A. N. et al. PTEN is required to maintain luminal epithelial homeostasis and integrity in the adult mammary gland. Dev Biol 409, 202-217, doi:10.1016/j.ydbio.2015.10.023 (2016).

9 Grego-Bessa, J. et al. The tumor suppressor PTEN and the PDK1 kinase regulate formation of

the columnar neural epithelium. Elife 5, doi:10.7554/eLife.12034 (2016).
10 Jagan, I., Fatehullah, A., Deevi, R. K., Bingham, V. & Campbell, F. C. Rescue of glandular dysmorphogenesis in PTEN-deficient colorectal cancer epithelium by PPARγ-targeted therapy. Oncogene 32, 1305-1315, doi:10.1038/onc.2012.140 (2012).
11 Berglund, F. M. et al. Disruption of epithelial architecture caused by loss of PTEN or by oncogenic mutant p110alpha/PIK3CA but not by HER2 or mutant AKT1. Oncogene 32, 4417-4426, doi:10.1038/onc.2012.459 (2013).
12 Garfin, P. M., Nguyen, T. & Sage, J. Loss of Pten Disrupts the Thymic Epithelium and Alters Thymic Function. PLoS One 11, e0149430, doi:10.1371/journal.pone.0149430 (2016).
13 Bardet, P. L. et al. PTEN controls junction lengthening and stability during cell rearrangement in epithelial tissue. Dev Cell 25, 534-546, doi:10.1016/j.devcel.2013.04.020 (2013).
14 Martin-Belmonte, F. et al. PTEN-mediated apical segregation of phosphoinositides controls epithelial morphogenesis through Cdc42. Cell 128, 383-397, doi:10.1016/j.cell.2006.11.051 (2007).
15 Fournier, M. V., Fata, J. E., Martin, K. J., Yaswen, P. & Bissell, M. J. Interaction of E-cadherin and PTEN Regulates Morphogenesis and Growth Arrest in Human Mammary Epithelial Cells. Cancer Research 69, 4545-4552, doi:10.1158/0008-5472.can-08-1694 (2009).
16 Baas, A. F. et al. Complete polarization of single intestinal epithelial cells upon activation of LKB1 by STRAD. Cell 116, 457-466 (2004).
17 Garbett, D. & Bretscher, A. PDZ interactions regulate rapid turnover of the scaffolding protein EBP50 in microvilli. J Cell Biol 198, 195-203, doi:10.1083/jcb.201204008 (2012).
18 Cuppen, E. et al. A FERM domain governs apical confinement of PTP-BL in epithelial cells. Journal of cell science 112 (Pt 19), 3299-3308 (1999).
19 Sotelo, N. S., Schepens, J.T.G., Valiente, M., Hendriks, W.J.A.J. & Pulido, R. PTEN–PDZ domain interactions: Binding of PTEN to PDZ domains of PTPN13. Methods 77-78, 147-156, doi:10.1016/j.ymeth.2014.10.017 (2015).
20 Langlois, M. J. et al. The PTEN phosphatase controls intestinal epithelial cell polarity and barrier function: role in colorectal cancer progression. PLoS One 5, e15742, doi:10.1371/journal.pone.0015742 (2010).
21 Cantrup, R. et al. Cell-type specific roles for PTEN in establishing a functional retinal architecture. PLoS One 7, e32795, doi:10.1371/journal.pone.0032795 (2012).
22 Bruurs, L. J. et al. ATP8B1-mediated spatial organization of Cdc42 signaling maintains singularity during enterocyte polarization. J Cell Biol 210, 1055-1063, doi:10.1083/jcb.201505118 (2015).
23 von Stein, W., Ramrath, A., Grimm, A., Muller-Borg, M. & Wodarz, A. Direct association of Bazooka/PAR-3 with the lipid phosphatase PTEN reveals a link between the PAR/aPKC complex and phosphoinositide signaling. Development 132, 1675-1686, doi:10.1242/dev.01720 (2005).
24 van Ree, J. H., Nam, H. J., Jeganathan, K. B., Kanakkanthara, A. & van Deursen, J. M. Pten regulates spindle pole movement through Dlg1-mediated recruitment of Eg5 to centrosomes. Nature cell biology 18, 814-821, doi:10.1038/ncb3369 (2016).
25 Wu, X. et al. Evidence for regulation of the PTEN tumor suppressor by a membrane-localized multi-PDZ domain containing scaffold protein MAGI-2. Proceedings of the National Academy of Sciences of the United States of America 97, 4233-4238 (2000).
26 Abaan, O. D. & Toretsky, J. A. PTPL1: a large phosphatase with a split personality. Cancer Metastasis Rev 27, 205-214, doi:10.1007/s10555-008-9114-2 (2008).

V

Mechanisms and functions of Rap2 signaling

5

Lucas J.M. Bruurs and Johannes L. Bos

Abstract
The Rap subfamily of Ras-like GTPases is composed of five members (Rap1A/B, Rap2A/B/C) that function as molecular switches in signaling processes that involve the actin cytoskeleton. Like other small GTPases, activity of Rap proteins is determined by their association with either GDP or GTP, which is regulated by the activity of GEFs and GAPs. The combined actions of GEFs and GAPs allow high spatial and temporal control over Rap signaling. This degree of control is necessary because Rap signaling often functions to mark a cellular region for local actin remodeling.
Although highly similar, it has become apparent that Rap1 and Rap2 proteins can signal independently and even antagonistically. Here we will review the mechanisms of Rap2 signaling and provide an overview of the biological functions in which Rap2 signaling is involved.

5

Introduction

Small GTPases of the Ras-related protein (Rap) subfamily are critical signaling hubs in processes that govern cell morphology. Like other small GTPases, Rap cycles between an inactive GDP-bound and an active GTP-bound state. In addition to intrinsic GTPase activity, the guanine nucleotide binding status of small GTPase proteins is regulated by the activity of guanine nucleotide exchange factors (GEFs) and GTPase activating proteins (GAPs). GEFs promote dissociation of GDP and replacement with the more available GTP, thereby enabling effector binding and activating downstream signaling. In contrast, GAPs stimulate intrinsic GTPase activity resulting in a GDP-bound inactive conformation. The combined activity of GEFs and GAPs allow strict regulation of Rap signaling both in time and space[1].

Although highly similar to other Ras family proteins, a Rap ortholog was already present in the last eukaryotic common ancestor (LECA)[2]. In contrast, Rap1 and Rap2 proteins appear to have emerged later in evolution and the different Rap1 and Rap2 isoforms are only present in vertebrates. Five Rap proteins have been identified in mammals and categorized in two subtypes based on sequence homology. The Rap2 isoforms (Rap2A/B/C) share 60% of the amino acid identity with the Rap1 isoforms (Rap1A/B) and as a consequence of this similarity Rap1 and Rap2 share many GEFs, GAPs and effectors. Therefore, it was suggested that Rap1 and Rap2 function in the same signaling pathway[3]. However, various reports have now demonstrated that Rap2 has independent signaling functions and in some cases can even antagonize Rap1 activity. The molecular mechanisms underlying unique signaling by the Rap isoforms are slowly being uncovered and it illustrates how highly similar small GTPases can signal independently.

Biochemistry of Rap2 proteins

Structurally, Rap proteins consist of an N-terminal 'business' region which is the part responsible for nucleotide binding. Additionally, this part is involved in GEF and GAP binding and it contains the docking site for Rap effectors. The five Rap isoforms are very similar in the N-terminal part of the protein, however a single substitution (Ser39Phe) in Rap2 allows discrimination by Rap2 specific GEFs and effectors[4-6].

In contrast, much variation is found in the C-terminal part of the Rap proteins. This part contains various localizations signals including the CAAX motif, which is posttranslationally modified by the addition of a hydrophobic isoprenoid moiety, thereby targeting the protein to membranous compartments[7]. Both Rap1 isoforms are modified with a C-20 geranylgeranyl moiety, however Rap2 isoforms are differentially isoprenylated: Rap2A is equipped with a C-15 farnesyl moiety whereas Rap2B is geranylgeranylated. Based on the sequence of the CAAX motif Rap2C was expected to be farnesylated, however Rap2C was also

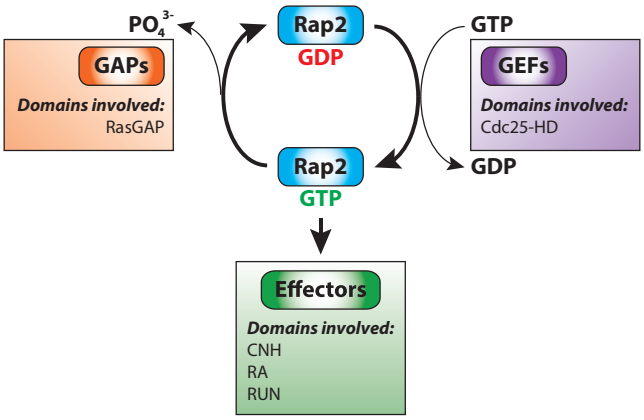

Figure 1: General regulatory mechanisms of Rap2 signaling and the domains involved

identified as a substrate for geranylgeranyl transferase type 1 in MCF-7 cells suggesting plasticity in the type of modification[8,9]. Differences in isoprenylation status critically affect cellular distribution as was demonstrated by the specific interaction between farnesylated Ras family proteins and the GDI-like solubilizing factor PDEδ[10,11]. PDEδ binding to farnesylated Rap2A and Rap2C solubilizes these proteins from the plasma membrane and aids cytoplasmic diffusion[10].

Next to the C-terminal CAAX motif Rap1 contains a polybasic region, which for Ras proteins mediates more stable membrane association via interactions with negatively charged membrane lipids[12]. As for Rap2, the C-terminus does not contain a polybasic region, but in addition to the CAAX motif contains two cysteine residues that can be dynamically palmitoylated[13]. For H- and NRas, palmitoylation at the Golgi apparatus directs these proteins to the plasma membrane, whereas depalmitoylated Ras proteins are redirected to the Golgi[10,14]. Biochemically, deletion of the two cysteine residues in Rap2B results in an altered fractionation pattern associated with loss of Rap2B from detergent-resistant membranes[15]. The functional importance of this mislocalization is highlighted by the finding that deletion of the two cysteines renders Rap2 incapable of activating the Rap2 specific effector TNIK[13].

In addition to lipid modifications on the Rap2 C-terminus, other posttranslational modifications were identified that affect Rap2 signaling. Ubiquitination by Nedd4-1 affects the ability of Rap2 to activate the Rap2 specific effectors TNIK and MINK[16]. In addition, Rap2 ubiquitination by a Cullin-5 containing ubiquitin ligase complex regulates plasma membrane localization of Rap2, which recruits Dishevelled (Dsh) and thereby regulates noncanonical Wnt signaling during *Xenopus laevis* gastrulation[17].

Mechanisms of Rap2 signaling

Because Rap1 and Rap2 are highly identical in the nucleotide binding region it is not surprising that most GEFs, GAPs and effectors are shared. Classic RapGEFs including EPAC, PDZGEF and CalDAG-GEF similarly activate Rap1 and Rap2 Nonetheless, C3G and RasGEF1 have been reported to specifically activate Rap1 or Rap2 respectively[4,18]. Interestingly, Rap2 appears to be more GTP-loaded under basal conditions then Rap1 which has been suggested to result from reduced sensitivity towards the activity of various RapGAPs[3,19]. Differential GEF and GAP activity towards Rap1 and Rap2 is allowed by a single amino acid substitution (Ser39Phe) in the switch I region of Rap2. This region is the site of interaction for most GEFs, GAPs and effectors and indeed the Rap2(Phe39Ser) mutant is not activated by the RasGEF1, the only GEF specific for Rap2[4]. Additionally Rap2(Phe39Ser) is unable to bind the Rap2 specific downstream effectors MAP4K4[20], TNIK[5], MINK[6] and the adapter protein RAPL[21].

Whereas RasGEF1 is the only selective Rap2GEF, multiple Rap2 specific downstream effector proteins have been identified. Although the canonical Ras association (RA) domain can bind Rap2 specifically in the GTP-bound conformation, it generally does not discriminate between Rap1 and Rap2. Nevertheless RA domains can have higher affinity towards Rap2 compared to Rap1 as was shown for the RA domain of the Rap effector RAPL[21].

An important class of specific Rap2 effectors are the Citron/NIK homology (CNH) domain containing kinases MAP4K4, TNIK and MINK via which Rap2 exerts a variety of effects on the actin cytoskeleton[5,6,20]. It is not known whether the CNH domain bears any structural resemblance to the RA domain, yet like the RA domain the CNH domain is only able to interact with GTP-loaded Rap2. Functionally, the CNH domain is suggested to maintain and to regulate the autoinhibition via which these kinases are kept inactive[22].

Other Rap2 specific effectors like RPIP9 and RPIPx are hallmarked by the presence of a RPIP8/UNC-14/NESCA (RUN) domain which is structurally distinct from the classical RA domain[23]. Although the RUN domain of RPIPx is able specifically interact with GTP-loaded Rap2, RUN domains in general are not dedicated Rap2 specific binding modules and can interact with other Rap and Rab family proteins[23,24]. Therefore specificity of the RUN domain is context dependent.

Curiously, the Rho GTPase activating protein ArhGAP29 is an atypical Rap2 effector since its association with active Rap2 is not mediated by a classical RA, CNH or RUN domain and because binding to GTP-Rap2 is suggested to inactivate ArhGAP29 functioning[25]. Although ArhGAP29 can associate with GTP-bound Rap2 resulting in inactivation, ArhGAP29 is activated by Rap1 via the Rap1

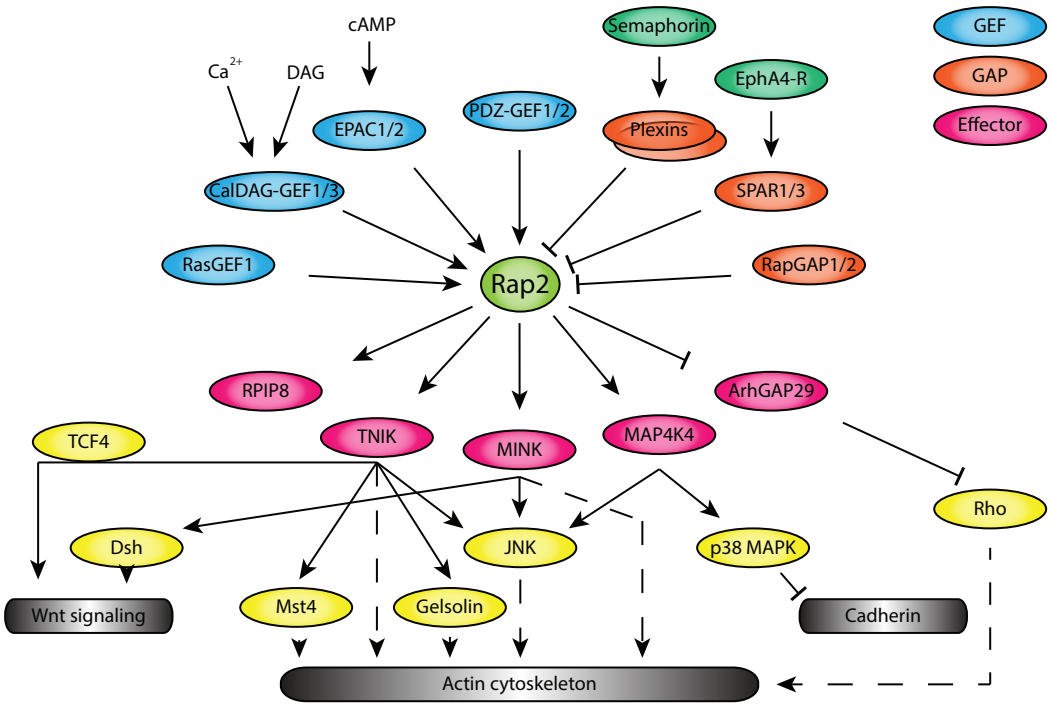

Figure 2: Molecules involved in Rap2 signaling during cell morphogenesis
GEFs (blue), GAPs (orange) and effector proteins (magenta) involved in the regulation of Rap2 signaling during various processes that contribute to cell shape. Proteins in green and yellow are proteins that regulate GAP activity and mediate effector signaling respectively. Dashed arrows indicate indirect regulation.

effector scaffolds Radil and Rasip[26]. Therefore, ArhGAP29 might function as a node of convergence in antagonistic Rap1 and Rap2 signaling pathways.

The existence of specific activators and effectors allows for signaling pathways that are uniquely transduced by Rap2. Pannekoek et al. described the first of such an isolated pathway in which both the GEF (RasGEF1C) and effector (MAP4K4) are Rap2-specific[27]. Interestingly, this pathway was shown to counteract the increase in endothelial barrier resistance induced by Rap1 activation. Nevertheless, whereas the effects of Rap1 on barrier tightness are mediated by remodeling radial and junctional stress fibers, Rap2 does not contribute to the actin remodeling observed during barrier tightness modulation[27]. This suggests that Rap1 and Rap2 employ completely different mechanisms to antagonistically regulate endothelial barrier function and highlights their signaling divergence.

This type of opposing outcome has been reported for Rap1 and Rap2 signaling in the context of neuronal growth cone size and T cell migration and strongly argues for independent signaling modules[21,28]. Often though, the crosstalk between Rap1 and Rap2 signaling is unclear. Although many RapGEFs, such as EPAC and PDZGEF, possess no *in vitro* specificity this does not necessarily imply they

are non-specific *in vivo*[29]. Since the different Rap isoforms function in distinct spatial pools it may well be possible that a promiscuous GEF only encounters one isoform and therefore displays an *in vivo* specificity.

Biological functions of Rap2 signaling

Like the Rap1 GTPases, Rap2 is engaged in signaling pathways involved in a plethora of biological processes. In general though, Rap2 signaling governs cell morphology by regulating the actin cytoskeleton or actin-driven transport. These are often local processes during which Rap activity is regulated under strict spatial and temporal control[1].

Rap2 signaling during brush border formation

The strict spatial regulation of Rap2 signaling is strikingly illustrated by its function during the formation of apical microvilli in the process of enterocyte polarity establishment. During polarization, enterocytes generate an asymmetrical distribution of membrane lipids including an apical enrichment of $PI(4,5)P_2$ and phosphatidic acid (PA)[30]. This creates a spatial cue for the RapGEF PDZGEF which is recruited to phosphatidic acid via its PDZ domain[31]. Because of this compartmentalization, a specific pool of Rap2A at the apical plasma membrane is activated by PDZGEF. Curiously, Rap2A signaling during brush border formation is strictly isolated from the other Rap2 isoforms. This signaling specificity originates from a dual mechanism involving differential localization and selective activation[32].

The selective activation of Rap2A at the apical plasma membrane results in local activation of the Rap2 effector kinase TNIK. Activated Rap2A, via TNIK, induces plasma membrane localization of the kinase Mst4, which in conjunction with other kinases and phosphatases, governs the phosphorylation status of the Ezrin, Radixin and Moesin (ERM) proteins to remodel the actin cytoskeleton and induce brush border formation[30,33-35]. Therefore, Rap2A signaling during brush border formation highlights how Rap2 functions to convert a spatial cue (apical phosphatidic acid) into localized remodeling of the actin cytoskeleton.

Rap2 in neuronal development

Rap2 and its effectors TNIK and MINK are highly expressed in the brain where Rap signaling regulates neuronal architecture[16,36-38]. In addition to regulating neuronal structure, Rap2 is involved in neuronal depotentiation by governing synaptic AMPA receptor levels[39]. Synaptic AMPA receptor levels are controlled by the concerted actions of both Ras and Rap GTPases[40]. Both Rap1 and Rap2 can induce AMPA receptor removal, thereby counteracting Ras signaling, which promotes synaptic delivery of AMPA receptors. Nevertheless, Rap1 and Rap2 do not act redundantly and engage different effector proteins to trigger the removal of unique subsets of AMPA receptors[39,40].

Rap2-mediated AMPA receptor removal can be triggered by activation of NMDA receptors. Still, the exact mechanism and the GEF and/or GAP involved in Rap2 activation upon NMDA receptor activation are unknown. Among the candidates for regulating Rap2 activity downstream of NMDA receptor activation are EPAC2 and the GAPs spine associated RapGAP (SPAR) and synaptic RasGAP (SynGAP). EPAC2 is localized to dendritic spines and its activation by the EPAC-selective agonist 8-CPT-2-Me-cAMP results in synaptic removal of GluR2/3, which is the pool of AMPA receptors regulated by Rap2[39,41]. On the other hand, SPAR and SynGAP RNAi similarly induce AMPA receptor removal as constitutively active Rap2 and both GAPs and Rap2 reside in the NMDA receptor complex[42-45].

Downstream of Rap2 activation, JNK signaling is engaged to remove AMPA receptors via the Rap2 effector kinases TNIK and MINK[36,39]. Although both TNIK and MINK can activate JNK signaling and are required for Rap2 induced AMPA receptor removal, these kinases are differentially engaged in this process[36,37,46-49]. Whereas TNIK activates JNK to remove AMPA receptors, overexpression of MINK restores the loss of AMPA receptors induced by Rap2 activation[36]. Interestingly, a similar antagonistic relationship between TNIK and MINK is suggested to occur in the regulation of canonical Wnt signaling by these kinases[22]. Nevertheless, it remains unclear under what conditions TNIK and MINK function antagonistically in relaying Rap2 signaling and which molecular mechanisms allow for opposing outcomes.

In addition to regulating AMPA receptor levels on the synaptic surface, Rap2 signaling affects neuronal cell shape by stimulating dendritic and axonal retraction and promoting synaptic pruning[36,38,49]. For this, Rap2 employs many of the GEFs, GAPs and effectors that are also involved in AMPA receptor removal, thus raising the question whether Rap2 regulates AMPA receptor recycling and neuronal morphology at the same time via one mechanism[36,41,42,45]. However, whereas Rap1 and Rap2 cooperate to remove AMPA receptors, both Raps are differentially involved in regulating neuronal morphology. Whereas overexpression of constitutively active Rap2(V12) potently reduces dendritic length, similar overexpression of Rap1(V12) has no effect[49]. Additionally, constitutively active Rap1 and Rap2 have opposing effects on growth cone size and are differentially involved in EphrinA mediated growth cone collapse[28]. Therefore, the observation that during AMPA receptor removal Rap1 and Rap2 operate in conjunction whereas they function antagonistically in regulating neuronal morphology suggests that Rap2 governs these processes via distinct signaling pathways.

Rap2 in the regulation of Wnt signaling

Wnt signaling is pivotal for tissue homeostasis and embryonic development by governing stem cell behavior and body axis establishment. Rap2 and its

effector TNIK have been implicated in modulating Wnt signaling output and can therefore affect these processes[50,51].
Exactly how Rap2 signaling impinges on Wnt signaling remains unclear. However, Rap2 signaling is required for plasma membrane localization of Dishevelled (Dsh) upon Frizzled (Fz) receptor activation[17,51]. For this, Rap2 needs to be ubiquitinated by a Cullin5-containing ubiquitin ligase complex, which functions to regulate the localization of Rap2[17]. Two Rap2 specific effectors are implicated in mediating the effects of Rap2 on Dsh localization: MINK and TNIK. In *Xenopus laevis*, activation of MINK and TNIK by Rap2 involves proteolytic cleavage resulting in liberation of the active kinase domain which is normally auto-inhibited[22].
How activated MINK and TNIK impose Dsh membrane localization is unclear, but may involve regulation of protein trafficking. Rap2 may have a general function to regulate receptor recycling and trafficking as it is also involved in the recycling of neuronal AMPA receptors and ALK receptors, via which it regulates Activin/Nodal signaling strength during embryonic patterning[52]. Additionally, Rap2 is implicated in the stability of LRP6, a co-receptor for Fz, which requires similar receptor internalization for signaling[53,54]. Therefore, Rap2, and its effectors MINK and TNIK, could regulate Wnt signaling via a general effect on receptor recycling.

Concluding remarks

Rap signaling is an evolutionary conserved signaling module that functions to regulate cell morphology predominantly via the actin cytoskeleton. Despite the high similarity on a biochemical level, Rap2 can signal independently of Rap1 by employing Rap2 specific GEFs or effectors. Furthermore, GEFs that are promiscuous *in vitro* can achieve selectivity *in vivo* allowing signaling pathways governed by a single Rap2 isoform[29,32].

Not only can Rap2 signal independently, in various cases the signaling output of Rap2 is antagonistic to Rap1. These opposing relationships between Rap1 and Rap2 have been reported to occur in the regulation of endothelial barrier function[27], neuronal growth cone size[28] and T cell migration[21]. The mechanisms that allow for these antagonistic outcomes remain unknown. An interesting candidate to function as a point of convergence for Rap1 and Rap2 is ArhGAP29, since its RhoGAP activity is directly inhibited by Rap2 whereas it is activated by Rap1, via the effectors Radil and Rasip[25,26]. Nevertheless, the point of convergence may be further downstream of Rap as was suggested for the antagonistic effects of Rap1 and Rap2 in the regulation of endothelial barrier tightness[27].
The biological processes in which Rap2 signaling has been implicated may appear haphazard. Nonetheless, all processes require extensive modulation of the actin cytoskeleton: upon Rap2 activation in enterocytes, actin is polymerized and bundled to generate the apical brush border and recycling receptors are

trafficked over actin filaments by Rab11/MyosinV positive endosomes[30,55-59]. Also neuronal cell morphology is a process that is largely dependent on remodeling of the actin cytoskeleton and involves elaborate regulation by other known actin remodeling proteins such as the Rho family of small GTPases[60,61]. Rap2 signaling may contribute to this actin remodeling via their effectors MINK and TNIK, which have actin severing capacities[5,6,13,37].

With the identification of dedicated Rap2 GEFs and effector it has become apparent that Rap2 forms an independent module of Rap signaling. Although many core constituents of Rap2 signaling, such as the GEFs, GAPs and effectors, have been identified, it remains largely unknown how these are connected with other signaling routes or how they are linked with a biological outcome. In particular the molecular origin of the complex connectivity with Rap1 signaling, which can be either synergistic or antagonistic, still remains elusive.

References

1 Gloerich, M. & Bos, J. L. Regulating Rap small G-proteins in time and space. Trends in cell biology 21, 615-623, doi:10.1016/j.tcb.2011.07.001 (2011).
2 van Dam, T. J., Bos, J. L. & Snel, B. Evolution of the Ras-like small GTPases and their regulators. Small GTPases 2, 4-16, doi:10.4161/sgtp.2.1.15113 (2011).
3 Ohba, Y. et al. Rap2 as a slowly responding molecular switch in the Rap1 signaling cascade. Molecular and cellular biology 20, 6074-6083 (2000).
4 Yaman, E., Gasper, R., Koerner, C., Wittinghofer, A. & Tazebay, U. H. RasGEF1A and RasGEF1B are guanine nucleotide exchange factors that discriminate between Rap GTP-binding proteins and mediate Rap2-specific nucleotide exchange. The FEBS journal 276, 4607-4616, doi:10.1111/j.1742-4658.2009.07166.x (2009).
5 Taira, K. et al. The Traf2- and Nck-interacting kinase as a putative effector of Rap2 to regulate actin cytoskeleton. The Journal of biological chemistry 279, 49488-49496, doi:10.1074/jbc.M406370200 (2004).
6 Nonaka, H. et al. MINK is a Rap2 effector for phosphorylation of the postsynaptic scaffold protein TANC1. Biochemical and biophysical research communications 377, 573-578, doi:10.1016/j.bbrc.2008.10.038 (2008).
7 Farrell, F. X., Yamamoto, K. & Lapetina, E. G. Prenyl group identification of rap2 proteins: a ras superfamily member other than ras that is farnesylated. The Biochemical journal 289 (Pt 2), 349-355 (1993).
8 Maurer-Stroh, S. et al. Towards complete sets of farnesylated and geranylgeranylated proteins. PLoS computational biology 3, e66, doi:10.1371/journal.pcbi.0030066 (2007).
9 Chan, L. N. et al. A novel approach to tag and identify geranylgeranylated proteins. Electrophoresis 30, 3598-3606, doi:10.1002/elps.200900259 (2009).
10 Chandra, A. et al. The GDI-like solubilizing factor PDEdelta sustains the spatial organization and signalling of Ras family proteins. Nature cell biology, doi:10.1038/ncb2394 (2011).
11 Nancy, V., Callebaut, I., El Marjou, A. & de Gunzburg, J. The delta subunit of retinal rod cGMP phosphodiesterase regulates the membrane association of Ras and Rap GTPases. The Journal of biological chemistry 277, 15076-15084, doi:10.1074/jbc.M109983200 (2002).
12 Hancock, J. F., Paterson, H. & Marshall, C. J. A polybasic domain or palmitoylation is required in addition to the CAAX motif to localize p21ras to the plasma membrane. Cell 63, 133-139 (1990)
13 Uechi, Y. et al. Rap2 function requires palmitoylation and recycling endosome localization. Biochemical and biophysical research communications 378,732-737,doi:10.1016/j.bbrc.2008.11.107 (2009).
14 Rocks, O. et al. An acylation cycle regulates localization and activity of palmitoylated Ras isoforms. Science 307, 1746-1752, doi:10.1126/science.1105654 (2005).

15 Canobbio, I., Trionfini, P., Guidetti, G. F., Balduini, C. & Torti, M. Targeting of the small GTPase Rap2b, but not Rap1b, to lipid rafts is promoted by palmitoylation at Cys176 and Cys177 and is required for efficient protein activation in human platelets. Cellular signalling 20, 1662-1670, doi:10.1016/j.cellsig.2008.05.016 (2008).
16 Kawabe, H. et al. Regulation of Rap2A by the ubiquitin ligase Nedd4-1 controls neurite development. Neuron 65, 358-372, doi:10.1016/j.neuron.2010.01.007 (2010).
17 Lee, R. H. et al. XRab40 and XCullin5 form a ubiquitin ligase complex essential for the noncanonical Wnt pathway. The EMBO journal 26, 3592-3606, doi:10.1038/sj.emboj.7601781 (2007).
18 van den Berghe, N., Cool, R. H., Horn, G. & Wittinghofer, A. Biochemical characterization of C3G: an exchange factor that discriminates between Rap1 and Rap2 and is not inhibited by Rap1A(S17N). Oncogene 15, 845-850, doi:10.1038/sj.onc.1201407 (1997).
19 Rubinfeld, B. et al. Molecular cloning of a GTPase activating protein specific for the Krev-1 protein p21rap1. Cell 65, 1033-1042 (1991).
20 Machida, N. et al. Mitogen-activated protein kinase kinase kinase kinase 4 as a putative effector of Rap2 to activate the c-Jun N-terminal kinase. The Journal of biological chemistry 279, 15711-15714, doi:10.1074/jbc.C300542200 (2004).
21 Miertzschke, M. et al. Characterization of interactions of adapter protein RAPL/Nore1B with RAP GTPases and their role in T cell migration. The Journal of biological chemistry 282, 30629-30642, doi:10.1074/jbc.M704361200 (2007).
22 Mikryukov, A. & Moss, T. Agonistic and antagonistic roles for TNIK and MINK in non-canonical and canonical Wnt signalling. PloS one 7, e43330, doi:10.1371/journal.pone.0043330 (2012).
23 Kukimoto-Niino, M. et al. Crystal structure of the RUN domain of the RAP2-interacting protein x. The Journal of biological chemistry 281, 31843-31853, doi:10.1074/jbc.M604960200 (2006).
24 Kitagishi, Y. & Matsuda, S. RUFY, Rab and Rap Family Proteins Involved in a Regulation of Cell Polarity and Membrane Trafficking. International journal of molecular sciences 14, 6487-6498, doi:10.3390/ijms14036487 (2013).
25 Myagmar, B. E. et al. PARG1, a protein-tyrosine phosphatase-associated RhoGAP, as a putative Rap2 effector. Biochemical and biophysical research communications 329,1046-1052,doi:10.1016/j.bbrc.2005.02.069 (2005).
26 Post, A. et al. Rasip1 mediates Rap1 regulation of Rho in endothelial barrier function through ArhGAP29. Proceedings of the National Academy of Sciences of the United States of America 110, 11427-11432, doi:10.1073/pnas.1306595110 (2013).
27 Pannekoek, W. J., Linnemann, J. R., Brouwer, P. M., Bos, J. L. & Rehmann, H. Rap1 and rap2 antagonistically control endothelial barrier resistance. PloS one 8, e57903, doi:10.1371/journal.pone.0057903 (2013).
28 Richter, M., Murai, K. K., Bourgin, C., Pak, D. T. & Pasquale, E. B. The EphA4 receptor regulates neuronal morphology through SPAR-mediated inactivation of Rap GTPases. The Journal of neuroscience : the official journal of the Society for Neuroscience 27, 14205-14215, doi:10.1523/JNEUROSCI.2746-07.2007 (2007).
29 Popovic, M., Rensen-de Leeuw, M. & Rehmann, H. Selectivity of CDC25 Homology Domain-Containing Guanine Nucleotide Exchange Factors. Journal of molecular biology 425, 2782-2794, doi:10.1016/j.jmb.2013.04.031 (2013).
30 Gloerich, M. et al. Rap2A links intestinal cell polarity to brush border formation. Nature cell biology 14, 793-801, doi:10.1038/ncb2537 (2012).
31 Consonni, S. V., Brouwer, P. M., van Slobbe, E. S. & Bos, J. L. The PDZ domain of the guanine nucleotide exchange factor PDZGEF directs binding to phosphatidic acid during brush border formation. PloS one 9, e98253, doi:10.1371/journal.pone.0098253 (2014).
32 Bruurs, L. J. & Bos, J. L. Mechanisms of Isoform Specific Rap2 Signaling during Enterocytic Brush Border Formation. PloS one 9, e106687, doi:10.1371/journal.pone.0106687 (2014).
33 ten Klooster, J. P. et al. Mst4 and Ezrin induce brush borders downstream of the Lkb1/Strad/Mo25 polarization complex. Developmental cell 16, 551-562, doi:10.1016/j.devcel.2009.01.016 (2009).
34 Dhekne, H. S. et al. Myosin Vb and rab11a regulate ezrin phosphorylation in enterocytes. Journal of cell science, doi:10.1242/jcs.137273 (2014).
35 Viswanatha, R., Ohouo, P. Y., Smolka, M. B. & Bretscher, A. Local phosphocycling mediated by

LOK/SLK restricts ezrin function to the apical aspect of epithelial cells. The Journal of cell biology 199, 969-984, doi:10.1083/jcb.201207047 (2012).
36 Hussain, N. K., Hsin, H., Huganir, R. L. & Sheng, M. MINK and TNIK differentially act on Rap2-mediated signal transduction to regulate neuronal structure and AMPA receptor function. The Journal of neuroscience : the official journal of the Society for Neuroscience 30, 14786-14794, doi:10.1523/JNEUROSCI.4124-10.2010 (2010).
37 Fu, C.A. et al. TNIK, a novel member of the germinal center kinase family that activates the c-Jun N-terminal kinase pathway and regulates the cytoskeleton. The Journal of biological chemistry 274, 30729-30737 (1999).
38 Ryu, J., Futai, K., Feliu, M., Weinberg, R. & Sheng, M. Constitutively active Rap2 transgenic mice display fewer dendritic spines, reduced extracellular signal-regulated kinase signaling, enhanced long-term depression, and impaired spatial learning and fear extinction. The Journal of neuroscience : the official journal of the Society for Neuroscience 28, 8178-8188, doi:10.1523/JNEUROSCI.1944-08.2008 (2008).
39 Zhu, Y. et al. Rap2-JNK removes synaptic AMPA receptors during depotentiation. Neuron 46, 905-916, doi:10.1016/j.neuron.2005.04.037 (2005).
40 Zhu, J. J., Qin, Y., Zhao, M., Van Aelst, L. & Malinow, R. Ras and Rap control AMPA receptor trafficking during synaptic plasticity. Cell 110, 443-455 (2002).
41 Woolfrey, K. M. et al. Epac2 induces synapse remodeling and depression and its disease-associated forms alter spines. Nature Neuroscience 12, 1275-1284, doi:10.1038/nn.2386 (2009).
42 Pak, D. T., Yang, S., Rudolph-Correia, S., Kim, E. & Sheng, M. Regulation of dendritic spine morphology by SPAR, a PSD-95-associated RapGAP. Neuron 31, 289-303 (2001).
43 Husi, H., Ward, M. A., Choudhary, J. S., Blackstock, W. P. & Grant, S. G. Proteomic analysis of NMDA receptor-adhesion protein signaling complexes. Nat Neurosci 3, 661-669, doi:10.1038/76615 (2000).
44 Lee, K. J. et al. Requirement for Plk2 in orchestrated ras and rap signaling, homeostatic structural plasticity, and memory. Neuron 69, 957-973, doi:10.1016/j.neuron.2011.02.004 (2011).
45 Krapivinsky, G., Medina, I., Krapivinsky, L., Gapon, S. & Clapham, D. E. SynGAP-MUPP1-CaMKII synaptic complexes regulate p38 MAP kinase activity and NMDA receptor-dependent synaptic AMPA receptor potentiation. Neuron 43, 563-574, doi:10.1016/j.neuron.2004.08.003 (2004).
46 Shkoda, A. et al. The Germinal Center Kinase TNIK Is Required for Canonical NF-kappaB and JNK Signaling in B-Cells by the EBV Oncoprotein LMP1 and the CD40 Receptor. PLoS biology 10, e1001376, doi:10.1371/journal.pbio.1001376 (2012).
47 Hu, Y. et al. Identification and functional characterization of a novel human misshapen/Nck interacting kinase-related kinase, hMINK beta. The Journal of biological chemistry 279, 54387-54397, doi:10.1074/jbc.M404497200 (2004).
48 Lim, J., Lennard, A., Sheppard, P. W. & Kellie, S. Identification of residues which regulate activity of the STE20-related kinase hMINK. Biochemical and biophysical research communications 300, 694-698, doi:10.1016/s0006-291x(02)02909-1 (2003).
49 Fu, Z. et al. Differential roles of Rap1 and Rap2 small GTPases in neurite retraction and synapse elimination in hippocampal spiny neurons. Journal of neurochemistry 100, 118-131, doi:10.1111/j.1471-4159.2006.04195.x (2007).
50 Mahmoudi, T. et al. The kinase TNIK is an essential activator of Wnt target genes. The EMBO journal 28, 3329-3340, doi:10.1038/emboj.2009.285 (2009).
51 Choi, S. C. & Han, J. K. Rap2 is required for Wnt/beta-catenin signaling pathway in Xenopus early development. The EMBO journal 24, 985-996, doi:10.1038/sj.emboj.7600571 (2005).
52 Choi, S. C. et al. Regulation of activin/nodal signaling by Rap2-directed receptor trafficking. Developmental cell 15, 49-61, doi:10.1016/j.devcel.2008.05.004 (2008).
53 Park, D. S., Seo, J. H., Hong, M. & Choi, S. C. Role of the Rap2/TNIK kinase pathway in regulation of LRP6 stability for Wnt signaling. Biochemical and biophysical research communications 436, 338-343, doi:10.1016/j.bbrc.2013.05.104 (2013).
54 Yamamoto, H., Komekado, H. & Kikuchi, A. Caveolin is necessary for Wnt-3a-dependent internalization of LRP6 and accumulation of beta-catenin. Developmental cell 11, 213-223, doi:10.1016/j.devcel.2006.07.003 (2006).

55 Crawley, S. W., Mooseker, M. S. & Tyska, M. J. Shaping the intestinal brush border. The Journal of cell biology 207, 441-451, doi:10.1083/jcb.201407015 (2014).
56 Hanley, J. G. Actin-dependent mechanisms in AMPA receptor trafficking. Frontiers in cellular neuroscience 8, 381, doi:10.3389/fncel.2014.00381 (2014).
57 Grant, B. D. & Donaldson, J. G. Pathways and mechanisms of endocytic recycling. Nature reviews. Molecular cell biology 10, 597-608, doi:10.1038/nrm2755 (2009).
58 Puthenveedu, M. A. et al. Sequence-dependent sorting of recycling proteins by actin-stabilized endosomal microdomains. Cell 143, 761-773, doi:10.1016/j.cell.2010.10.003 (2010).
59 Schuh, M. An actin-dependent mechanism for long-range vesicle transport. Nature cell biology 13, 1431-1436, doi:10.1038/ncb2353 (2011).
60 Neukirchen, D. & Bradke, F. Neuronal polarization and the cytoskeleton. Seminars in cell & developmental biology 22, 825-833, doi:10.1016/j.semcdb.2011.08.007 (2011).
61 Stankiewicz, T. R. & Linseman, D. A. Rho family GTPases: key players in neuronal development, neuronal survival, and neurodegeneration. Frontiers in cellular neuroscience 8, 314, doi:10.3389/fncel.2014.00314 (2014).

VI

Mechanisms of isoform specific Rap2 signaling during enterocytic brush border formation

Lucas J.M. Bruurs and Johannes L. Bos

6

Published in:
PLoS One.
2014 Sep 9;9(9):e106687.

Abstract
Brush border formation during polarity establishment of intestinal epithelial cells is uniquely governed by the Rap2A GTPase, despite expression of the other highly similar Rap2 isoforms (Rap2B and Rap2C). We investigated the mechanisms of this remarkable specificity and found that Rap2C is spatially segregated from Rap2A signaling as it is not enriched at the apical membrane after polarization. In contrast, both Rap2A and Rap2B are similarly located at Rab11 positive apical recycling endosomes and inside the brush border. However, although Rap2B localizes similarly it is not equally activated as Rap2A during brush border formation. We reveal that the C-terminal hypervariable region allows selective activation of Rap2A, yet this selectivity does not originate from the known differential lipid modifications of this region.
In conclusion, we demonstrate that Rap2 specificity during brush border formation is determined by two distinct mechanisms involving segregated localization and selective activation.

Introduction

GTPases of the Rap family function as molecular switches that relay signals under strict control of spatial and temporal cues. Three Rap2 proteins exist (Rap2A, Rap2B and Rap2C) that are over 90% identical in protein sequence. As a result of this sequence similarity none of the currently known Rap2GEFs, GAPs and effectors have preferred activity towards a single isoform *in vitro*[1]. Nevertheless, isoform specific signaling routes have been described raising the question how these highly similar GTPases can achieve signaling selectivity *in vivo*[2-4].

In the context of the closely related K-, H- and N-Ras proteins, isoform selectivity originates from the C-terminal hypervariable region (HVR)[5,6]. The HVR constitutes the major localization signal for GTPases as it is the site for both irreversible CAAX prenylation and dynamic cysteine palmitoylation. These lipid modifications allow for membrane association that in combination with the presence of a polybasic region or additional sorting signals in the HVR determine the localization of the Ras GTPases[7,8]. However, in comparison with the HVRs of the Ras isoforms, the Rap2 isoforms have very similar HVR compositions. Nevertheless, the Rap2 HVRs differ in amino acid sequence and in CAAX-box modification: whereas Rap2A and Rap2C are farnesylated, the Rap2B isoform is modified with a geranylgeranyl moiety[9,10] (Fig. 1a).

In the intestinal epithelial Ls174T:W4 cell line, single cells can polarize upon doxycycline-induced expression of STRAD and the subsequent cytosolic stabilization and activation of LKB1[11]. Previously, we identified a pathway

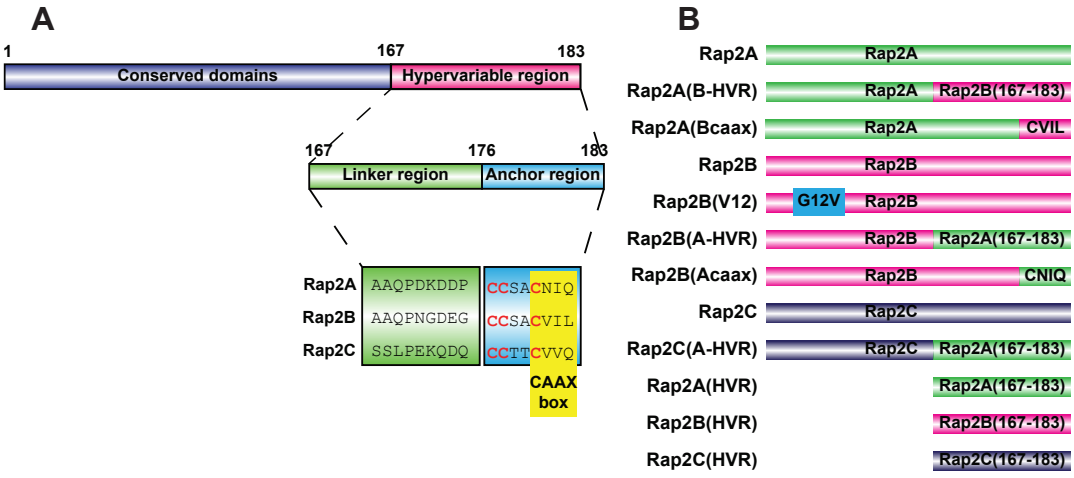

Figure 1: General structure of the Rap2 proteins and constructs used in this study
(**a**) Domain structure of Rap2 isoforms. Proteins differ most extensively in the C-terminal hypervariable region (HVR), which comprises a linker and anchor region. Cysteine residues in the anchor region (highlighted in red) are posttranslationally subjected to CAAX box isoprenylation and dynamic cysteine palmitoylation. (**b**) Schematic structure of various Rap2 constructs used in this study.

in which the small GTPase Rap2A regulates apical brush border formation downstream of LKB1[2]. Interestingly, only knockdown of Rap2A prevents brush border formation during Ls174T:W4 polarization, whereas knockdown of the other Rap2 isoforms present in this cell line has no effect. Notably, neither the upstream activator (PDZGEF) nor the downstream effector (TNIK) of Rap2A in this pathway have specificity towards any of the Rap2 isoforms[1,9].

Therefore, we set out to investigate the mechanisms via which isoform specific Rap2 signaling is achieved during brush border formation. Using an imaging approach in combination with mutant analysis we find that Rap2C is spatially isolated from Rap2A signaling. In contrast, Rap2B, although identically localized, is not similarly activated as Rap2A during brush border formation. We identify the C-terminal hypervariable region to be responsible for differential activation between Rap2A and Rap2B. Therefore, we conclude that the hypervariable region of Rap2 can regulate protein activity independent of its effects on localization and thereby allows for isoform specific Rap2 signaling during brush border formation.

Results

Since Rap GTPases are known to signal from distinct spatial pools, we assessed localization of the different Rap2 proteins in Ls174T:W4 cells[12]. After doxycycline-induced polarization, we observe enrichment of Rap2A at the apical brush border as judged by colocalization with the actin cytoskeleton marker Lifeact-Ruby[13] (Fig. 2a). Interestingly, Rap2B shows a similar localization upon polarization as Rap2A: both isoforms are predominantly located in the brush border membrane and in cytosolic vesicles subjacent to the brush border. These vesicles colocalize with the apical recycling endosome marker Rab11 (Fig. 2b). Recycling endosomes are pivotal for the establishment of apical membranes by sorting multiple signaling proteins to the apical membrane[14,15]. Thus, we identify two distinct pools of Rap2 at the apical aspect of polarized Ls174T:W4 cells: a pool residing on Rab11 positive endosomes en route to the apical plasma membrane and a second pool residing at the plasma membrane in the brush border.

Whereas Rap2A and Rap2B become enriched at the apical aspect upon polarization, Rap2C remains localized in vesicles that do not colocalize with dsRed-Rab11 (Fig. 2b). Therefore, we conclude that for Rap2C, but not Rap2B, differential localization most likely underlies the failure to function in brush border formation.

To get further insight in why Rap2C is differentially and Rap2B is similarly localized as Rap2A we assessed the localization of the isolated C-terminal HVRs as this region is most divergent between Rap2 isoforms and is known to regulate localization of other GTPases[6,8]. After Ls174T:W4 cell polarization, both GFP-Rap2A(HVR) and GFP-Rap2B(HVR) localize on recycling endosomes and at

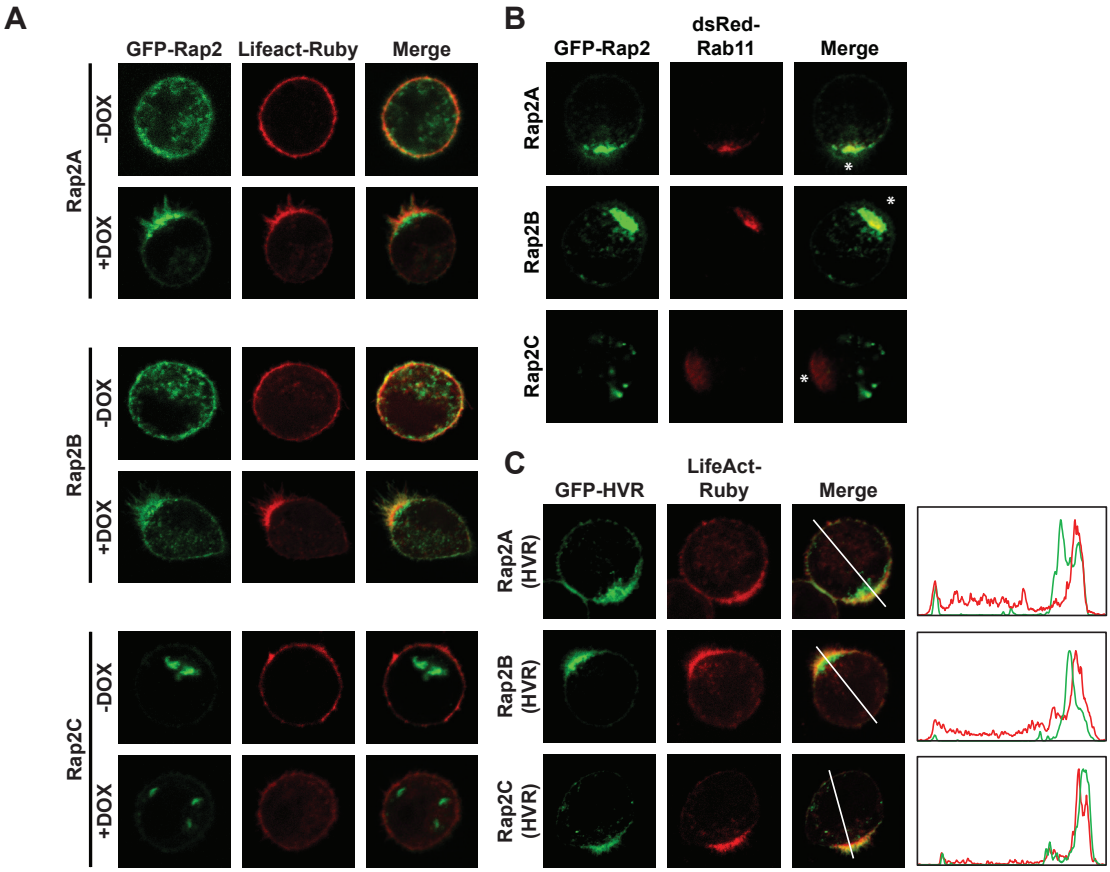

Fig. 2: Localization of Rap2 isoforms in polarized Ls174T:W4 cells
(**a**) GFP-tagged Rap2 isoform were cotransfected with the actin marker Lifeact-Ruby in W4 cells and imaged in unpolarized and polarized (i.e. doxycycline-stimulated) cells. (**b**) GFP-Rap2 localization compared with the recycling endosomal marker dsRed-Rab11 in polarized W4 cells. Asterisks indicate the apical aspect as judged by polarized Rab11 distribution. (**c**) Localization of the isolated hypervariable regions of the Rap2 isoforms. Profile plots show normalized fluorescence intensities over the indicated line scans. DOX = doxycycline

the brush border membrane, reflecting distribution of the full length proteins (Fig. 2c). In contrast, GFP-Rap2C(HVR) only localizes at the brush border and not on recycling endosomes. Therefore, we conclude that the HVR of Rap2A and Rap2B contains the dominant localization signals for these proteins, whereas for Rap2C localization of the isolated HVR (plasma membrane bound) does not reflect localization of the full length protein (vesicular), indicating that for Rap2C additional sorting signals overrule HVR-imposed localization. Furthermore, differences in the HVR of Rap2A and Rap2B compared to the HVR of Rap2C imposes specific localization at the recycling endosomes for Rap2A and Rap2B. Taken together, this demonstrates that the HVR of Rap2A and Rap2B selectively imposes localization of the full length proteins in polarized W4 cells.

Since localization does not explain specificity of Rap2A over Rap2B we questioned

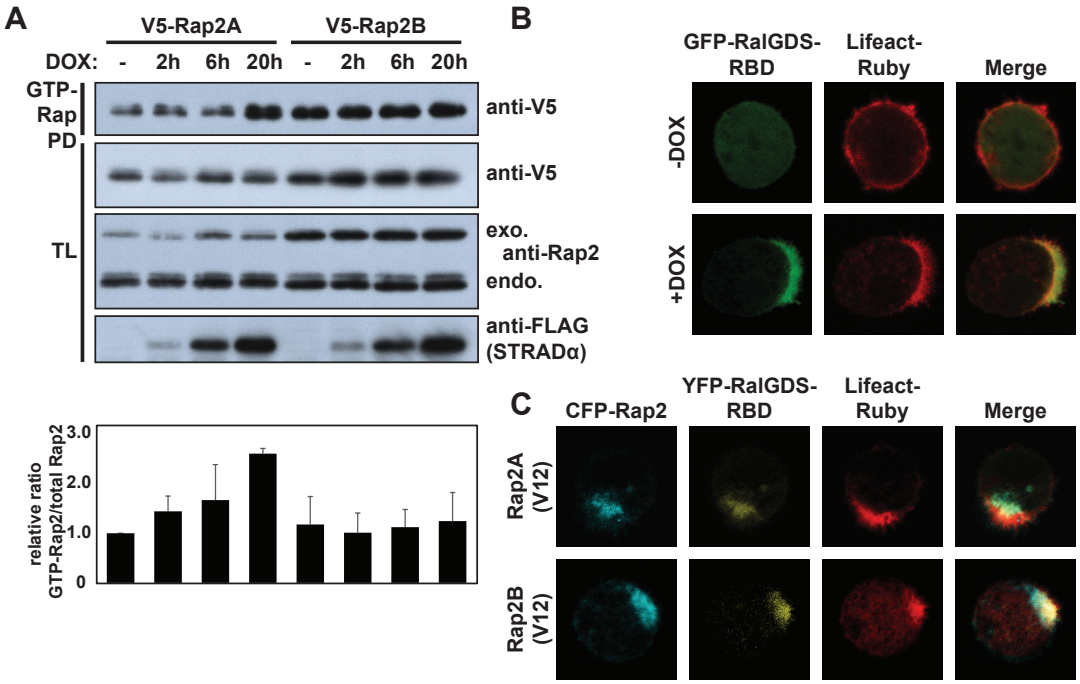

Figure 3: Rap2A and Rap2B are differentially activated during Ls174T:W4 cell polarization (**a**) Pulldown of GTP-bound V5-Rap2A and V5-Rap2B from W4 cells stimulated with doxycycline for various durations. Total lysates were probed for V5, Rap2 and FLAG. FLAG-STRADα levels were assessed to demonstrate differential induction over the different time points. Results from three independent experiments were averaged and expressed as the ratio of GTP-Rap2 vs. total Rap2 signal relative to unstimulated V5-Rap2A. Error bars represent standard deviations. (**b**) Distribution of GTP-bound Rap proteins in unpolarized and polarized W4 cells as visualized by localization of the Ras-binding domain (RBD) of RalGDS. (**c**) Localization of YFP-RalGDS-RBD in polarized W4 cells expressing constitutively activated CFP-Rap2A(V12) or CFP-Rap2B(V12). GTP-Rap PD: GTP-bound Rap pulldown, DOX = doxycycline, exo. exogenous, endo. endogenous

whether the activity of Rap2B is similarly induced as Rap2A during brush border formation. To assess this, we transfected V5-tagged Rap2A and Rap2B and subsequently used the Ras-binding domain of RalGDS (RalGDS-RBD) to specifically pulldown GTP-loaded Rap proteins[16]. After doxycycline treatment to induce brush border formation, an increase in GTP-bound Rap2A is observed whereas no induction in Rap2B (and Rap2C) activity is detected (Fig. 3a and supporting information Fig. S2). This indicates that Rap2B activity is not similarly controlled as Rap2A during brush border formation and suggests that for these proteins isoform specificity results from differential activation.

In order to visualize the site of Rap activation we expressed GFP-RalGDS-RBD in W4 cells and found that after polarization it is exclusively recruited to the brush border and not to the recycling endosomes (Fig. 3b). In contrast, when either constitutively activated CFP-Rap2A(V12) or CFP-Rap2B(V12) were present, YFP-RalGDS-RBD was able to localize to the recycling endosomes (Fig.

3c). These results indicate that the pool of Rap2A and Rap2B on the recycling endosomes are maintained in an inactive conformation and that Rap2A is selectively activated upon disassembly of the recycling endosomes at the apical membrane.

To further test the hypothesis that Rap2A and Rap2B differ in their activation state at the brush border, we scored brush formation in W4 cells stably depleted of endogenous Rap2A in which various Rap2 mutants were added back (Fig. 1b). Importantly, overexpression of wild type GFP-Rap2B and GFP-Rap2C cannot overcome the brush border formation defect imposed by Rap2A depletion (Fig. 4a,b). This again emphasizes that Rap2A is the dominant isoform during brush border formation and also demonstrates that isoform selectivity is maintained under overexpression conditions. In contrast, when overexpressing a constitutively active Rap2B(V12) mutant, brush border formation was restored in Rap2A-depleted W4 cells. The Rap2B(V12) mutant is similarly localized as wild type Rap2B, yet it is highly GTP-loaded because of reduced sensitivity towards GAP-mediated inactivation (Fig. 4a,b). No rescue of brush border formation was observed when Rap2C(V12) was expressed in Rap2A depleted W4 cells (Supporting information Fig. S3). Together with the failure of Rap2B to become activated after polarization, these findings suggest that although properly localized, Rap2B is not similarly activated as Rap2A and as a result of this does not contribute to brush border formation.

Next, we addressed whether the hypervariable region of Rap2A allows for selective Rap2A activation at the brush border. For this we generated chimeric Rap2 proteins in which the hypervariable region of Rap2B (and Rap2C) was replaced by the HVR of Rap2A (Fig. 1b). When expressed in W4 cells depleted of endogenous Rap2A, GFP-Rap2B(A-HVR) was able to restore brush border formation (Fig. 4a,b). In agreement with this, we find that V5-Rap2B(A-HVR) is more GTP-loaded in polarized W4 cells compared to wild type V5-Rap2B (Fig. 4d). Furthermore, a chimeric Rap2A(B-HVR) mutant loses the ability to induce brush border formation in Rap2A depleted W4 cells and is less active in polarized W4 cells compared to Rap2B(A-HVR) (Fig. 4e,f and Supporting information Fig. S4). Therefore, we conclude that differences in signaling by Rap2A and Rap2B can be attributed solely to differences in the hypervariable region. In contrast, GFP-Rap2C(A-HVR) is unable to rescue brush border formation in Rap2A depleted cells (Fig. 4a,b). In agreement with this, localization of GFP-Rap2C is not affected by replacing the hypervariable region, again indicating that the dominant localization signal of Rap2C is outside the HVR (Fig. 4a).

A striking difference between the HVRs of Rap2A and Rap2B is their differential CAAX box modification. Whereas the CAAX motif of Rap2A results in a farnesylated protein, the Rap2B CAAX motif is modified with a geranylgeranyl

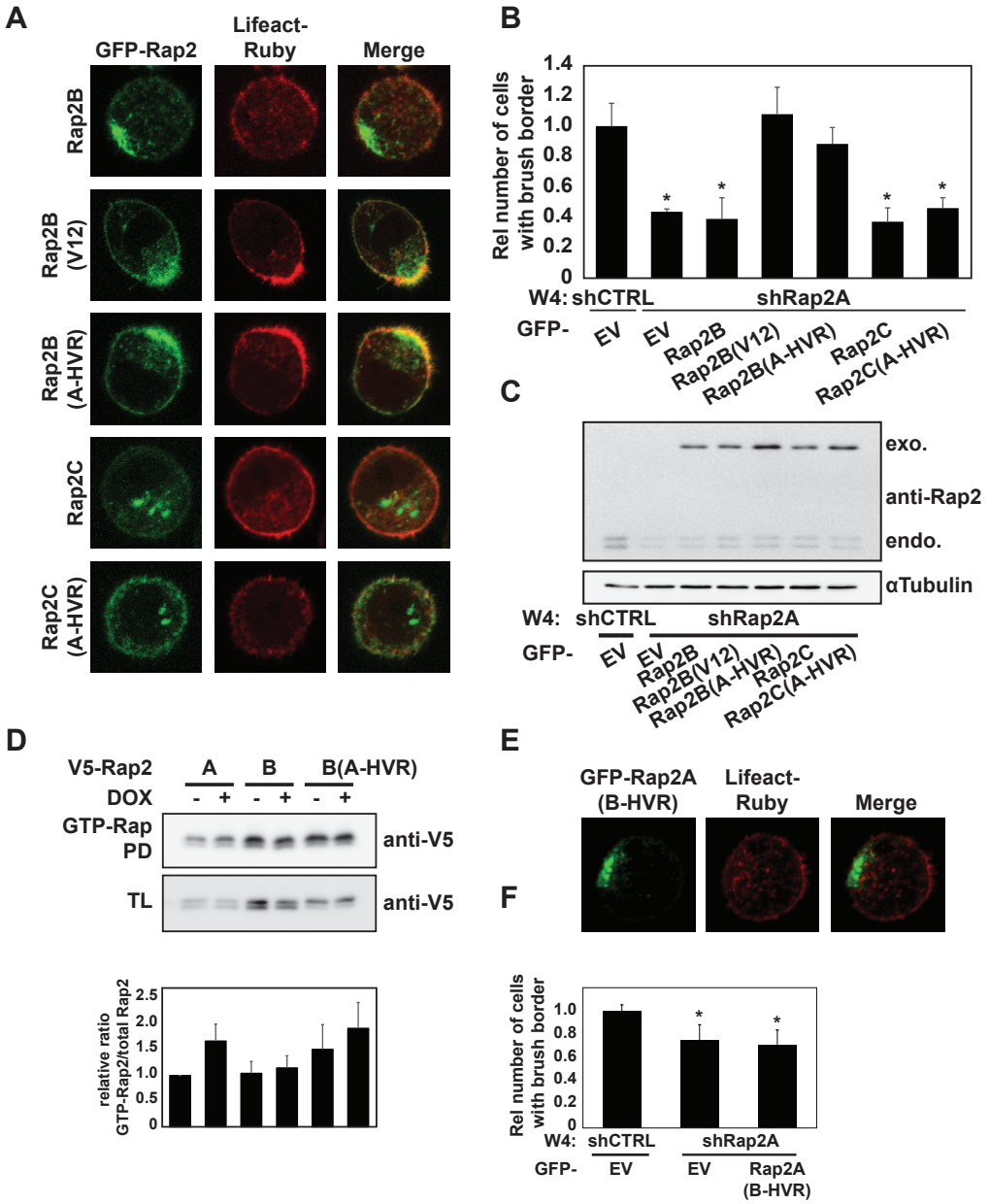

Figure 4: Constitutively activated Rap2B(V12) or a chimeric Rap2B(A-HVR) mutant can rescue brush border formation in Rap2A depleted Ls174T:W4 cells

(**a**) Images of Rap2A-depleted polarized W4 cells expressing various GFP-tagged Rap2 constructs and LifeAct-Ruby. (**b**) Quantification of brush border formation in GFP-positive cells in three independent experiments. (total counts ~150 cells per condition). * $p < 0{,}05$ using paired samples t-test. (**c**) Western blot of lysates from a rescue experiment probed with Rap2 antibody and anti-αTubulin as a loading control. exo. exogenous, endo. endogenous (**d**) GTP-Rap pulldown from unpolarized and polarized W4 cells expressing V5-Rap2A, V5-Rap2B or V5-Rap2B(A-HVR). Results from three independent experiments were quantified and averages were expressed as ratio of GTP-Rap2 vs. total Rap2 relative to unstimulated Rap2A. (**e**) Image of Rap2A-depleted W4 cell expressing GFP-Rap2A(B-HVR) and Lifeact-Ruby. (**f**) Quantification of brush border formation in Rap2A depleted W4 cells in which GFP or GFP-Rap2A(B-HVR) was introduced. (Total counts ~300 cells per condition) * $p < 0{,}05$ using paired samples t-test.

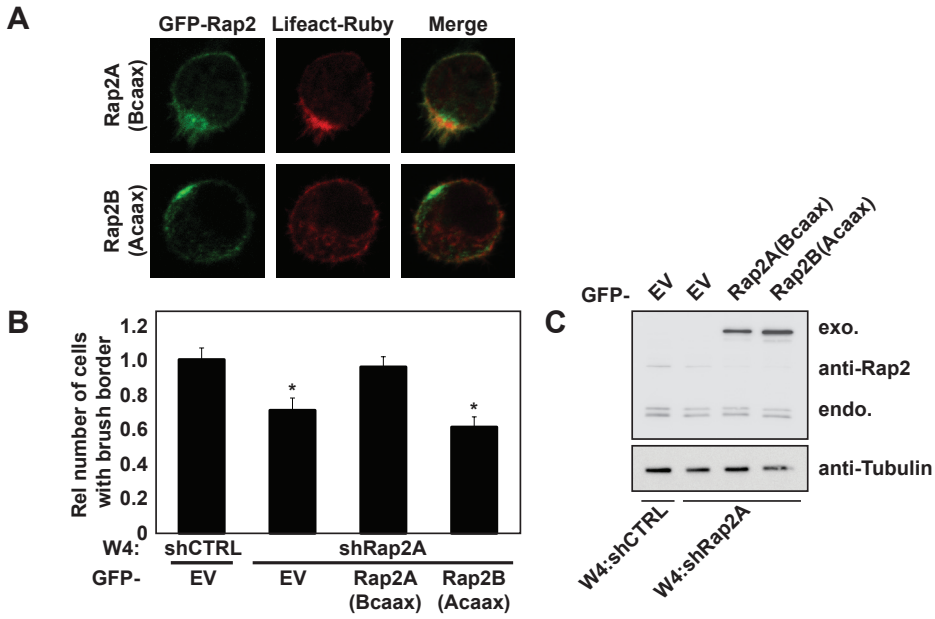

Figure 5: CAAX-box swopped Rap2A and Rap2B mutants function indistinguishable from the wild type Rap2 proteins.
(**a**) Images of Rap2A depleted W4 cells expressing GFP-tagged CAAX-swopped Rap2 constructs and Lifeact-Ruby. (**b**) Quantification of brush border formation in Rap2A-depleted W4 cells in which GFP-tagged CAAX-box mutant Rap2A and Rap2B were expressed. (Total counts ~ 150 cells per condition) * $p < 0{,}05$ using paired samples t-test. (**c**) Western blot of lysates from a rescue experiment probed with anti-Rap2 antibody and anti-αTubulin as a loading control. exo. exogenous, endo. endogenous

moiety[17]. To investigate whether different isoprenyl modifications cause selective activation we generated Rap2A and Rap2B mutants in which CAAX box sequences were interchanged and performed a rescue experiment in Rap2A depleted W4 cells. We find that both geranylgeranylated Rap2A and farnesylated Rap2B are functionally indistinct from wild type Rap2A and Rap2B (Fig. 5a,b). Therefore, we conclude that differential CAAX modification does not underlie specificity between Rap2A and Rap2B during brush border formation.

Discussion

Although the Rap2 GTPases are highly similar, they are engaged in isoform specific signaling pathways. For instance, during intestinal polarity establishment isoform specific signaling by Rap2A regulates the formation of the apical brush border. Since the Rap2 proteins are most divergent in their hypervariable region, which affects protein localization, differential localization would be the simplest explanation for isoform specificity. We indeed show that in polarized intestinal epithelial cells Rap2C is localized in cytoplasmic vesicles, whereas Rap2A is at the plasma membrane and apical recycling endosomes. Nevertheless, Rap2B localizes similar to Rap2A implying that other factors than localization must determine specificity between Rap2A and Rap2B.

We show that in contrast to Rap2A, Rap2B is not activated at the apical plasma membrane during brush border formation. Furthermore, a constitutively activated Rap2B(V12) mutant is able to restore brush border formation in Rap2A-depleted cells, indicating that the failure of Rap2B to become activated determines specificity between Rap2A and Rap2B.

We show that differential activation is imposed by the C-terminal hypervariable region, which also determines localization of Rap2A and Rap2B. Importantly, the hypervariable region regulates Rap2 activity independently of its effects on proteins localization as both Rap2A and Rap2B localize similarly in polarized epithelial cells.

Exactly what feature of the HVR allows for selective activation of Rap2A remains unknown. The hypervariable region of Rap2 comprises the C-terminal 14 amino acids of which four residues differ between Rap2A and Rap2B. Importantly, next to these four residues the HVR of Rap2A and Rap2B is differentially isoprenylated as a result of different CAAX motifs: whereas Rap2A is modified with a farnesyl moiety, Rap2B is equipped with a geranylgeranyl moiety. Although differential isoprenylation could allow for isoform specific binding partners[10], we find that differential CAAX modification does not underlie signaling specificity between Rap2A and Rap2B during brush border formation.

Our study thus suggests that subtle differences in het HVR sequence affect the ability of PDZGEF to activate Rap2B. The involvement of the C-terminus in determining specificity of a GEF is not without precedence. For instance, a proline-rich sequence in the carboxy-terminus of Rac1 allows specific binding of the SH3-domain containing GEF ß-PIX[18]. In addition, the C-terminus can regulate activity of GTPases by other means than providing a direct binding site for GEFs. For example, a polybasic motif in the hypervariable region of Rac1 allows binding of Extracellular Signal-Regulated Kinase (ERK) that by phosphorylating Rac1 at position T108 affects GEF binding[19]. For Rap2, so far no isoform specific interaction partners have been documented that could explain selective activation of Rap2A. However, our data suggests that the HVRs of Rap2A and Rap2B engage in isoform specific interactions that results in the selective activation of Rap2A.

In conclusion, we identify a function for the hypervariable region of the Rap2 proteins in regulating protein activity independent of its function in regulating protein localization during brush border formation.

Methods

Cell culture and constructs

Ls174T:W4 cells[11] were cultured in RPMI1640 (Lonza) supplemented with 10%

tetracycline-free FBS (Lonza) and antibiotics. For transient transfection, cells, while in suspension, were transfected with X-tremeGene 9 (Roche) according to the manufacturer's protocol. To induce polarization, cells were trypsinized and seeded in doxycycline-containing medium (1 μg/ml) for at least 16h.
N-terminally GFP-, CFP- and V5- tagged Rap2 constructs were cloned using Gateway recombination (Invitrogen) in a pcDNA3 backbone. HVR- and CAAX-mutants were generated by site-directed mutagenesis and the isolated HVR constructs were generated by directly ligating annealed oligo's into pEGFP-C2 using the EcoRI and SalI restriction sites.

Lentiviral knockdown
Ls174T:W4 cells were infected for two successive days with lentiviral shRNA constructs (Mission library, Sigma). Three days after the first round of infection, infected cells were selected with puromycin (10 μg/ml) for three days. For stable knockdown, four shRNAs targeting the Rap2A mRNA were pooled (Targeting sequences shRNA #1: 5'-CGGCACCTTCATCGAGAAATA-3', shRNA #2: 5'-CCTTTATGGAAACTTCCGCTA-3', shRNA #3: 5'-GACGAACTCTTTGCAGAAATT-3', shRNA #4: 5'-GTATGAGAAAGTGCCAGTCAT-3') , whereas for rescue experiments with Rap2A(B-HVR) and CAAX mutants a single Rap2A shRNA was used, targeting the sequence encoding the Rap2A HVR. (Targeting sequence shRNA #5: 5'-GTTCTGCATGTAACATACAAT-3') shRNAs were validated to have no compensatory effects on Rap2B and Rap2C mRNA levels. (Supporting information Fig. S1 and[2])

Life cell imaging
Two days after transfection, cells were stimulated with doxycycline and seeded on glass bottom dishes (WillCo Wells). After at least 16h, cells were imaged in Hepes-buffered (pH 7.4) Leibovitz's L-15 medium (Invitrogen) at 37°C on an Axioskop2 LSM510 confocal microscope (Zeiss). Brush border formation was quantified in three independent experiments for a total of at least 150 cells and averages before normalization were compared with control transfected W4 cells using paired samples t-test.

Rap activity assay
V5-Rap2 constructs were transfected in W4 cells and cells were stimulated with doxycycline for various time points. Cells were gently scraped in cold lysis buffer [1% Nonidet P-40 substitute; 10% glycerol; 50 mM Tris-HCl pH 7.4; 2.0 mM $MgCl_2$; 200 mM NaCl; protease and phosphatase inhibitors] and cleared by centrifugation at 4°C. Protein concentration of the cleared lysates was quantified using the BCA protein assay (Thermo) and equal amounts of protein were subjected to precipitation with glutathione-agarose beads coupled with the GST fusion protein of the Ras-binding domain of RalGDS (GST-RalGDS-RBD)[16]. Beads were washed, eluted in Laemmli sample buffer and resolved by SDS

PAGE. Western blots were probed with anti-panRap2 (BD Biosciences), anti-V5 (Invitrogen), anti-αTubulin (Calbiochem) and anti-FLAG (M2) (Sigma).
Blots from three independent experiments were quantified using ImageJ software. For this the ratio between band intensities of the V5 signal in pulldown and total lysates was determined and expressed relative to V5-Rap2A without doxycycline stimulation (or V5-Rap2B in Fig. S4 of the supporting information). Quantifications show the average ratios in three experiments with error bars representing standard deviations.

Quantitative PCR
RNA from W4 cells infected with four different or a single (#5) shRap2A hairpin was isolated using the RNeasy Mini Kit (Qiagen). RNA concentration was quantified and 2 µg of RNA was converted to cDNA using the iScript cDNA synthesis kit (Bio-Rad). cDNA from control infected W4 cells was diluted to generate a reference dilution series and cDNA levels were quantified by SYBR green real-time PCR on a C1000 Thermal Cycler (Bio-Rad). The following primer sequences were used: Rap2A-FW 5'-CATGCTGTTCTGCATGTAAC-3', Rap2A-RV 5'-CAAGTTCTGCAGTGGAGTAG-3', Rap2B-FW 5'-GACTGATTGCGATTCTGAGG-3', Rap2B-RV 5'-CACACTGTATTGGCATCAGT-3', Rap2C-FW 5'-CAGGATATCAAGCCAATGAG-3', Rap2C-RV 5'-CTGAAGACATAACCTCTCTTTC-3'. Expression levels were normalized to HPRT1 and GAPDH mRNA levels. Relative expression levels of thee QPCR experiments were averaged and pooled standard deviations were calculated. Average relative expression levels of the two W4:shRap2A samples were compared to the W4:shCTRL reference using independent samples Students' t-test.

Acknowledgements
We would like to thank F.J. Zwartkruis and W.J. Pannekoek for critical evaluation of the manuscript and all lab members for continuous support and discussion.

References
1 Popovic, M., Rensen-de Leeuw, M. & Rehmann, H. Selectivity of CDC25 Homology Domain-Containing Guanine Nucleotide Exchange Factors. Journal of molecular biology 425, 2782-2794, doi:10.1016/j.jmb.2013.04.031 (2013).
2 Gloerich, M. et al. Rap2A links intestinal cell polarity to brush border formation. Nature cell biology 14, 793-801, doi:10.1038/ncb2537 (2012).
3 Evellin, S. et al. Stimulation of phospholipase C-epsilon by the M3 muscarinic acetylcholine receptor mediated by cyclic AMP and the GTPase Rap2B. The Journal of biological chemistry 277, 16805-16813, doi:10.1074/jbc.M112024200 (2002).
4 Stope, M. B. et al. Rap2B-dependent stimulation of phospholipase C-epsilon by epidermal growth factor receptor mediated by c-Src phosphorylation of RasGRP3. Molecular and cellular biology 24, 4664-4676, doi:10.1128/

MCB.24.11.4664-4676.2004 (2004).
5 Hancock, J. F. Ras proteins: different signals from different locations. Nature reviews. Molecular cell biology 4, 373-384, doi:10.1038/nrm1105 (2003).
6 Laude, A. J. & Prior, I. A. Palmitoylation and localisation of RAS isoforms are modulated by the hypervariable linker domain. Journal of cell science 121, 421-427, doi:10.1242/jcs.020107 (2008).
7 Hancock, J. F., Paterson, H. & Marshall, C. J. A polybasic domain or palmitoylation is required in addition to the CAAX motif to localize p21ras to the plasma membrane. Cell 63, 133-139 (1990).
8 Ahearn, I. M., Haigis, K., Bar-Sagi, D. & Philips, M. R. Regulating the regulator: post-translational modification of RAS. Nature reviews. Molecular cell biology 13, 39-51, doi:10.1038/nrm3255 (2012).
9 Uechi, Y. et al. Rap2 function requires palmitoylation and recycling endosome localization. Biochemical and biophysical research communications 378, 732-737, doi:10.1016/j.bbrc.2008.11.107 (2009).
10 Chandra, A. et al. The GDI-like solubilizing factor PDEdelta sustains the spatial organization and signalling of Ras family proteins. Nature cell biology, doi:10.1038/ncb2394 (2011).
11 Baas, A. F. et al. Complete polarization of single intestinal epithelial cells upon activation of LKB1 by STRAD. Cell 116, 457-466 (2004).
12 Gloerich, M. & Bos, J. L. Regulating Rap small G-proteins in time and space. Trends in cell biology 21, 615-623, doi:10.1016/j.tcb.2011.07.001 (2011).
13 Riedl, J. et al. Lifeact: a versatile marker to visualize F-actin. Nature methods 5, 605-607, doi:10.1038/nmeth.1220 (2008).
14 Bryant, D. M. et al. A molecular network for de novo generation of the apical surface and lumen. Nature cell biology 12, 1035-1045, doi:10.1038/ncb2106 (2010).
15 Dhekne, H. S. et al. Myosin Vb and rab11a regulate ezrin phosphorylation in enterocytes. Journal of cell science, doi:10.1242/jcs.137273 (2014).
16 van Triest, M., de Rooij, J. & Bos, J. L. Measurement of GTP-bound Ras-like GTPases by activation-specific probes. Methods in enzymology 333, 343-348 (2001).
17 Farrell, F. X., Yamamoto, K. & Lapetina, E. G. Prenyl group identification of rap2 proteins: a ras superfamily member other than ras that is farnesylated. The Biochemical journal 289 (Pt 2), 349-355 (1993).
18 ten Klooster, J. P., Jaffer, Z. M., Chernoff, J. & Hordijk, P. L. Targeting and activation of Rac1 are mediated by the exchange factor beta-Pix. The Journal of cell biology 172, 759-769, doi:10.1083/jcb.200509096 (2006).
19 Tong, J., Li, L., Ballermann, B. & Wang, Z. Phosphorylation of Rac1 T108 by extracellular signal-regulated kinase in response to epidermal growth factor: a novel mechanism to regulate Rac1 function. Molecular and cellular biology 33, 4538-4551, doi:10.1128/MCB.00822-13 (2013).

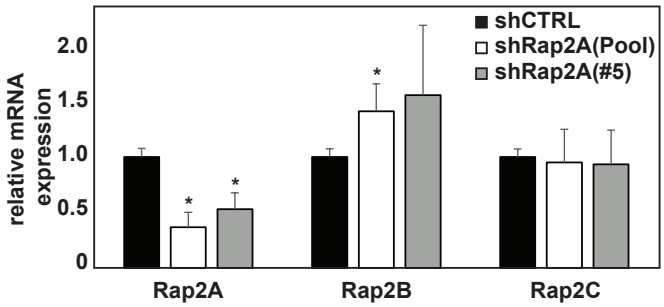

Figure S1: Relative expression levels of Rap2 isoforms in W4 cells infected with pooled shRap2A hairpins or a single (#5) shRap2A hairpin.
RNA from W4:shRap2A cells was extracted and subjected to QPCR for the Rap2 isoforms. Average relative expression levels were determined in three QPCR experiments from independent RNA extractions. Error bars indicate standard deviation. * $p < 0,05$

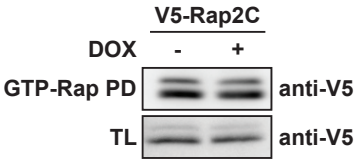

Figure S2: Rap2C activity is not induced during W4 cell polarization.
Pulldown of GTP-bound Rap from W4 cells transfected with V5-Rap2C with or without 20h of doxycycline stimulation.

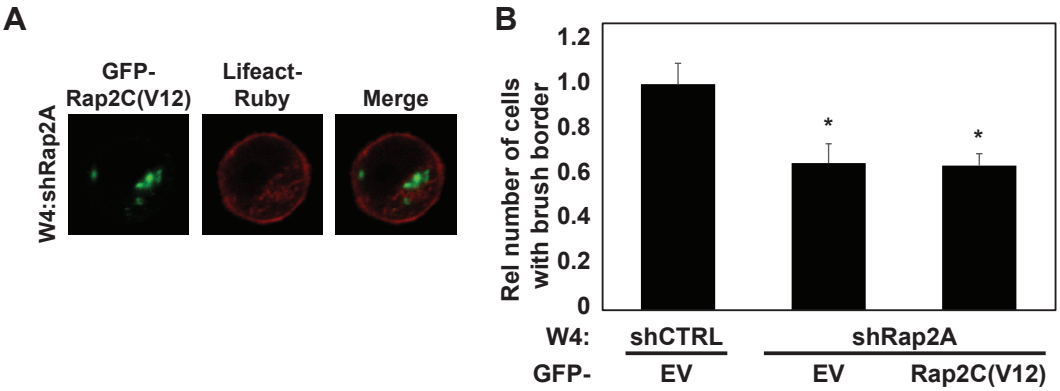

Figure S3: Constitutively activated Rap2C(V12) can not restore brush border formation in Rap2A depleted W4 cells.
(**a**) Image of Rap2A-depleted cell expressing GFP-Rap2C(V12) and the actin marker Lifeact-Ruby. (**b**)Quantification of brush border formation in W4 cells stably depleted of endogenous Rap2A expressing GFP or GFP-tagged Rap2C(V12) (total counts ~200 cells per condition). * $p < 0,05$ using paired samples t-test.

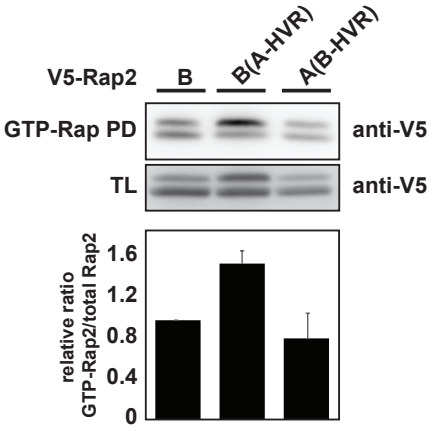

Figure S4: Rap2A(B-HVR) is less active compared to Rap2B(A-HVR) in polarized W4 cells. GTP-Rap pulldown from W4 cells transfected with V5-Rap2B, V5-Rap2B(A-HVR) or V5-Rap2A(B-HVR) after doxycline-induced polarization. Results from three independent pulldown experiments were quantified and expressed as ratios of GTP-Rap2 vs. total Rap2 relative to Rap2B. Error bars represent the standard deviation in the ratios of independent experiments.

VII

Summarizing Discussion

7

Breaking of cellular symmetry in order to establish an apico-basal polarity axis initiates *de novo* formation of cell polarity. However, symmetry breaking provides a formidable challenge from a signaling perspective, because by definition no spatial cues are present to instruct axis establishment. Instead, symmetry breaking is driven by amplification of stochastic fluctuations in signaling activity. A concomitant problem of this is that polarization can occur at multiple sites; a situation that could be detrimental to the cell. Therefore, cells must be able to restrict polarization to a single domain.

Throughout evolution, small GTPases, and Cdc42 in particular, are involved in the control of symmetry breaking events. By engaging different GEFs, GAPs and effectors, Cdc42 signaling is orchestrated with pinpoint precision to control the various cellular processes that contribute to cell polarization. In this thesis, novel signaling pathways have been presented that establish functional asymmetry during enterocyte polarization.

Cdc42 controls singularity in apical domain specification

Cell-cell junctions are generally considered to safeguard singularity in apical domain specification. However, the finding that epithelial cells that polarize in the absence of junctions rarely form multiple apical domains suggests that cell-intrinsic mechanisms ensure singularity in apical domain specification[1,2]. We reveal a crucial function for Cdc42 in ensuring singularity in polarization as demonstrated by the finding that a large fraction of Cdc42 knockout cells present with multiple apical domains.

To enforce singularity in polarization, Cdc42 is under spatial control of ATP8B1, a flippase that is mutated in progressive familial intrahepatic cholestasis type 1 (PFIC1) patients. ATP8B1 functions to limit Cdc42 mobility, thereby spatially restricting Cdc42 signaling at the apical plasma membrane. As a consequence, loss of ATP8B1 impairs Cdc42 confinement and results in cells with an enlarged apical membrane and cells with multiple apical domains (Fig. 1a, b).
The formation of an enlarged apical plasma membrane is also observed in enterocytes of small intestinal organoid cultures from ATP8B1-deficient mice. This finding therefore indicates that regulation of apical domain size by ATP8B1/Cdc42 also contributes to epithelial architecture when cell-cell junction are present. Furthermore, the finding that apical membrane morphology is affected in PFIC patients also suggests that loss of this regulation underlies human pathologies.

How does Cdc42 ensure the formation of a single apical domain? During yeast cell polarization, singularity in apical membrane formation originates from a winner-takes-all competition between multiple, growing polarity clusters for limited polarity factors[3]. Analogous to this, two findings suggest that a similar

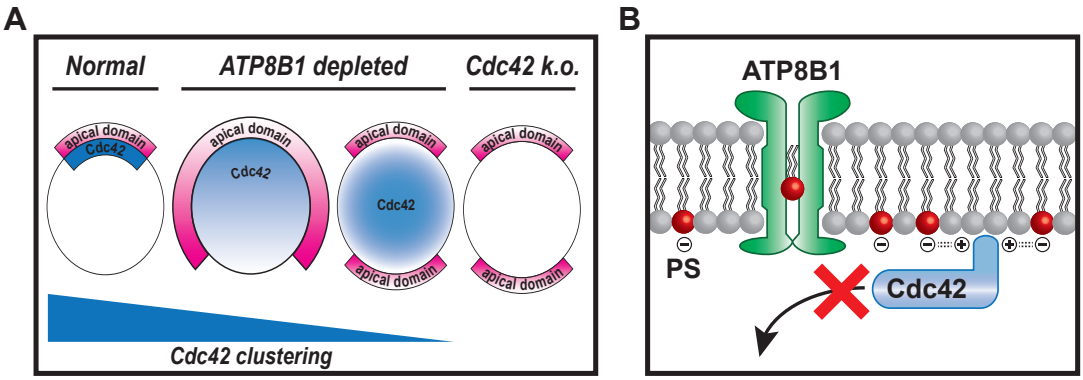

Figure 1: Graphical summary of chapter two
(**a**) The ability to restrict apical domain formation correlates with degree of Cdc42 clustering at the apical plasma membrane. In polarized Ls174T:W4 cells, clustered localization of Cdc42 (blue) results in the formation of a clustered apical domain (pink). If Cdc42 is not properly confined, as in ATP8B1-depleted cells, the apical domain is enlarged or multiple apical domains are formed. Absence of Cdc42 results in the formation of multiple apical domains. (**b**) Mechanism of spatial regulation of Cdc42 by ATP8B1. ATP8B1, by catalyzing the internalization, or flipping, of phosphatidylserine (PS, red) reduces Cdc42 mobility at the apical membrane. The interaction between negatively charged PS with positively charged residues in the C-terminus of Cdc42 is critical for this. Curved arrow represents Cdc42 eviction.

competition for Cdc42 may underlie singularity in epithelial cell polarization. Firstly, we show that impairing the ability to confine Cdc42 into a cluster, by increasing Cdc42 mobility, resulted in the formation of multiple apical domains. Secondly, the competition between polarity clusters during yeast cell polarization is dependent on RhoGDI-mediated transfer of Cdc42[3,4]. We show that singularity in polarization can not be ensured when Cdc42 is unable to bind RhoGDI, which may indicate the presence of a similar competition for Cdc42 in enterocytes.

Although many parallels between yeast cell polarization and enterocyte polarization can be observed, there are several notable differences. Firstly, whereas Cdc42 is absolutely required for yeast cell polarization and bud formation, Cdc42 is not required for apical membrane formation in Ls174T:W4 cells[5]. Instead Cdc42 is only responsible for the clustered positioning of the apical domain. Secondly, whereas Cdc42 is also regulated by flippases during yeast cell polarization, these flippases function to promote Cdc42 membrane dissociation, which is the opposite of ATP8B1[6,7]. Thirdly, whereas loss of flippase activity in yeast causes the formation of elongated buds, no yeast flippases are associated with singularity defects[6].

Activity-dependent regulation of Cdc42 mobility
Given the crucial role of Cdc42 mobility in safeguarding singularity in apical membrane formation, we questioned how activation affects Cdc42 mobility. We demonstrate that Cdc42 is subjected to a drastic immobilization upon GTP-loading which originates from a dual mechanism: on the one hand, Cdc42

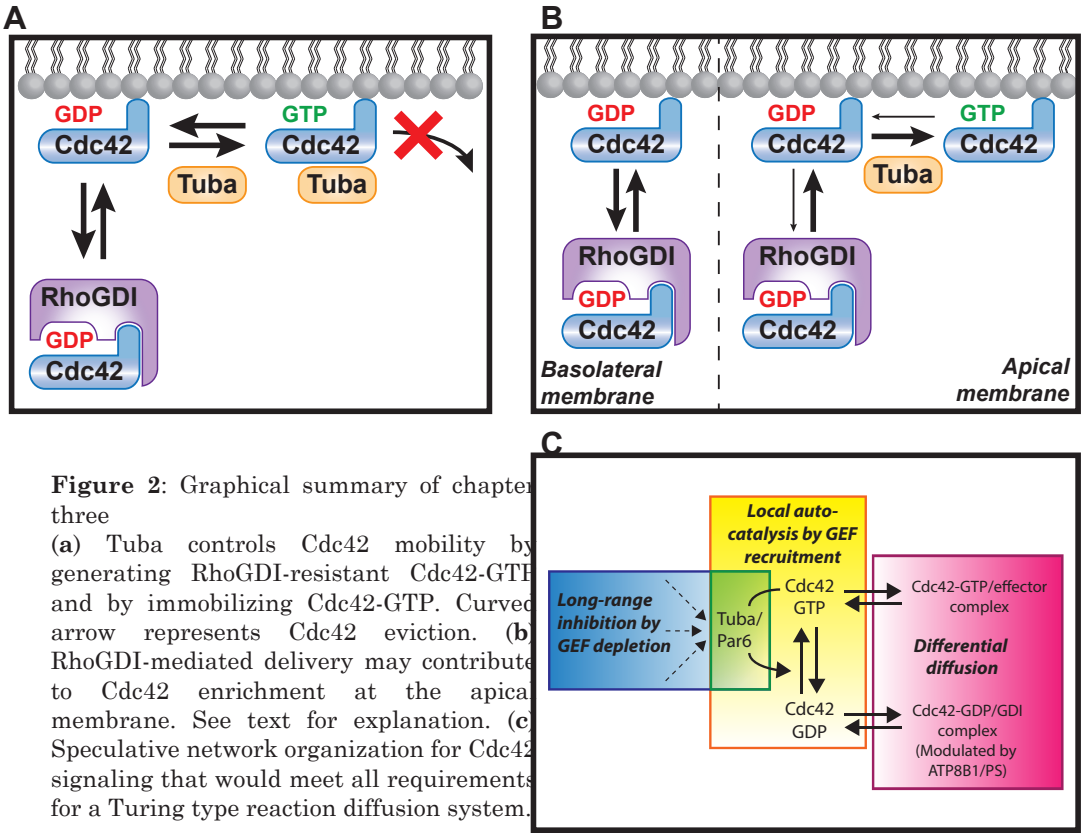

Figure 2: Graphical summary of chapter three
(**a**) Tuba controls Cdc42 mobility by generating RhoGDI-resistant Cdc42-GTP and by immobilizing Cdc42-GTP. Curved arrow represents Cdc42 eviction. (**b**) RhoGDI-mediated delivery may contribute to Cdc42 enrichment at the apical membrane. See text for explanation. (**c**) Speculative network organization for Cdc42 signaling that would meet all requirements for a Turing type reaction diffusion system.

activation abolishes RhoGDI-dependent membrane dissociation. On the other hand, GTP-loaded Cdc42 is immobilized by the Cdc42GEF Tuba. We demonstrate that interference with either mechanism affects Cdc42 mobility and function (Fig. 2a).
An important consequence of the notion that RhoGDI only dissociates Cdc42-GDP and not Cdc42-GTP from the membrane is that RhoGDI may contribute to apical enrichment of Cdc42. RhoGDI-dependent membrane extraction is reversible and therefore extraction is normally balanced by delivery. However, at sites of Tuba activity where Cdc42-GDP is converted into Cdc42-GTP, RhoGDI-mediated delivery of Cdc42-GDP exceeds membrane extraction. As a result, RhoGDI may create an influx of Cdc42 molecules into a cluster of Cdc42 activity, thereby contributing to Cdc42 enrichment at the apical membrane (Fig. 2b).

The large difference between Cdc42-GDP and Cdc42-GTP mobility poses the question to what extent regulation of Cdc42 membrane association by ATP8B1 is relevant in the context of activity-dependent mobility regulation. Because the effect of ATP8B1 on Cdc42 mobility was demonstrated using the isolated hypervariable region (HVR) of Cdc42, this difference reflects a reduction in membrane association that is independent of RhoGDI-binding and GDP/GTP cycling. However, also in the context of full length Cdc42, we measured

in an increased mobility for Cdc42(D185) that was largely dependent on the interaction with RhoGDI (data not shown). This suggests that the decreased membrane association caused by ATP8B1 makes Cdc42 more prone to RhoGDI-mediated membrane dissociation. Because the polybasic region of Cdc42 directly interacts with RhoGDI, it may be that the interaction between the PBR and PS inhibits Cdc42 membrane dissociation by RhoGDI by preventing RhoGDI binding[8]. Therefore it is likely that both decreased membrane association and increased RhoGDI-mediated membrane extraction cooperate to impose the diffuse localization of Cdc42 in ATP8B1-depeleted cells.

Differential mobility between an active and inactive signaling molecule is one of the requirements for a Turing type reaction-diffusion network. Because Cdc42 dynamics during yeast cell polarization can be modeled according to a Turing type mechanism and because it can mathematically account for symmetry breaking and singularity, it is tempting to speculate that Cdc42 signaling during Ls174T:W4 cell polarization also embodies a Turing type network[9-12]. Next to differential diffusion, a classic Turing network also comprises a positive feedback mechanism to amplify a stochastic fluctuation in signaling and a means of long-range inhibition to prevent ectopic cluster formation[12].

During yeast cell polarization, a positive feedback loop for Cdc42-GTP production is established by recruitment of the Cdc42GEF, Cdc24, by means of the scaffold protein, Bem1, which directly binds activated Cdc42[13,14]. A similar feedback mechanism may operate during enterocyte polarization, since various Cdc42 effectors directly bind GEFs and could thereby recruit GEF activity to sites of Cdc42 activity[15,16]. Indeed, Tuba directly binds to the Cdc42 effector NWASP and the Tuba/NWASP complex is implicated in various Cdc42-dependent polarization processes[17-19]. We however could neither find an apparent polarity phenotype in NWASP knockout Ls174T:W4 cells nor was the mobility of Cdc42 affected in these cells (data not shown). Preliminary findings suggests, that Tuba directly associates with the Cdc42 effector Par6, suggesting that formation of a Tuba/Cdc42/Par6 complex could establish a positive feedback mechanism for the generation of Cdc42-GTP and additionally could contribute to the Tuba-dependent immobilization of active Cdc42.

Next to a positive feedback mechanism that may depend on a GEF/effector complex, amplification of a Cdc42 cluster at the apical membrane could involve Cdc42 delivery by apical recycling endosomes. This feedback recruitment mechanism was shown to operate during yeast cell polarization and is responsible for Cdc42 enrichment at the leading edge of migrating fibroblast[20-22]. However, we do not see obvious localization of Cdc42 to recycling endosomes. Furthermore, for yeast it has been debated whether the Cdc42 concentration on vesicles is sufficient to contribute to Cdc42 cluster expansion[23].

The final Turing requirement involves a mechanism to suppress ectopic cluster formation, either by means of long-range inhibition or by depletion of an essential 'substrate'[10]. In the model for yeast cell polarization, the essential substrate is the Cdc24/Bem1 complex which is depleted from the cytosol by membrane-bound Cdc42[9]. In support of a similar organization of substrate depletion during Ls174T:W4 cell polarization is the finding that Tuba localization to the plasma membrane is exclusively apical.

Because Turing type signaling networks can account for symmetry breaking and singularity in polarization, it provides an attractive framework to study polarity signaling. A speculative signaling model that would meet the requirements for a Turing network is shown in figure 2c.

Apical domain specification by PTEN

The lipid phosphatase PTEN is best known for antagonizing PI3K-dependent activation of PKB/Akt signaling. However, PTEN also plays a role in cell polarization via which it contributes to epithelial tissue architecture and this could contribute to the tumor suppressive properties of PTEN. We reveal that PTEN is required to restrict apical membrane formation to a limited part of the cell as PTEN knockout Ls174T:W4 cells form an apical brush border that spans the entire plasma membrane. To ensure apical membrane clustering, PTEN binds to the PDZ-domain containing phosphatase PTPL1 and this interaction is required to enrich PTEN at the apical plasma membrane (Fig. 3).

Because loss of PTEN and PTPL1 both result in an apical membrane clustering defect similar to loss of ATP8B1 and Cdc42, the question arises whether they operate in the same pathway. In support of this idea, PTEN is suggested to regulate Cdc42 localization by generating $PI(4,5)P_2$ at the apical plasma membrane, thereby recruiting Annexin2, which in turn binds and localizes activated Cdc42[24]. Several findings argue against this link and suggest that both pathways are non-redundant: firstly, the increase in apical membrane size in ATP8B1-depleted cells was rescued by expression of a Cdc42 mutant

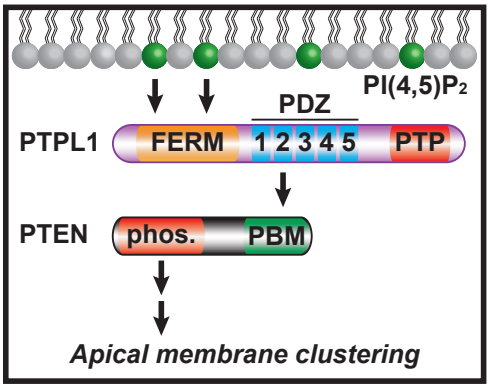

Figure 3: Graphical summary of chapter four
PTPL1-mediated apical membrane recruitment of PTEN is required for apical membrane clustering. PTPL1 is localized to the apical plasma membrane by binding to $PI(4,5)P_2$ (green) via its 4.1, Ezrin, Radixin, Moesin (FERM) domain. PTEN binds to the second PDZ domain of PTPL1 by means of its PDZ binding motif (PBM) and this is required for apical enrichment of PTEN and consequently apical membrane clustering. PTP = protein tyrosine phosphatase domain, phos. = phosphatase domain.

that was localized to $PI(4,5)P_2$. If Cdc42 is normally localized to $PI(4,5)P_2$ via Annexin2 this Cdc42-PH mutant would likely not be required to bypass the need for PS/ATP8B1. Secondly, whereas expression of a Cdc42 mutant with reduced mobility (Cdc42(2xPBR)) was able to rescue the clustering defect of ATP8B1-depleted, it could not restore normal apical membrane size in PTPL1-depleted cells (data not shown). Thirdly, we show that Cdc42 mobility is tightly regulated for its function in apical membrane clustering, yet we find no effect of PTEN or PTPL1 loss on Cdc42 mobility (data not shown). Finally, knockdown of Annexin2 did not result in apical membrane enlargement or the formation of multiple brush border (data not shown).

If the PTEN/PTPL1 and ATP8B1/Cdc42 pathways are not closely connected how do they relate to one another? It might be that both clustering pathways, although similar in Ls174T:W4 cells, are required during different processes that require regulation of apical domain size. In support of this, ATP8B1 is predominantly expressed in terminally differentiated polarized epithelial cells where control over apical membrane size is required to ensure proper lumen morphology[25]. PTEN has been implicated in controlling apical membrane size of polarized neuroepithelial cells in the process of neural tube closure[26]. In this process, constriction of the apical membrane allows invagination of the epithelial sheet which ultimately forms the neural tube. Therefore, we speculate that PTEN/PTPL1-dependent clustering may be more relevant in the dynamic control over apical membrane size, whereas ATP8B1/Cdc42-mediated clustering may mostly operate under static conditions.

A closer look at the phenotypes of PTEN and Cdc42 already indicates that both clustering modules are different: whereas some Cdc42 knockout cells form a brush border that covers the complete plasma membrane it is much less frequent then in PTEN knockout cells. Conversely, PTEN (or PTPL1) loss results in an enlarged brush border, but cells rarely form multiple apical domains, indicating that singularity regulation is not affected.

The notion that the tumor suppressor PTEN controls apical membrane clustering solicits the question to what extent this regulation may be relevant in tumorigenesis. Epithelial tissue architecture is a barrier in oncogenic progression and this barrier might be broken by inadequate control over apical membrane clustering[27-29]. An increased apical domain might for instance result in cell eviction in the central lumen, a process that has been implicated in breast cancer progression[28]. Alternatively, loss over tissue architecture might disrupt the establishment of chemical gradients that control normal tissue homeostasis[30]. Furthermore, if epithelial barrier function is affected by an increased apical membrane size, cancer cells may more readily metastasize to the underlying tissue[31]. Although these examples are only speculative mechanisms via which

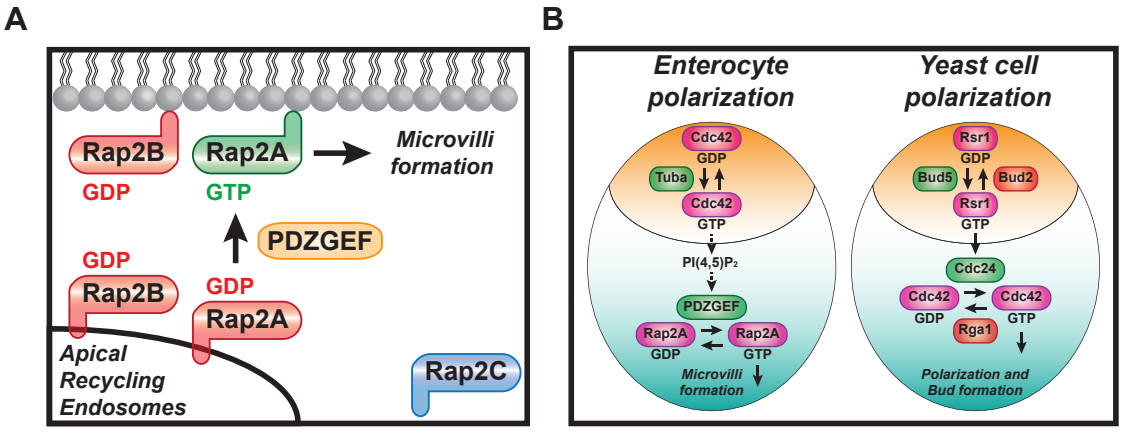

Figure 4: Graphical summary of chapter six
(**a**) Isoform-specific signaling by Rap2A during microvilli formation is enabled via two mechanisms: Rap2C is not translocated to the apical membrane via recycling endosomes during cell polarization and does therefore not contribute to signaling. On the other hand Rap2B, although properly localized, is not activated by PDZGEF at the apical domain. (**b**) Hierarchical organization of Cdc42 and Rap signaling during enterocyte and yeast cell polarization. GTPases are in pink, GEFs in green and GAPs in red. The nascent apical domain is depicted in orange.

apical membrane size could affect tumorigenesis, the notion that ATP8B1, PTPL1 and PTEN are frequently mutated and lost in epithelial malignancies is an argument that control over apical membrane size might suppress oncogenic progression[32-34].

Isoform specific Rap2 signaling during brush border formation

A fundamental question in GTPase signaling is how highly similar small GTPases can signal independently without signal interference. Rap2A is the sole Rap2 isoform that engages in brush border formation, despite expression of the other Rap2B and Rap2C isoforms[35]. We reveal that this isoform specific signaling originates from differential localization of the Rap2C isoform and selective activation of Rap2A over Rap2B. Crucial differences in the C-terminal HVR of Rap2B enable this selective activation of Rap2A (Fig. 4a).

Since the C-terminal HVR is primarily implicated in controlling the localization of small GTPases, the selective activation of Rap2A over Rap2B might also originate from a differential localization. However, Rap2A and Rap2B localize apparently similarly and constitutively active Rap2B(V12) is able to rescue Rap2A depletion, indicating that Rap2B at least is able to access the correct location to initiate brush border formation. Because PDZGEF, the RapGEF involved in Rap2A activation during brush border formation, does not discriminate between Rap2 isoforms *in vitro*, an interesting alternative would be the existence of a GAP that is able keep Rap2B inactive[36].

In general, isoform-specific signaling ensures that two processes do not interfere with one another. For brush border formation, this would mean that selective activation of Rap2A ensures that Rap2B signaling is not disturbed. Indeed, Rap2B itself engages in isoform-specific signaling at the plasma membrane and therefore this regulation may prevent interference between Rap2A and Rap2B signaling[37,38]. Rap2C is instead located in cytosolic structures suggesting that Rap2C has a specific function at these sites.

How is brush border formation by Rap2A linked with apical domain specification by Cdc42? As the pioneering factor for cell polarization, Cdc42 signaling at the nascent apical membrane establishes the spatial cues that instruct Rap2A signaling. Apical $PI(4,5)P_2$ may be the prime spatial cue as its clustering requires Cdc42 and because it has been implicated in the recruitment of PDZGEF[35]. How Cdc42 controls $PI(4,5)P_2$ lipid distribution at the apical membrane remains unclear, but this might involve PIP5K as Cdc42 can directly activate PIP5K *in vitro*[39].

Interestingly, whereas in enterocytes Cdc42 signaling provides the spatial cue for Rap2 signaling, this hierarchy is inverse during yeast cell polarization. In yeast, the Rap orthologue Rsr1, together with its GEF Bud5 and GAP Bud2, is part of the bud site selection machinery which prevents re-usage of previous bud sites[40]. For this, activated Rsr1 binds the GEF Cdc24 and activates its GEF activity towards Cdc42 thereby spatially controlling Cdc42-dependent symmetry breaking (Fig. 4b)[41,42]. Irrespective of the hierarchy, in both systems Rap signaling functions to mark a cortical site which is then subjected to remodeling of the actin cytoskeleton.

Concluding remarks

The generation of cellular asymmetry creates functionally distinct domains within a cell and is therefore a fundamental process in biology. Polarized enterocytes in the intestine epitomize this functional asymmetry by developing highly specialized apical and basal domains that are crucial for enterocyte function. Here, we have identified novel signaling mechanisms that contribute to symmetry breaking by controlling apical membrane clustering, singularity in apical domain specification and brush border formation. Importantly, we reveal that singularity in apical domain specification is actively safeguarded in polarized epithelial cells by Cdc42 signaling and implicate this regulation in human pathologies.

References

1 Baas, A. F. et al. Complete polarization of single intestinal epithelial cells upon activation of LKB1 by STRAD. Cell 116, 457-466 (2004).
2 Gon, H., Fumoto, K., Ku, Y., Matsumoto, S. & Kikuchi, A. Wnt5a signaling promotes apical and basolateral polarization of single epithelial cells. Molecular biology of the cell 24, 3764-3774, doi:10.1091/mbc.E13-07-0357 (2013).
3 Wu, C. F. et al. Role of competition between polarity sites in establishing a unique front. Elife 4, doi:10.7554/eLife.11611 (2015).
4 Freisinger, T. et al. Establishment of a robust single axis of cell polarity by coupling multiple positive feedback loops. Nature communications 4, 1807, doi:10.1038/ncomms2795 (2013).
5 Johnson, D. I. & Pringle, J. R. Molecular characterization of CDC42, a Saccharomyces cerevisiae gene involved in the development of cell polarity. The Journal of cell biology 111, 143-152 (1990).
6 Saito, K. et al. Transbilayer phospholipid flipping regulates Cdc42p signaling during polarized cell growth via Rga GTPase-activating proteins. Developmental cell 13, 743-751, doi:10.1016/j.devcel.2007.09.014 (2007).
7 Das, A. et al. Flippase-mediated phospholipid asymmetry promotes fast Cdc42 recycling in dynamic maintenance of cell polarity. Nature cell biology 14, 304-310, doi:10.1038/ncb2444 (2012).
8 Hoffman, G. R., Nassar, N. & Cerione, R. A. Structure of the Rho family GTP-binding protein Cdc42 in complex with the multifunctional regulator RhoGDI. Cell 100, 345-356 (2000).
9 Goryachev, A. B. & Pokhilko, A. V. Dynamics of Cdc42 network embodies a Turing-type mechanism of yeast cell polarity. FEBS letters 582, 1437-1443, doi:10.1016/j.febslet.2008.03.029 (2008).
10 Wu, C. F. & Lew, D. J. Beyond symmetry-breaking: competition and negative feedback in GTPase regulation. Trends in cell biology 23, 476-483, doi:10.1016/j.tcb.2013.05.003 (2013).
11 Huang, S. Where to Go: Breaking the Symmetry in Cell Motility. PLoS biology 14, e1002463, doi:10.1371/journal.pbio.1002463 (2016).
12 Turing, A. M. The Chemical Basis of Morphogenesis. Philosophical Transactions of the Royal Society of London B: Biological Sciences 237, 37-72 (1952).
13 Irazoqui, J. E., Gladfelter, A. S. & Lew, D. J. Scaffold-mediated symmetry breaking by Cdc42p. Nature cell biology 5, 1062-1070, doi:10.1038/ncb1068 (2003).
14 Kozubowski, L. et al. Symmetry-breaking polarization driven by a Cdc42p GEF-PAK complex. Current biology : CB 18, 1719-1726, doi:10.1016/j.cub.2008.09.060 (2008).
15 Feng, S. et al. A Rab8 guanine nucleotide exchange factor-effector interaction network regulates primary ciliogenesis. The Journal of biological chemistry 287, 15602-15609, doi:10.1074/jbc.M111.333245 (2012).
16 Manser, E. et al. PAK kinases are directly coupled to the PIX family of nucleotide exchange factors. Molecular cell 1, 183-192 (1998).
17 Otani, T., Ichii, T., Aono, S. & Takeichi, M. Cdc42 GEF Tuba regulates the junctional configuration of simple epithelial cells. The Journal of cell biology 175, 135-146, doi:10.1083/jcb.200605012 (2006).
18 Kovacs, E. M. et al. N-WASP regulates the epithelial junctional actin cytoskeleton through a non-canonical post-nucleation pathway. Nature cell biology 13, 934-943, doi:10.1038/ncb2290 (2011).
19 Salazar, M. A. et al. Tuba, a novel protein containing bin/amphiphysin/Rvs and Dbl homology domains, links dynamin to regulation of the actin cytoskeleton. The Journal of biological chemistry 278, 49031-49043, doi:10.1074/jbc.M308104200 (2003).
20 Slaughter, B. D., Das, A., Schwartz, J. W., Rubinstein, B. & Li, R. Dual modes of cdc42 recycling fine-tune polarized morphogenesis. Developmental cell 17, 823-835, doi:10.1016/j.devcel.2009.10.022 (2009).
21 Slaughter, B. D. et al. Non-uniform membrane diffusion enables steady-state cell polarization via vesicular trafficking. Nature communications 4, 1380, doi:10.1038/ncomms2370 (2013).
22 Osmani, N., Peglion, F., Chavrier, P. & Etienne-Manneville, S. Cdc42 localization and cell polarity depend on membrane traffic. The Journal of cell biology 191, 1261-1269, doi:10.1083/jcb.201003091 (2010).

23 Watson, L. J., Rossi, G. & Brennwald, P. Quantitative analysis of membrane trafficking in regulation of Cdc42 polarity. Traffic 15, 1330-1343, doi:10.1111/tra.12211 (2014).
24 Martin-Belmonte, F. et al. PTEN-mediated apical segregation of phosphoinositides controls epithelial morphogenesis through Cdc42. Cell 128, 383-397, doi:10.1016/j.cell.2006.11.051 (2007).
25 van Mil, S. W. et al. Fic1 is expressed at apical membranes of different epithelial cells in the digestive tract and is induced in the small intestine during postnatal development of mice. Pediatric research 56, 981-987, doi:10.1203/01.PDR.0000145564.06791.D1 (2004).
26 Grego-Bessa, J. et al. The tumor suppressor PTEN and the PDK1 kinase regulate formation of the columnar neural epithelium. Elife 5, doi:10.7554/eLife.12034 (2016).
27 Partanen, J. I., Nieminen, A. I., Makela, T. P. & Klefstrom, J. Suppression of oncogenic properties of c-Myc by LKB1-controlled epithelial organization. Proceedings of the National Academy of Sciences of the United States of America 104, 14694-14699, doi:10.1073/pnas.0704677104 (2007).
28 Leung, C. T. & Brugge, J. S. Outgrowth of single oncogene-expressing cells from suppressive epithelial environments. Nature, doi:10.1038/nature10826 (2012).
29 Martin-Belmonte, F. & Perez-Moreno, M. Epithelial cell polarity, stem cells and cancer. Nature reviews. Cancer 12, 23-38, doi:10.1038/nrc3169 (2012).
30 Levin, M. Morphogenetic fields in embryogenesis, regeneration, and cancer: non-local control of complex patterning. Biosystems 109, 243-261, doi:10.1016/j.biosystems.2012.04.005 (2012).
31 Martin, T. A. The role of tight junctions in cancer metastasis. Seminars in cell & developmental biology 36, 224-231, doi:10.1016/j.semcdb.2014.09.008 (2014).
32 Eldai, H. et al. Novel genes associated with colorectal cancer are revealed by high resolution cytogenetic analysis in a patient specific manner. PloS one 8, e76251, doi:10.1371/journal.pone.0076251 (2013).
33 Wang, Z. et al. Mutational analysis of the tyrosine phosphatome in colorectal cancers. Science 304, 1164-1166, doi:10.1126/science.1096096 (2004).
34 Li, J. et al. PTEN, a putative protein tyrosine phosphatase gene mutated in human brain, breast, and prostate cancer. Science 275, 1943-1947 (1997).
35 Gloerich, M. et al. Rap2A links intestinal cell polarity to brush border formation. Nature cell biology 14, 793-801, doi:10.1038/ncb2537 (2012).
36 Popovic, M., Rensen-de Leeuw, M. & Rehmann, H. Selectivity of CDC25 Homology Domain-Containing Guanine Nucleotide Exchange Factors. Journal of molecular biology 425, 2782-2794, doi:10.1016/j.jmb.2013.04.031 (2013).
37 Evellin, S. et al. Stimulation of phospholipase C-epsilon by the M3 muscarinic acetylcholine receptor mediated by cyclic AMP and the GTPase Rap2B. The Journal of biological chemistry 277, 16805-16813, doi:10.1074/jbc.M112024200 (2002).
38 Stope, M. B. et al. Rap2B-dependent stimulation of phospholipase C-epsilon by epidermal growth factor receptor mediated by c-Src phosphorylation of RasGRP3. Molecular and cellular biology 24, 4664-4676, doi:10.1128/MCB.24.11.4664-4676.2004 (2004).
39 Weernink, P. A. et al. Activation of type I phosphatidylinositol 4-phosphate 5-kinase isoforms by the Rho GTPases, RhoA, Rac1, and Cdc42. The Journal of biological chemistry 279, 7840-7849, doi:10.1074/jbc.M312737200 (2004).
40 Park, H. O. & Bi, E. Central roles of small GTPases in the development of cell polarity in yeast and beyond. Microbiol Mol Biol Rev 71, 48-96, doi:10.1128/MMBR.00028-06 (2007).
41 Shimada, Y., Wiget, P., Gulli, M. P., Bi, E. & Peter, M. The nucleotide exchange factor Cdc24p may be regulated by auto-inhibition. The EMBO journal 23, 1051-1062, doi:10.1038/sj.emboj.7600124 (2004).
42 Wu, C. F., Savage, N. S. & Lew, D. J. Interaction between bud-site selection and polarity-establishment machineries in budding yeast. Philos Trans R Soc Lond B Biol Sci 368, 20130006, doi:10.1098/rstb.2013.0006 (2013).

7

Etc

Appendices

Nederlandstalige Samenvatting

Veel celtypes vormen functioneel verschillende apicale ('voor') en basale ('achter') domeinen die belangrijk zijn voor de functie van de cel. Een voorbeeld van deze apicaal-basale polariteit is de enterocyt, die de deel uitmaakt van het darmepitheel. Dit celtype vormt een zeer gespecialiseerd apicaal domein, dat verantwoordelijk is voor opname van voedingsstoffen uit het darmkanaal, en een basaal domein, dat zorgt voor de afgifte van nutriënten aan het bloed. Verlies van deze functionele asymmetrie is de directe oorzaak van verscheidene ziektes (o.a. microvillus inclusie ziekte) en is een kenmerk van epitheliale kankers. De totstandkoming van cel polariteit is daarom een proces dat onder strenge regie verloopt.

De novo vorming van cel polariteit vereist het doorbreken van initiële cellulaire symmetrie. Vanuit een signaleringsperspectief is dit een grote uitdaging omdat er per definitie geen ruimtelijke informatie is die het polarisatieproces kan instrueren. Signalering door kleine GTPase eiwitten is betrokken bij verschillende symmetrie doorbrekende processen en één eiwit uit deze familie in het bijzonder is een evolutionair geconserveerde centrale regulator van cel polariteit: Cdc42.

In hoofdstuk twee en drie onderzoeken we de rol van Cdc42 in de totstandkoming van enterocyten polariteit. Hiervoor maken we gebruik van een gemodificeerde darmkankercellijn die in staat is te polariseren in de afwezigheid van cel-cel juncties en andere ruimtelijke informatie. We zien dat waar deze cellen normaal altijd één apicaal domein vormen, cellen zonder Cdc42 vaak meerdere apicale domeinen maken. Dit toont aan dat singulariteit in de vorming van een apicaal membraan actief gereguleerd wordt door polariserende epitheelcellen en dat dit Cdc42 signalering vereist.

In hoofdstuk 2 tonen we verder aan dat deze Cdc42 signalering georkestreerd wordt door ATP8B1, een flippase-eiwit dat gemuteerd is in patiënten met progressieve familiale intrahepatische cholestase type 1 – in Nederland bekend als de Spakenburgse ziekte. ATP8B1 lokaliseert in het apicale plasma membraan van enterocyten waar het, door het internaliseren van het membraan lipide phosphatidylserine te katalyseren, de mobiliteit van Cdc42 verlaagd. Verlies van ATP8B1 zorgt voor een hogere mobiliteit van Cdc42, waardoor het niet verrijkt blijft op het apicale membraan. Het gevolg hiervan is een diffuse lokalisatie van Cdc42 in de cel en een verlies van Cdc42-afhankelijke apicaal membraan clustering. Als gevolg hiervan vormen cellen zonder ATP8B1 een groter apicaal membraan en meerdere apicale domeinen per cel.

We laten vervolgens zien dat verlies van ATP8B1 ook een groter apicaal membraan geeft in intestinale 'organoïde' culturen en tonen daarmee aan dat regulatie van apicaal membraan clustering ook relevant is in de context van

een epitheliale cellaag; dus in de aanwezigheid van ruimtelijke instructies afkomstig van cel-cel juncties. Bovendien laten we zien dat de vorm van het apicaal membraan van enterocyten veranderd is in intestinale biopten van PFIC patiënten en impliceren daarmee dat verlies van apicaal membraan clustering een oorzaak is van PFIC.

In hoofdstuk 3 onderzoeken we hoe de mobiliteit van Cdc42 is gereguleerd tijdens cel polarisatie. We vinden dat de activator van Cdc42, de GEF Tuba, de mobiliteit van Cdc42 op twee manieren reguleert. Aan de ene kant remt Tuba, door Cdc42 te activeren, membraan-dissociatie van Cdc42 door RhoGDI, een eiwit dat normaal zorgt voor een hoge mobiliteit van inactief Cdc42-GDP. Aan de andere kant verlaagt Tuba de mobiliteit van actief Cdc42-GTP, vermoedelijk door de vorming van een trimeer complex bestaande uit Tuba, Cdc42 en een effector eiwit. Het gecombineerde effect van deze regulatiemechanismes is een drastische immobilisatie van Cdc42 na activatie door Tuba. We laten zien dat deze immobilisatie noodzakelijk is voor lokale Cdc42 signalering en daarmee voor clustering van het apicale membraan.

In hoofdstuk 4 beschrijven we hoe de lipide fosfatase en tumor suppressor PTEN betrokken is bij de vorming van een geclusterd apicaal membraan. We vinden dat verlies van PTEN leidt tot de vorming een apicaal membraan dat de volledige omtrek van de cel omspant. Voor clustering van het apicaal membraan is het nodig dat PTEN een interactie aangaat met het platform-eiwit PTPL1. Binding aan PTPL1 zorgt ervoor dat PTEN lokaliseert naar het apicale membraan om zo clustering te bewerkstelligen. PTEN en PTPL1 vormen dus een alternatieve module in de regulatie van apicaal membraan grootte.

In hoofdstuk 5 bieden we een overzicht van de signaleringsmechanismes van de Rap2 GTPases. Aan de hand van dit overzicht laten we zien dat Rap2 een markeringsfunctie heeft en regio's in de cel aanduidt waar het actine cytoskelet herschikt moet worden.

In hoofdstuk 6 onderzoeken we hoe zeer identieke GTPase eiwitten afzonderlijk kunnen signaleren zonder interferentie. Enkel Rap2A, en niet de isovormen Rap2B en Rap2C, is betrokken bij de signalering die zorgt voor de formatie van microvilli op het apicale membraan van gepolariseerde enterocyten. We laten zien dat waar Rap2A lokaliseert in het apicale membraan en in de apicale recyclerende endosomen, Rap2C enkel aanwezig is in cytosolische structuren en als gevolg daarvan niet betrokken is bij microvilli formatie. Desalniettemin, Rap2B lokaliseert ogenschijnlijk identiek aan Rap2A, maar wordt in tegenstelling tot Rap2A niet geactiveerd aan het apicale plasma membraan. Kritieke verschillen in de C-terminale aminozuursequentie van Rap2B zorgen voor dit verschil.

Kortom, we beschrijven nieuwe signaleringsmechanismes die bijdragen aan het doorbreken van cellulaire symmetrie. Specifiek zijn deze mechanismes betrokken bij de clustering van het apicale membraan, het naleven van singulariteit in apicaal domein specificatie en de vorming van microvilli. Hiermee bieden we fundamentele inzichten in de organisatie van polariteitssignalering en de mechanismes van weefselvorming.

Abbreviations

ATP8B1	ATPase class I type 8b member 1
Cdc42	Cell devision control protein 42 homolog
CRISPR	clustered regularly interspaced short palindromic repeats
CTRL	control
DAPI	4,6-diamidino-2-phenylindole
DOX	doxycycline
EBP50	Ezrin-binding protein 50
EV	empty vector
GAP	GTPase-activating protein
GDI	Guanosine nucleotide dissociation inhibitor
GDP	guanosine diphosphate
GEF	Guanine nucleotide exchange factor
GTP	guanosine triphosphate
HVR	hypervariable region
IP	immunoprecipitation
LKB1	Liver kinase B1
MDCK	Madin-Darby Canine Kidney
MINK	Misshapen-like kinase 1
MTOC	microtubule organizing center
NEC	no endogenous Cdc42
P4-ATPases	type 4 subfamily of P-type ATPases
PA	phosphatidic acid
Par	partitioning defective
PBM	PDZ-binding motif
PBR	polybasic region
PD	pulldown
PDZ	post synaptic density protein 95 (PSD95), disc large homolog 1 (Dlg1), and zonula occludens-1 protein (ZO-1)
PFIC1	progressive familial intrahepatic cholestasis type 1
PH	pleckstrin homology
$PI(4,5)P_2$	phosphatidylinositol 4,5-bisphosphate
PS	phosphatidylserine
PTEN	phosphatase and tensin homolog
PTPL1	protein tyrosine phosphatase like 1
Rap	Ras-related protein
shRNA	short hairpin RNA
STRAD	STE20-related kinase adapter protein
TL	total lysate
TNIK	TRAF2 and NCK-interacting protein kinase
W4	Ls174T:W4
WT	wild type

Curriculum Vitae

Lucas Bruurs was born on april 21st, 1988 in Serooskerke, the Netherlands. After obtaining his 'gymnasium' diploma at the Christelijke Scholengemeenschap Walcheren in 2006 he started a bachelor program in pharmacy at Utrecht University. As his final research project, he performed a six month research internship in the group of prof. Albert Heck at Utrecht University, focussing on the development of a chemical labeling approach to study protein conformation using native mass spectrometry.

After this, he started the master program drug innovation at Utrecht University in 2009. For this he first performed an intership in the lab of prof. René Bernards at the Netherlands cancer institute (NKI) in Amsterdam, investigating the mechanisms via which epigentically silenced tumor suppressor genes in colorectal cancer cells can be pharmacologically reactivated. In a second internship in the group of prof. Hidde Ploegh, at the Whitehead Institute in Boston, he developed bio-orthogonal protein labeling strategies using sortase technology.

After obtaining his master diploma in 2011 he started his PhD training in the group of prof. Hans Bos at the University Medical Center Utrecht.

Outside of the lab Lucas is a sports enthousiast, who enjoys riding his racing bike on the Utrechtse Heuvelrug and is a loyal visitor of FC Utrechts' Bunnik side.

Publications

1. Bruurs LJM, Donker L, Zwakenberg S, Zwartkruis FJ, Begthel H, Knisely AS, Posthuma G, van de Graaf SF, Paulusma CC, Bos JL. 2015. ATP8B1-mediated spatial organization of Cdc42 signaling maintains singularity during enterocyte polarization. J Cell Biol 210:1055-1063.

2. Bruurs LJM, Bos JL. 2014. Mechanisms of Isoform Specific Rap2 Signaling during Enterocytic Brush Border Formation. PLoS One 9:e106687.

3. Cai Y, Geutjes EJ, de Lint K, Roepman P, Bruurs L, Yu LR, Wang W, van Blijswijk J, Mohammad H, de Rink I, Bernards R, Baylin SB. 2013. The NuRD complex cooperates with DNMTs to maintain silencing of key colorectal tumor suppressor genes. Oncogene 33: 2157-2168.

Nawoord
Met veel plezier heb ik de afgelopen vijf jaar het onderzoek verricht waarvan de bevindingen in dit proefschrift te lezen zijn. Ik ben iedereen dankbaar die gedurende deze tijd een bijdrage heeft geleverd aan de totstandkoming van dit proefschrift. In het bijzonder wil ik de volgende mensen bedanken:

Ik dank Hans voor de vrijheid om mijn eigen weg te kiezen zonder ooit het gevoel te hebben gehad er alleen voor te staan. Jouw vertrouwen heeft me erg gestimuleerd en ondanks dat we het wetenschappelijk niet altijd met elkaar eens waren, waren onze discussies altijd nuttig. Je hebt een omgeving geschept waar passie en creativiteit kunnen floreren en het was een voorrecht om daarin te mogen werken.
Cruciaal was het bediscussiëren van nieuwe experimenten en ideeën met WJ, Fried, Harmjan, Boudewijn, Holger, Hugo en Bas. Jullie opinie heeft op deze momenten mijn enthousiasme getemperd of juist aangewakkerd maar was altijd leerzaam. Bas, jouw microscopie expertise heeft mij veel geholpen. Grote dank ook voor Susan en Fried, onze helden van CRISPR. Jullie CRISPR creaties hebben een onmisbare bijdrage geleverd aan drie hoofdstukken. Ook dank ik Stan en Coen voor de aangename samenwerking met betrekking tot het ATP8B1 werk.
Ik heb het geluk gehad drie getalenteerde studenten te mogen begeleiden. Lisa, Axel en Mirjam hebben elk cruciale bijdragen geleverd aan dit werk waarvoor ik ze erg dankbaar ben. Mirjam, jouw hulp in mijn laatste jaar heeft mij enorm veel werk uit handen genomen. Enorm bedankt dat je na je stage nog voor me wilde blijven werken.

Ontspanning buiten het werk heeft mij veel ideeën opgeleverd maar ook voor de nodige afleiding gezorgd. Ik dank alle huidige en vroegere leden van het Heuvelrug Butchers fietscollectief voor het geweldige afzien. Veel dank aan WJ en Koen voor alle zaterdagen en zondagen langs de lijn. Ook dank ik Jouke-Thiemo, Jelle, Pieter en Anouk voor afleiding van het lableven in welke vorm dan ook.

Verder dank ik iedereen die mij op de been heeft geholpen toen dat nodig was.
Ik dank mijn familie voor alle steun die ik heb mogen ontvangen. De rust van een weekend in Veere is voor mij een bron van energie die de calorische waarde van de altijd aanwezige taarten ruimschoots overstijgt.
Ten slotte dank ik Iris; voor je blijvende interesse in mijn onderzoek en voor jouw onvoorwaardelijke steun en liefde.